Mass balance and related topics of the Greenland ice sheet

Niels Reeh and Hans Oerter
(editors)

Open File Series 93/5

April 1993

GRØNLANDS GEOLOGISKE UNDERSØGELSE
Ujarassiortut Kalaallit Nunaanni Misissuisoqarfiat
GEOLOGICAL SURVEY OF GREENLAND

GRØNLANDS GEOLOGISKE UNDERSØGELSE
Ujarassiortut Kalaallit Nunaanni Misissuisoqarfiat
GEOLOGICAL SURVEY OF GREENLAND
Øster Voldgade 10, DK-1350 Copenhagen K, Denmark

The Geological Survey of Greenland (GGU) is a research institute affiliated to the Mineral Resources Administration for Greenland (MRA) within the Danish Ministry of Energy. As with all other activities involving the non-living resources in Greenland, GGU's investigations are carried out within the framework of the policies decided jointly by the Greenland Home Rule Authority and the Danish State.

Open File Series

The Open File Series consists of unedited reports and maps that are made available quickly in limited numbers to the public. They are a non-permanent form of publication that may be cited as sources of information. Certain reports may be replaced later by edited versions.

Citation form

Open File Series Grønlands Geologiske Undersøgelse

conveniently abbreviated to:

Open File Ser. Grønlands geol. Unders.

GGU's Open File Series består af uredigerede rapporter og kort, som publiceres hurtigt og i et begrænset antal. Disse publikationer er midlertidige og kan anvendes som kildemateriale. Visse af rapporterne vil evt. senere blive erstattet af redigerede udgaver.

ISSN 0903-7322

GRØNLANDS GEOLOGISKE UNDERSØGELSE
Open File Series 93/5

Report of the
3rd Workshop on

Mass balance and related topics of the Greenland ice sheet

Niels Reeh and Hans Oerter
(editors)

held at
Alfred-Wegener-Institute for Polar- and Marine Research
Bremerhaven, Germany
30th November - 2nd December 1992

April 1993

Contents

Page intentionally left empty in printed version

INTRODUCTION

The Workshop on "Mass Balance and Related Topics of the Greenland Ice Sheet" held at Alfred-Wegener Institute for Polar- and Marine Research (AWI), Bremerhaven, Germany on 30th November - 2nd December 1992 was the third workshop dedicated to mass and energy balance studies of the Greenland ice sheet. Since the first workshop on this subject held at the Geological Survey of Greenland (GGU), Copenhagen 14.-16. November 1990 via the second workshop held in Zermatt, Switzerland 2.-4. December 1991, the number of participants and subjects covered have steadily increased, and the workshop in Bremerhaven was the hitherto most comprehensive.

The workshops were started up as a forum for exchanging and discussing results of mass and energy balance studies carried out in Greenland by Austrian, Danish, Dutch, German and Swiss groups. Despite studies by W. Ambach, A. Bauer and C.S. Benson in the 1950s and 1960s, GGU was the only institution active in this kind of investigations in Greenland until 1989. In 1989, AWI initiated mass balance studies in Northeast Greenland and University of Utrecht (IMAU), The Netherlands and ETH Zurich, Switzerland started mass and energy balance studies in West Greenland. Originally, the investigations by AWI, GGU and IMAU took place under The EPOCH programme "Climate Change, Sea Level Rise and Associated Impacts in Europe" funded by the EC. The EPOCH programme has now finished, but the three institutions continue the studies on Greenland mass and energy balance and ice sheet dynamics under the EC ENVIRONMENT programme 1993-1994.

The increasing interest for the workshops, also from other groups, indicates that there is a general need for meetings dealing with Greenland glaciology, and it is hoped that the workshops may eventually develop into real symposia dealing with all aspects of Greenland glaciology as a counterpart to the already institutionalized International Symposia on Antarctic Glaciology.

At the workshop at AWI it was decided for the first time to publish a report of extended abstracts of the presentations given at the meeting. GGU has offered to publish the abstracts from the AWI workshop as a GGU Open File Report, and furthermore, in collaboration with future host institutions, to publish similar abstract volumes for future workshops.

March, 1993

Niels Reeh

Participants and adresses

Ayako **Abe-Ouchi**
ETH Zürich, Geograhisches Institut, Wintherthurerstr. 190, CH-8057 Zürich, Switzerland
Tel.: +41-1-257-5208 Fax.: +41-1-362-5197

Carl Egede **Bøggild**
AWI, Sektion Geophysik/Glaziologie, Postfach 120161, D-2850 Bremerhaven, FR Germany
Tel.: +49-471-4831-174 Fax.: +49-471-4831-149

Dr. Roger J. **Braithwaite**
GGU, , Øster Volgade 10, DK-1350 Copenhagen K, Denmark
Tel.: +45-33-118866 Fax.: +45-33-935352

Reinhard **Calov**
Technische Hochschule, Inst. für Mechanik III, Hochschulstraße 1, D-W 6100 Darmstadt, FR Germany
Tel.: +49-6151-16-5370 Fax.: +49-6151-16-6869

Dr. Jürgen **Determann**
Alfred-Wegener-Institut, Columbus Straße, D-W 2850 Bremerhaven, FR Germany
Tel.: +49-471-4831-413 Fax.: +49-471-4831-149

Dr. P. G. **Duynkerke**
Inst. for Marine and Atmospheric Research, , Princetonplein 5, NL-3584 CC Utrecht, The Netherlands
Tel.: +31-30-532909 Fax.: +31-30-543163

Kerstin **Fleg**
Alfred-Wegener-Institut, Columbus Straße, D-W 2850 Bremerhaven, FR Germany
Tel.: +49-471-4831-255 Fax.: +49-471-4831-149

Hubertus **Fischer**
Universität Heidelberg, Institut für Umweltphysik, Im Neuenheimer Feld 366, 6900 Heidelberg, FR.Germany
Tel.: +49-6221-56-3310 Fax.: +49-6221-56-3405

Jann **Forrer**
ETH Zürich, Geograhisches Institut, Wintherthurerstr. 190, CH-8057 Zürich, Switzerland
Tel.: +41-1-257-5221 Fax.: +41-1-362-5197

Dr. Wouter **Greuell**
Inst. of Marine and Atmospheric Research, Princetonplein 5, NL-3584 Utrecht, Niederlande
Tel.: +31-30-533268 Fax.: +31-30-543163

Ralf **Greve**
Technische Hochschule, Inst. für Mechanik III, Hochschulstraße 1, D-W 6100 Darmstadt, FR Germany
Tel.: +49-6151-16-3093 Fax.: +49-6151-16-6869

Marcel **Haefliger**
ETH Zürich, Geograhisches Institut, Wintherthurerstr. 190, CH-8057 Zürich, Switzerland
Tel.: +41-1-257-5226 Fax.: +41-1-362-5197

Ludwig **Hempel**
Universität Münster, Forschungsstelle f. phys. Glaziologie, Corrensstraße 24, 4400 Münster, FR Germany
Tel.: +49-251-83-3590 Fax.: +49-251-83-8397

E.A.C. **Henneken,** M.Sc.
Vrije Universiteit Amsterdam, Faculty of Eart Sciences, De Boelelaan 1085, NL-1081 HV Amsterdam, Niederlande
Tel.: +31-20-5485772 Fax.: +31-20-6462457

Christa **Homann**
Technische Universität, Inst. für Vermessungskunde, Pockelstraße 4, D-W 3300 Braunschweig , FR Germany
Tel.: +49-531/391-7494 Fax.: +49-531/391-5599

Prof. Kolumban **Hutter,** Ph.D.
Technische Hochschule, Inst. für Mechanik III, Hochschulstraße 1, D-W 6100 Darmstadt, FR Germany
Tel.: +49-6151-16-2991 Fax.: +49-6151-16-6869

Dr. Philippe **Huybrechts**
Alfred-Wegener-Institut, Columbus Straße, D-W 2850 Bremerhaven, FR Germany
Tel.: +49-471-4831-194 Fax.: +49-471-4831-149

Dr. Almut **Iken**
VAW, , ETH-Zentrum, CH-8092 Zürich,
Tel.: +41-1-2564092 Fax.: +41-1-2520158

Prof. Dipl.-Ing. Achim **Karsten**
Fachhochschule Hamburg, Fachber. Vermessungswesen, Hebebrandstraße 1, D-2000 Hamburg 60, FR Germany
Tel.: +49-40-59105-682 Fax.: +49-40-59105-685

Dr. Josef **Kipfstuhl**
AWI, Sektion Geophysik/Glaziologie, Postfach 120161, D-2850 Bremerhaven, FR Germany
Tel.: +49-471-4831-175 Fax.: +49-471-4831-149

Hinrich **Kock**
Techn. Universität, Inst. für Vermessungskunde, Pockelsstraße 4 , D-W 3300 Braunschweig, FR Germany
Tel.: +49-531-391-7491 Fax.: +49-531-391-5599

Dr. Antoon G C A **Meesters**
Vrije Universiteit Amsterdam, Faculty of Earth Sciences, De Boelelaan 1085, NL-1081 HV Amsterdam, Niederlande
Tel.: +31-20-5485311 Fax.: +31-20-6462457

Dr. Jaap J M **v d Meer**
Fysisch Geografisch & Bodemkundig Lab., University of Amsterdam, Nieuwe Prinsengracht 130, 1018 VZ Amsterdam, The Netherlands
Tel.: +31-20-525-74 20 Fax.: +31-20-525-74 31

Prof. Dr. Heinz **Miller**
AWI, Sektion Geophysik/Glaziologie, Postfach 120161, D-2850 Bremerhaven, FR Germany
Tel.: +49-471-4831-210 Fax.: +49-471-4831-149

Dr. Friedrich **Obleitner**
Universität Innsbruck, Institut für Geophysik und Meteorologie, Innrain 52, A-6020 Innsbruck, FR.Germany
Tel.: +43-512-724 Fax.: +43-512-507-2170

Dr.-Ing. Hans **Oerter**
AWI, Sektion Geophysik/Glaziologie, Postfach 120161, D-2850 Bremerhaven, FR Germany
Tel.: +49-471-4831-347 Fax.: +49-471-4831-149

Prof. Dr. Atsumu **Ohmura**
ETH Zürich, Geograhisches Institut, Wintherthurerstr. 190, CH-8057 Zürich, Switzerland
Tel.: +41-1-257-5220 Fax.: +41-1-362-5197

Dr. Hisashi **Ozawa**
ETH Zürich, Geograhisches Institut, Wintherthurerstr. 190, CH-8057 Zürich, Switzerland
Tel.: +41-1-257-5217 Fax.: +41-1-362-5197

Niels **Reeh**
Danish Polar Center, c/o GGU, Øster Volgade 10, DK-1350 Copenhagen K, Denmark
Tel.: +45-33-118866 Fax.: +45-33-935352

Dr. Oskar **Reinwarth**
Kommission für Glaziologie der Bayerischen Akademie der Wissenschaften, Marstallplatz 8, D-W8000 München 22, FR Germany
Tel.: +49-89-23031-196 Fax.: +49-89-23031-240

Dr. Andrew J. **Russell**
Kingston University, School of Geography, Penrhyn Road, Kingston upon Thames, Surrey KTI 2EE, UK
Tel.: +44-81-547-2000 ext 2511 Fax.: +44-81-547-7419

Prof. Dr.-Ing. Manfred **Stober**
FH f. Technik Stuttgart, Fachber. Vermessung, Postfach 101452, 7000 Stuttgart 10, FR Germany
Tel.: +49-711-121-2563 Fax.: +49-711-121-2666

Thorsteinn **Thorsteinsson**
Alfred-Wegener-Institut, Columbus Straße, D-W 2850 Bremerhaven, FR Germany
Tel.: +49-471-4831-348 Fax.: +49-471-4831-149

Prof. Dr. Franz **Thyssen**
Universität Münster, Forschungsstelle f. phys. Glaziologie, Corrensstraße 24, 4400 Münster, FR Germany
Tel.: +49-251-83-3592 Fax.: +49-251-83-8397

Dr. Seiho **Uratsuka**
Alfred-Wegener-Institut, Columbus Straße, D-W 2850 Bremerhaven, FR Germany
Tel.: +49-471-4831-174 Fax.: +49-471-4831-149

Prof. Dr. Hans F **Vugts**
Vrije Universiteit Amsterdam, Institute of Earth Sciences, De Boelelaan 1085, NL-1081 HV Amsterdam, The Netherlands
Tel.: +31-20-5484151 Fax.: +31-20-6462457

Dr. Dietmar **Wagenbach**
Universität Heidelberg, Institut für Umweltphysik, Im Neuenheimer Feld 366, 6900 Heidelberg, FR.Germany
Tel.: +49-6221-56-3310 Fax.: +49-6221-56-3405

Presentations at the Workshop

Ice sheet related modelling

Philippe Huybrechts	Modelling the present and future evolution of the Greenland ice sheet
Kolumban Hutter	On the thermal regime of the Greenland ice sheet
Ralf Greve	A polythermal ice sheet model
Martin Funk Almut Iken Keith Echelmeyer	Modelled and measured englacial temperatures in Jakobshavn Isbrae
Reinhard Calov	A time dependent parameter study on the evolution of the Greenland ice sheet
Ayako Abe-Ouchi	Climatic impact on Greenland ice sheet: A modelling approach

Energy balance, ablation and run off

Atsumu Ohmura	ETH Greenland ice sheet climate Program: an overview
Jan Forrer	Turbulence measurements in the stable atmospheric boundary layer at the ETH camp
Marcel Haefliger	Surface temperature derived from AVHRR for the Greenland ice sheet
Hisashi Ozawa	Climate conditions on temperate, cold and inversion type glaciers
Wouter Greuell	Parameterization of short and long-wave radiation for the Greenland ice sheet
E. A. C. Henneken	Energy balance and melt at the VU-Camp
P. G. Duynkerke	Katabatic flow and surface energy balance near the boundary line between glacier and tundra during GIMEX-91
Antoon G. C. A. Meesters	Simulation of the katabatic wind and its influence on the energy balance

Hans F Vugts	Is there a fifteen hour inertial oscillation in the windfield at Greenland?
Carl E Bøggild Hans Oerter Niels Reeh	Ablation and mass balance approach for Storstrømmen, NE-Greenland
Roger Braithwaite	Meltwater refreezing in the lower accumulation area of the Greenland ice sheet
Russell, A. J.	Controls on the varying morphology and sedimentology of three proglacial outwash systems near Kangerlussuaq, Søndre Strømfjord, Greenland

discussion on future work

Dynamics, accumulation and paleoclimate

Hinrich Kock	Height determinations along the EGIG line and the GRIP area
Christa Homman	Strain and velocity determination on the Greenland ice sheet
Atsumu Ohmura	Re-evaluation of the EGIG profile change.
Ludwig Hempel FranzThyssen M. Jonas	Accumulation during the last 2000 years along the EGIG line derived from radio-echo soundings
Dietmar Wagenbach	Isotopic, chemical and glacio-meteorological studies along the EGIG line
Jaap J M van der Meer,	Glaciation of the Søndre Strømfjord - Itiudleq Fjord System
Niels Reeh Carl E Bøggild Hans Oerter	On the dynamics of Storstrømmen, NE-Greenland
Hans Oerter Niels Reeh	^{18}O studies on the margin of Storstrømmen, NE-Greenland.

final discussion

Modelling the present evolution of the Greenland ice sheet

Philippe Huybrechts

Alfred-Wegener-Institut für Polar-und Meeresforschung,
Postfach 120161, D-W2850 Bremerhaven, FR Germany

Introduction

The present state of balance of the Greenland ice sheet is an important initial condition to assess the ice sheet's contribution to future sea levels. From a physical point of view, regarding the long time scales introduced by isostasy, thermo-mechanical coupling and the slow advection of harder Holocene ice in the basal shear layers, it is unlikely that the Greenland ice sheet would have adjusted completely to its past history. Based on various methods and only a limited amount of measurements, it seems that at present an imbalance of up to 30% of the annual mass turnover cannot be detected in a definite way (Warrick and Oerlemans, 1990). Here I use an alternative method to approach this problem, and obtain the imbalance by first simulating the past history of the ice sheet and subsequently analyzing the evolution pattern which results for the present day. Theoretically, this approach would be exact provided both the past boundary conditions (mass balance, surface temperature, ...) over a time scale at least as long as the longest response time scale of the system and the ice dynamics were perfectly described.

Experimental setup

I use a 3-D, time-dependent thermomechanical ice sheet model which includes all of the relevant mechanisms believed to play a role in the ice sheet's evolution (fig. 1). The environmental forcing is made up by both prescribing the eustatic sea level stand, which determines the coast line beyond which the ice sheet cannot expand, and a uniformly distributed background temperature change, which drives the mass-balance model. The latter consists of two components: the accumulation part is based on presently observed values and varies by 5.3% for every degree of temperature change. The ablation model is based on the degree-day method and accounts for the daily and annual temperature cycle, a different degree-day factor for ice and snow melting and superimposed ice formation (Huybrechts et al., 1991)

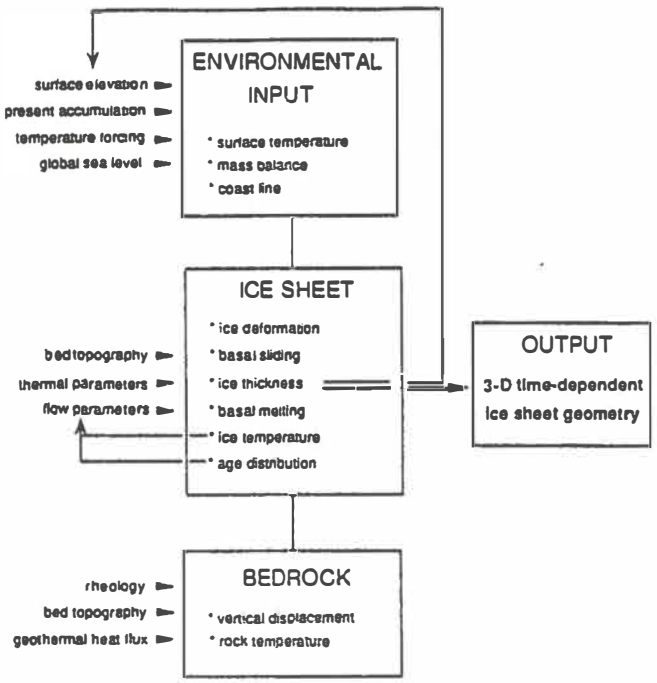

fig. 1: Structure of the model used in this investigation. Inputs are given at the left- hand side. Prescribed environmental variables drive the model, which has grounded ice and bedrock adjustment as major components. Temperature and age of the ice determine the ice flow properties. Ice thickness feeds back on surface elevation, an important parameter for the calculation of the mass balance. The main output is the 3-D time-dependent ice sheet geometry, which is freely generated by the model.

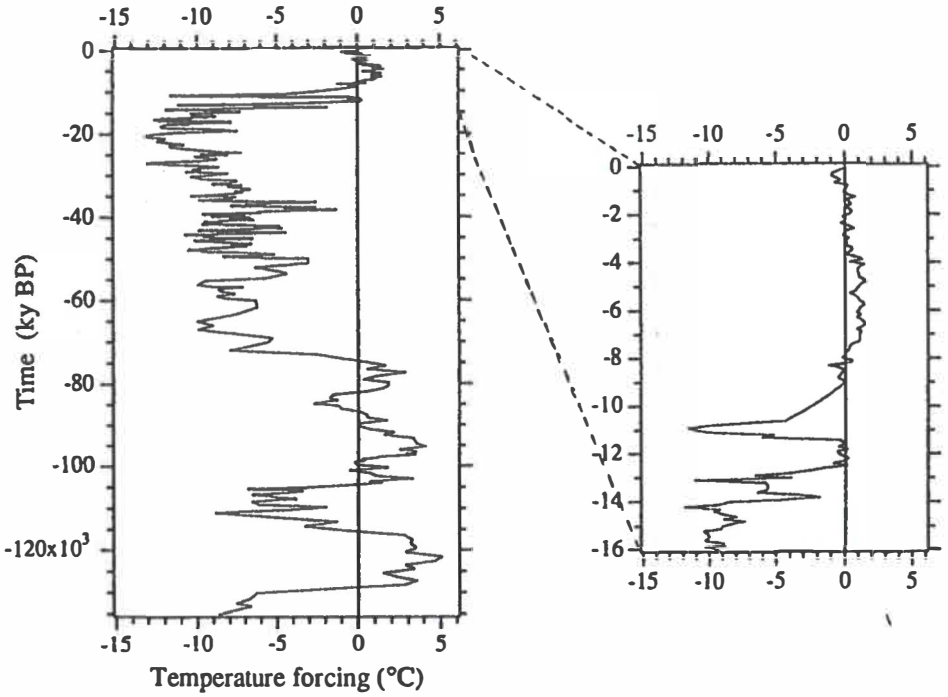

fig. 2: Temperature record used as forcing during the last glacial-interglacial cycle. The part older than 10800 years BP originates from the Pakitsoq $\delta^{18}O$ record obtained from surface ice sampling in central West Greenland (Reeh et al., 1991). The Holocene part was collated from the Dye3 and Camp Century records The enlargement at the right covers the period between the Last Glacial Maximum and the present-day.

A steady-state simulation of the ice sheet in a glacial climate was used as an initial configuration at 135000 years ago, when calculations started. The model forcing consists of a temperature record for central Greenland, which was assembled from various sources (fig. 2). This record resolves features down to a period of 100 years, meaning that only the somewhat longer-term trend is expected to show up in the results.

Results

The calculations indicate that the ice sheet as a whole is at present thickening slightly at a mean rate of 14 km^3 of ice or almost 1 cm/year, corresponding to a world-wide sea-level lowering of 3.5 mm during the last hundred years. However, large spatial differences occur (fig. 3). Central and northern parts high up in the accumulation area show a slight thinning which is mainly due to a slow but consistent basal warming in response to the last glacial-interglacial transition. Marginal thinning, most notably in the northeast and along major parts of the west coast, on the other hand, is principally due to increased melting caused by higher temperatures subsequent to the Little Ice Age. The most striking feature is a rather important thickening in the southwestern part of the ice sheet, which appeared to be robust against all realistic changes in environmental and ice-dynamical factors. It is suggested that this represents a long-term trend caused by a purely dynamic reaction to the geometry which came out of the last glacial-interglacial transition.

References

Huybrechts, P., submitted. The present evolution of the Greenland ice sheet: an assessment by modelling. *Palaeogeogr., Palaeoclimatol., Palaeoecol. (Global Planet. Change Sect.) special issue on Greenland.*

Huybrechts, P., Letreguilly, A., and Reeh, N., 1991. The Greenland ice sheet and greenhouse warming. *Palaeogeogr., Palaeoclimatol., Palaeoecol. (Global Planet. Change Sect.) 89:* 399-412.

Letreguilly, A., Reeh, N., and Huybrechts, P., 1991. The Greenland ice sheet through the last glacial-interglacial cycle. *Palaeogeogr., Palaeoclimatol., Palaeoecol. (Global Planet. Change Sect.) 90:* 385-394.

Reeh, N., Oerter, H., Letreguilly, A., Miller, H., and Hubberten, H.-W., 1991. A new, detailed ice-age oxygen-18 record from the ice sheet margin in central West Greenland. *Palaeogeogr., Palaeoclimatol., Palaeoecol. (Global Planet. Change Sect.) 90:* 373-383.

Warrick, R., and Oerlemans, J., 1990. Sea level rise. In: Houghton, J.T., Jenkins, G.J., and Ephraums, J.E. (eds.), *Climate Change, the IPCC Scientific Assessment*, Cambridge University Press, pp. 257-282.

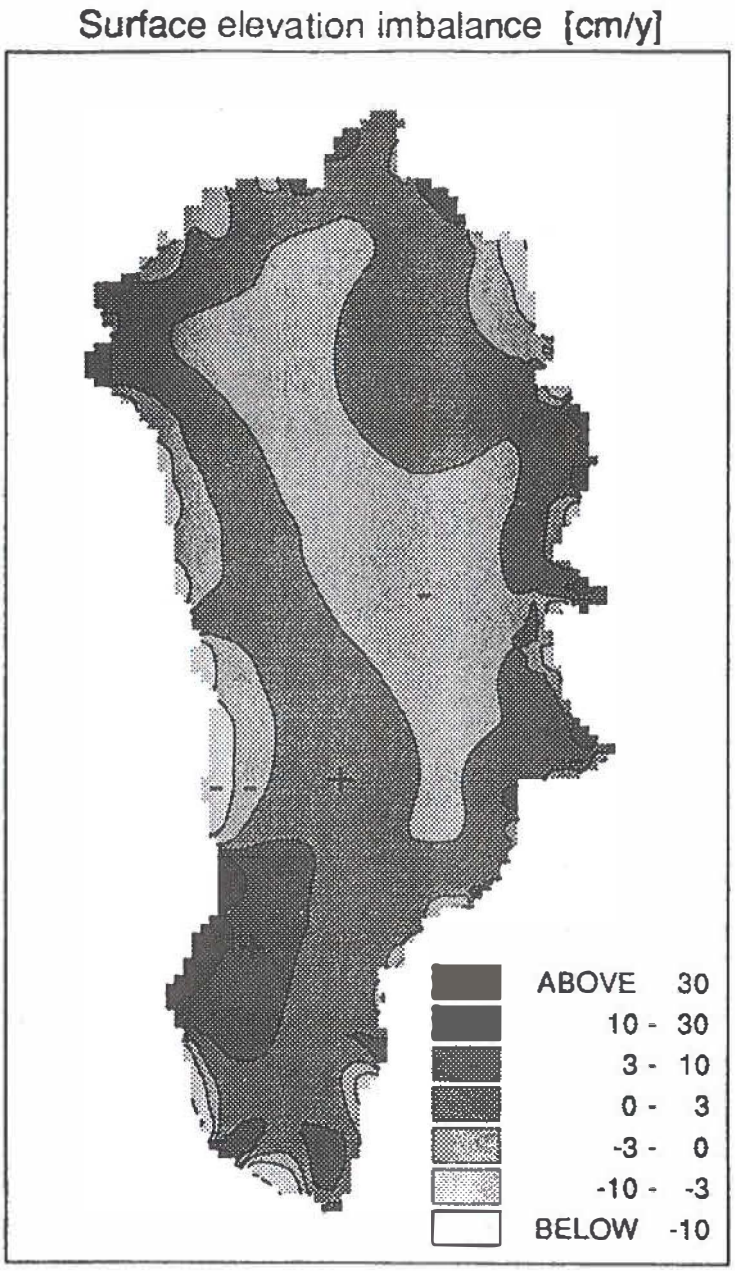

fig. 3: **Rate of surface elevation** change averaged over **the last 200 years as obtained after modelling the last glacial-interglacial** cycle. Positive values **indicate a thickening, negative values are for a thinning,** as marked by the respective **symbols. The pattern for the ice thickness evolution resembles this** one to a large extent, **but values tend to differ slightly by a few mm/year due to isostatic adjustments.**

Thermal response of the Greenland Ice Sheet through the last Ice Age to Present

Kolumban Hutter, Reinhard Calov

Institut für Mechanik, Technische Hochschule
Hochschulstr. 1, D-W-6100 Darmstadt, Germany

Modelling the flow of ice is such a complex problem that it is reasonable to focus interest on one single effect and neglect other processes in order to understand the principles underlying that effect. In this work we consider the evolution of the temperature distribution, and in particular, the evolution of the basal temperature of the Greenland Ice Sheet through time by neglecting the change in ice thickness. Our aim is to understand the principles of the atmospheric temperature variation through the Ice Age(s) on the Greenland Ice Sheet. Obviously, since according to ice core date "Dye 3" and "Camp Century" were ice free during the Eemian Interglacial, our computations are likely to deliver somewhat higher basal temperatures with inferences or the safe side for temperate patchiness. Computations are being performed for a finite difference model of the well known shallow ice equations (1). The present surface temperature distribution is a mathematical fit to the data of Ohmura (2). Its temporal evolution follows modified time series of the Vostok data (3), *fig. 1.* Scenarios I and II are approximate upper and lower bounds, respectively to this temperature driving, prolonged into the past by one period to let the model swing into the proper initial temperature distribution 145 kyrs BP. The geothermal heat flow is chosen to be 42×10^{-3} Wm^{-2} either prescribed at the ice rock interface (scenarios are then called I and II, respectively), or 4 km below in a rigid, but thermally responding rock bed (in which case scenarios are called I-S and II-S, respectively). Computations are also performed for hard holocene ice (with enhancement factor E = 1) and softer pleistocence ice with E = 3).

Results show the following typical qualities:

- Because of the considerable thermal inertia of the rock bed, the temperature distribution of the Greenland Ice Sheet may contain some remnants of the Illinoian Ice Age.

- Its base has always had temperate (hot) patches, the size of which varied through time, see *Table 1* but the bore hole sites "Dye 3", "Camp Century" and "Summit" have always been cold.

- The basal temperature and the areal coverage of the base with temperate patches depends considerably on the thermal inertia of the rock bed. *Fig. 2* shows present homologous temperatures at the bed for scenario I - S.

A detailed report on this will appear in Refs. (4), (5), (6)

Table 1: Comparision of scenarios. Present temperate patches of the base of the Greenland Ice Sheet for various scenarios.

Scenario	E	A' x 10^3 km^2	$\frac{A'}{A}$ x 100
Steady	1	208.0	12.0 %
Steady	3	35.4	2,0 %
I (or II)	1	100.0	6,0 %
I-S	1	60.0	3,5 %
I-S	3	11.2	0,7 %

References:

1. K. Hutter, *Theroretical glaciology; material science of ice and the mechanics of glaciers and ice sheets*. D. Reidel, Dortrecht, 1983
2. A. Ohmura, *Zeitschrift für Gletscherkunde und Glazialgeologie, 13*, (1987)
3. J. M. Barnola, D. Raynaud, Y. S. Korotkevich, C. Lorius, *Nature, 329*, 408 (1987)
4. R. Calov, K. Hutter, 1993 pending publication
5. R. Calov, 1993 pending dissertations
6. R. Calov, K. Hutter, 1993 DFG-Fortsetzungsantrag

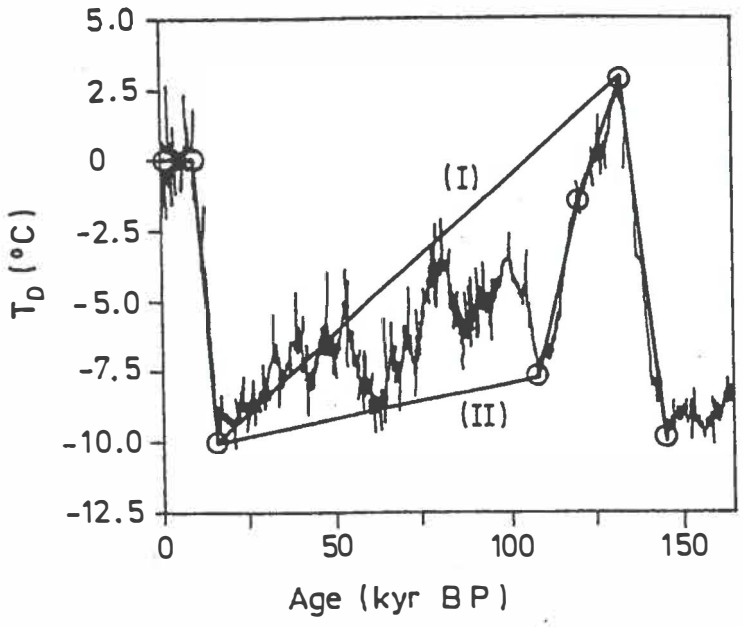

Figure 1: Surface driving temperature as inferred from the Vostok data and upper (I) and lower (II) bounds to these data. The ice age cycles I and II are continued back to 274 kyrs BP, to "swing-in" the computational model.

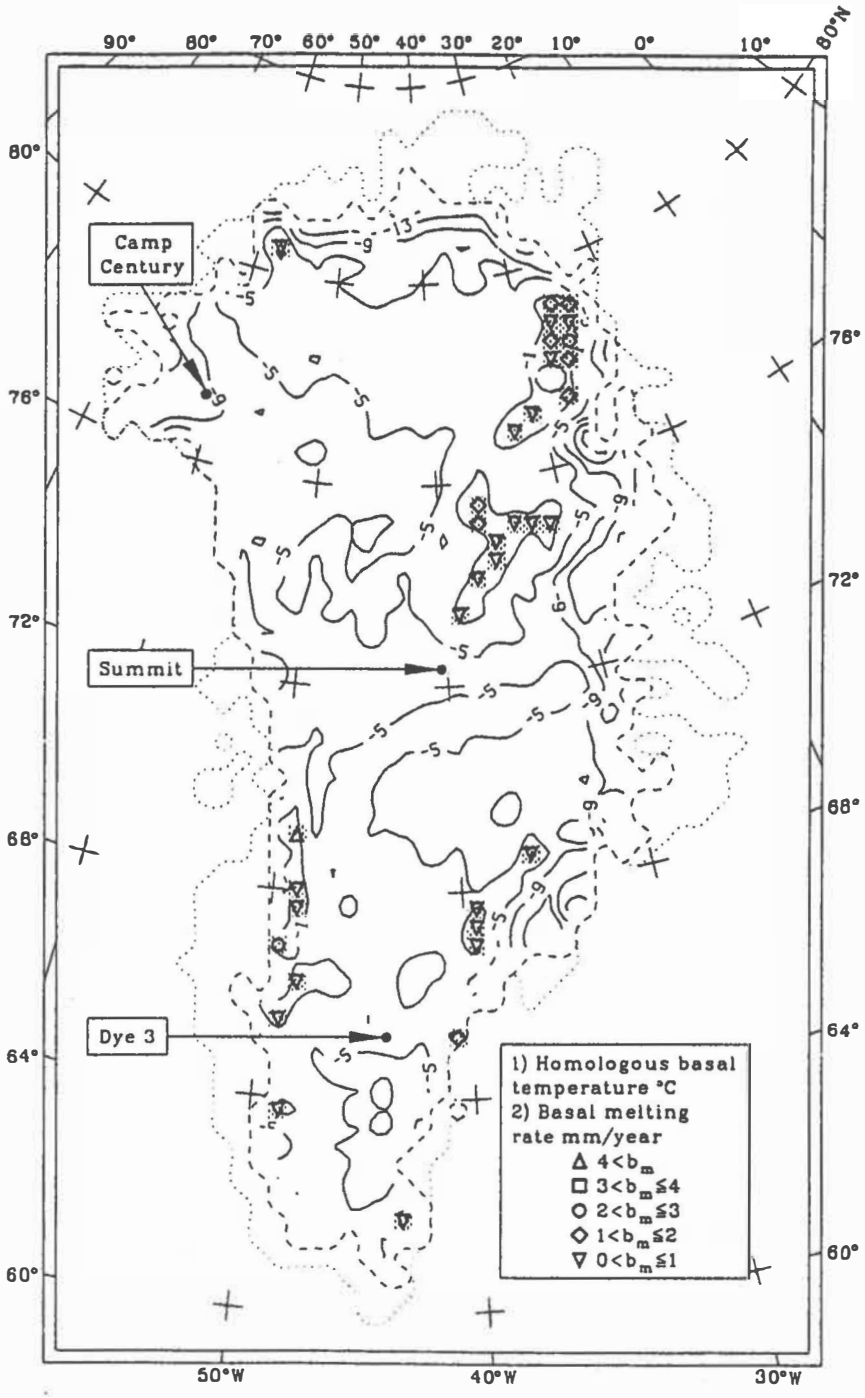

Figure 2: Today's computed homologous basal temperatures of the Greenland Ice Sheet for scenario I-S and E=1. Homologous isotherms are shown for T_B' = - 1, - 5, - 9, ...° C and regions with temperate basal ice are shaded. Symbols indicate the annual basal melting rate in intervals shown in the inset.

Climatic impact on Greenland Ice Sheet: approach by an ice sheet dynamics model

Ayako Abe-Ouchi
Geographisches Inst. ETH, Switzerland

The Greenland ice sheet is seldom in steady state, because of the climate change and transient ice dynamical response. The observations on elevation both by geodetic method on ground (Seckel, 1977) and by satellite altimetry (Zwally et al, 1989) suggest a slightly increase in elevation by the order of magnitude of 10mm per year at the center part of the ice sheet. Since it is not yet clear whether the thickening is the result of the change in ice physical properties (ice is soft/hard in Wisconsin/Holocene) (Reeh, 1985) or the result of a recent increase in accumulation (precipitation) rate (Zwally, 1989), several numerical experiments by an ice sheet model were carried out in this study.

A two dimensional ice sheet model was used, which calculates the ice sheet surface and bed geometry, ice velocity, dating of the ice (isochrone) and ice temperature time dependently (Abe-Ouchi and Blatter, 1993, Abe-Ouchi and others, 1993). The model was applied along the EGIG flow line, where the data for the input and verification are best documented in Greenland. A climate scenario was given as a forcing, where the Wisconsin-like *glacial* stage of 80,000 yrs. is followed by a 20,000 years Holocene-like *interglacial* stage. At the transition, the forcing parameters were changed stepwise: the precipitation was doubled, the equilibrium line altitude was raised by 1000m, the surface temperature increased by 10 °C and the ice made three times harder. Four glacial/interglacial cycles were repeated. The conclusion can be summarized as following:

Elevation change

1) Within 1000 years after the termination of the ice age, the present ice sheet has become thicker than that during ice age, mainly due to the increase of accumulation, and 2) at present, about 10,000 years after the transition, the ice sheet is still reacting to the change in the ice temperature and the downwards advection of harder Holocene ice, but, 3) the central part of the ice sheet may be slightly thinning by about 4mm per year. This is mainly due to the change in ice temperature at the transition, which dominates the effect of change in the ice physical properties at the transition.

Thermal history

4) The doubling of the accumulation at the transition has a substantial influence on the thermal regime of the ice sheet, especially on the basal temperature distribution, because the more the accumulation, the higher the ice flow velocity and the larger the strain rate heating (dissipation), which leads to the thinning trend of the ice sheet. 5) Under the summit, where the heat dissipation is very small, the basal temperature decreases after the transition, due to the increase in the accumulation rate and in the cold vertical advection .

Since the simulated rate of change of the summit elevation induced by the glacial/interglacial cycle is at most 4 mm per year and below detection threshold, the observed elevation change (either thickning or thinning) must be explained by the higher frequency variability in the accumulation rate. Here we conclude the importance of precipitation history for reconstructing and interpreting both the change in elevation and thermal regime of the ice sheet.

Reference

Abe-Ouchi, A. Doctor thesis in preparation.

Abe-Ouchi, A., Blatter, H. 1993. On the initiation of ice sheets. *Ann. Glaciology*, 18. (in press).

Abe-Ouchi, A., Blatter, H. and Ohmura, A. How does the Greenland Ice Sheet geometry remember the ice age? Submitted to the special issue in *Paleogeography, Paleoclimatology and Paleoecology (Global and Planetary change section).*

Reeh, N. 1985. Was the Greenland ice sheet thinner in the late Wisconsinan than now? *Nature*, **317**, 797-799.

Seckel, H. 1977. Höhenänderungen im grönländische Inlandeis zwischen 1959 und 1968. *Medd.Gronl.*, **187**(4), 58pp.

Zwally, H.J. 1989. Growth of Greenland ice sheet: Interpretation. *Science* 246, 1589-1591.

Zwally, H.J., Brenner, A.C., Major, J.A., Bindschalder, R.A. and Marsh, J.G. 1989. Growth of Greenland ice sheet: Measurement. *Science*, 246, 1587-1589.

An improved polythermal ice sheet model

Ralf Greve

Institut für Mechanik
Technische Hochschule Darmstadt
Hochschulstr.1, D-W-6100 Darmstadt

Natural ice sheets and glaciers may (if additional contents of salt and sediments are neglected) consist of two different phases. *Cold ice* has a temperature below the pressure corrected melting point, it can be described as an incompressible, viscous and heat-conducting one-component fluid. The temperature of *temperate ice*, however, is exactly on the melting point; thus, temperate ice also contains some water and is therefore a binary mixture. It can be described as an incompressible, viscous two-component fluid; the heat flux in temperate ice can be neglected because the temperature gradients due to the pressure correction of the melting point are very small. Ice sheets and glaciers containing both cold and temperate regions are called *polythermal*.

A continuum-mechanical model for polythermal ice consists of balance equations and constitutive relations for the cold and the temperate regions, boundary conditions at the free surface and the base and transition conditions at the surface of phase change between cold and temperate ice (the so-called cold-temperate transition surface, in the following referred to as CTS). For the cold region we have balance equations for mass, momentum and energy, added by three constitutive relations, a stress-stretching relation, a relation expressing the internal energy as a function of temperature and Fourier's heat conduction law. The temperate region is modelled by a mass balance, a momentum balance and an energy balance for the mixture ice plus water, a mass balance for the water itself (its content is assumed to be small, thus it is treated like a tracer), a stress-stretching relation, a relation expressing the internal energy as a function of the water content and a Fick-type diffusion law describing the flow of water relative to the barycentric velocity.

At the free surface a kinematic condition holds that describes the height evolution of the ice sheet as a function of accumulation and ablation. Furthermore, the stress vector is approximately equal to zero, and the temperature shall be prescribed in case of a cold free surface (if it is temperate, instead of this the water content or its normal derivative must be given). At the cold base adhesion is assumed, i. e., the velocity vector vanishes. Moreover, an energy jump condition is needed that relates the basal temperature gradient to the prescribed geothermal heat flux. In case of a temperate base, impenetrability shall be assumed; thus, the normal components of the barycentric velocity and the diffusive water flux vanish. Since the water may behave as a lubricant, we do not want to assume adhesion here, but a sliding law shall be adopted relating the tangential barycentric velocity to the tangential basal stress.

As for the transition conditions at the CTS, we have once more a kinematic condition describing the evolution of its position; furthermore, it can be deduced that the temperature, the velocity vector and the stress vector must be continuous. Moreover, we have a jump condition for the water content and a jump condition for the energy. In the former, the possibility of surface production or annihilation of water at the CTS due to melting and freezing processes is included, and the latter relates the temperature gradient at the cold side of the CTS to the water content at the temperate side. From the additional condition that the temperature in the cold region reaches its maximum at the CTS it can be inferred that the water surface production term in the jump

condition for the water content can only be negative or zero; this means that in case of melting conditions (ice flow from the cold to the temperate zone) the water surface production vanishes and thus the temperature gradient at the cold side and the water content at the temperate side are equal to zero. In case of freezing conditions (ice flow from the temperate to the cold zone), however, due to the negative water surface production these two quantities need not vanish; they may suffer jumps at the CTS.

These two different possibilities are demonstrated by analytical solutions for a two-dimensional, infinetely long, inclined (angle γ), polythermal ice plate (parallel-sided slab, fig. 1) with an upper cold layer and a lower temperate layer under steady-state conditions. Fig. 2 shows the distribution of the horizontal velocity v_x (panel a), the temperature T in the cold region and the water content ω in the temperate region (panel b) as a function of the height z in case of melting conditions (positive accumulation-ablation function $a_s^\perp$; hence the vertical velocity points downward), fig. 3 shows the same for freezing conditions (negative accumulation-ablation function $a_s^\perp$; hence the vertical velocity points upward). Obviously the behaviour of the horizontal velocity is the same in both cases; its value increases monotonically from the given basal velocity to the maximum at the top. The distribution of the water content and the temperature, however, is completely different: in case of melting conditions, the water content decreases from the bottom to the CTS where it becomes equal to zero, and accordingly, the temperature gradient at the cold side is also equal to zero; thus, these quantities are continuous at the CTS. In case of freezing conditions, however, the water content increases from the bottom to the CTS and reaches a non-zero value there. This water freezes out by passing the CTS (negative surface production), and the latent heat becoming free by this is conducted into the cold region by the nonvanishing negative temperature gradient. This means that indeed the water content and the temperature gradient suffer jumps in this case.

Reference:
Greve, R. & Hutter, K. 1992 *An extended theory for polythermal ice.* (Submitted to Geophys. Astrophys. Fluid Dynamics.)

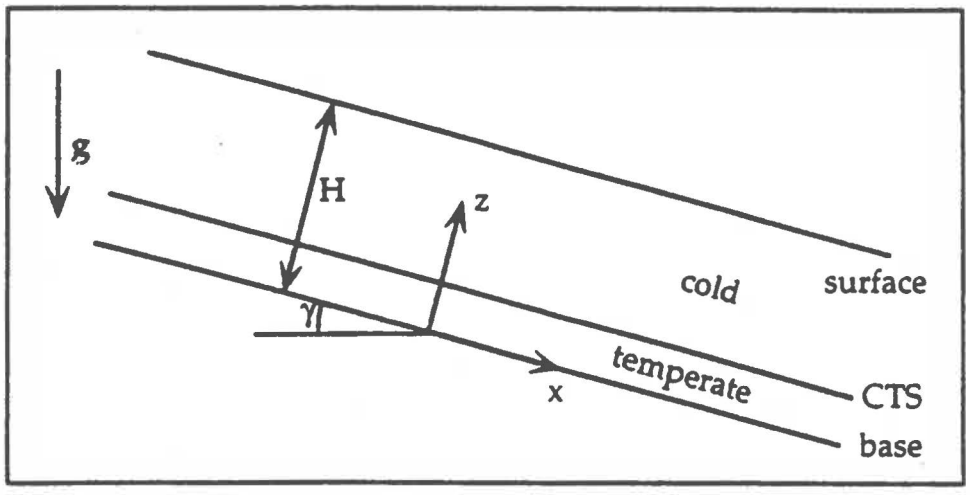

Fig. 1: Polythermal parallel-sided slab

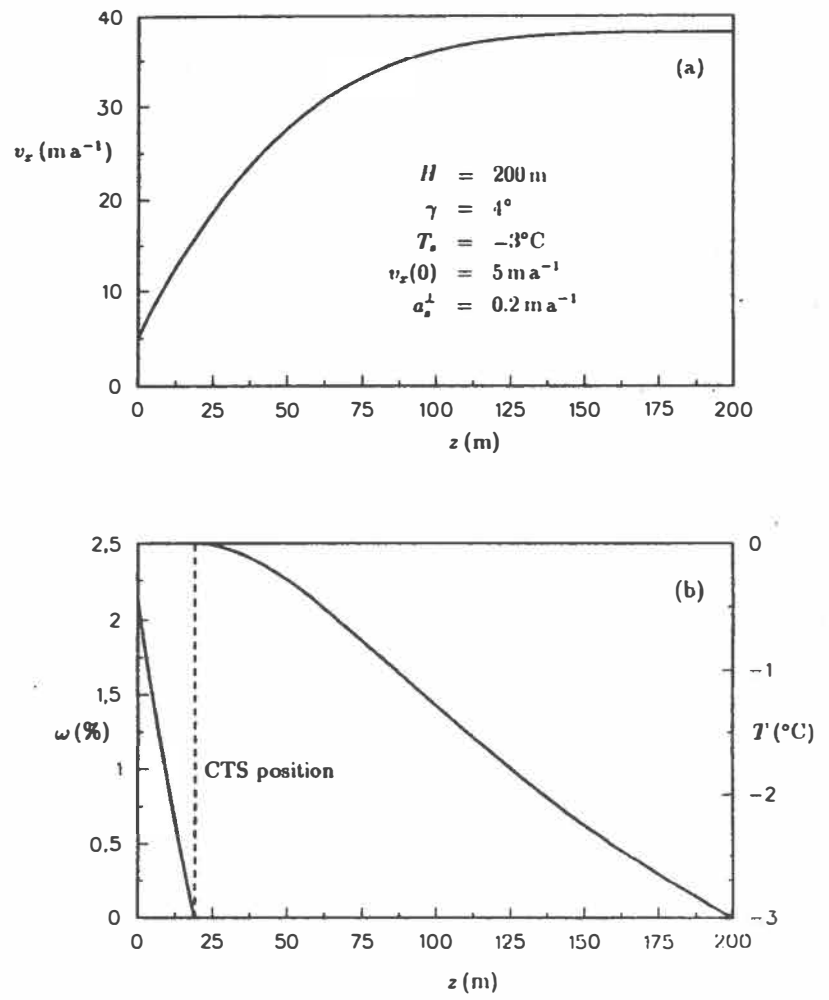

Fig. 2: Slab solutions for melting conditions

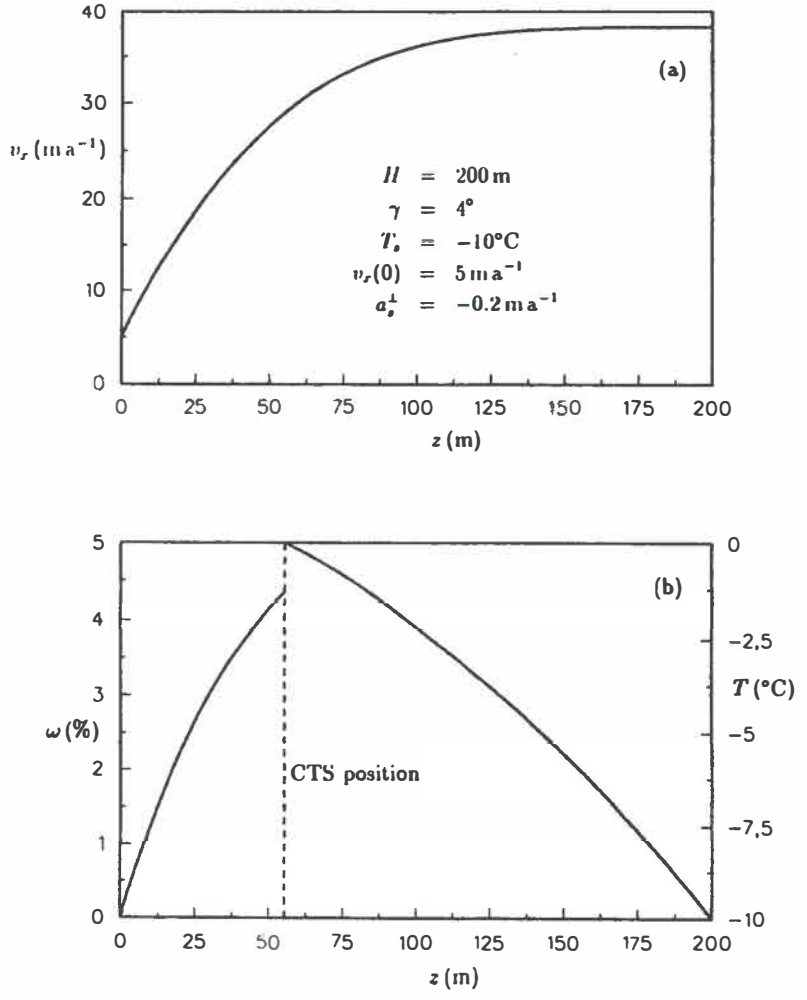

Fig. 3: Slab solutions for freezing conditions

Modelled and measured englacial temperatures in Jakobshavns Isbrae. Conclusions on vertical strain in the ice stream

Keith Echelmeyer
Geophysical Institute, University of Alaska
Fairbanks - AK 99775-0800, USA

Martin Funk, Almut Iken
VAW, Eidgenössische Technische Hochschule (ETH)
CH - 8092 Zurich, Switzerland

Jakobshavns Isbrae is a large ice stream in West Greenland. It flows at high velocities with a maximum of 7 km/a near the calving front. It produces about 27 km^3 icebergs per year. The ice stream flows through a deeply incised bedrock channel which extends 80 km inland. Surface velocity fields, strain rates, mass balance, near-surface ice temperatures, ice depth and surface morphology have been investigated in detail by members of the University of Alaska [Clarke and Echelmeyer (1989); Echelmeyer and Harrison (1990); Echelmeyer and others (1991) and (1992)]. In 1988 and 1989 several boreholes have been drilled in the ice stream, 50 km upstream from the calving front, to depths of some 1550m with a hot-water-drill (Iken and others 1988). The centerline depth of the ice stream is, however, 2500m. In these boreholes englacial temperatures and, where they reached the bed, subglacial water pressures have been measured (Iken and others, in press).

In order to obtain information on the temperature distribution below the depth reached with the drill, a model for the calculation of englacial temperatures has been developed. This model applies to flow in an ice sheet or along the centerline of an ice stream. It calculates the depth distribution of the velocity components, subject to the condition that the calculated velocities match the prescribed surface- and sliding velocities. The model allows for:

- Glen's flow law with the temperature-dependence of the rate factor as suggested by Smith and Morland (1981)
- 3-D strain rates, except transverse shear strain rates
- basal sliding
- 2-D thermal advection and conduction
- strain heating
- formation of a temperate layer and development of an unfrozen water content.

Input of the model are surface- and bed-elevation along a flowline from the ice cap center to the terminus, surface velocities, sliding velocities, mass balance, surface temperatures, geothermal heat flow and a shape factor accounting for friction along the ice stream boundaries. The following **assumptions** are made:

1. The driving stress varies linearly with depth.
2. The transverse shear stress, referring to shearing between flow lines is negligible.
3. Surface - and bed-slopes are small, and $\tau_{b\parallel} \cos(2\beta) >> \sigma'_{x\parallel} \sin(2\beta)$. ($\tau_{b\parallel}$ is the bed-parallel basal shear stress, $\sigma'_{x\parallel}$ is the bed-parallel basal stress deviator, β is the bed slope).
4. The distance between flow lines does not vary with depth.

Assumption 1 holds only approximately in the ice stream.

Assumption 4 is equivalent to stating that the transverse strain which develops while the ice flows a certain distance down stream, is independent of depth. This condition is not fulfilled where the ice stream flows through a subsurface-bedrock channel which becomes deeper and

narrower with distance downstream. The convergent subsurface channel imposes a strong transverse compression and a vertical extension on the ice flowing through it. Thus, it seems likely that the transverse and the vertical strain increase with depth, contrary to assumption 4 (Iken and others, in press). This effect should be reflected in a difference in shape of the modelled temperature-depth profile (which complies with assumption 4) as compared to the measured profile. In the model, the heat diffusion equation is solved for subsequent ice columns along a flow line with a finite difference scheme in a body-fitted coordinate system. Horizontal grid size is 1 km; vertical grid size decreases towards the bed or the temperate layer; the smallest vertical grid size is 2 metres. Velocity and temperature distributions are calculated iteratively. The model and the results of modeling are discussed in detail by Funk and others (submitted to the Journal of Glaciology).

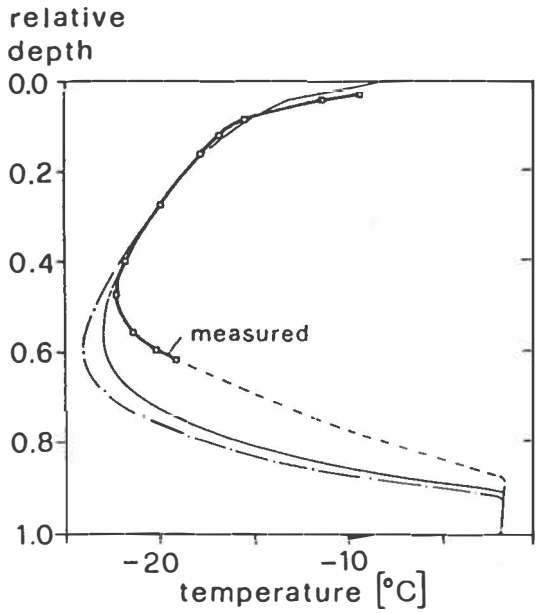

Fig. 1:
Measured and modelled englacial temperatures at the centerline of Jakobshavns Isbrae, 50 km inland from the calving front. The ice depth is there 2500 m.

Heavy line:	measured temperatures.
Thin, full line:	modelled, assuming a steady state at the present climatic conditions.
Thin line, dash-dotted:	time-dependent model (see text).

Fig. 1 shows the temperature profile, measured at the centerline (heavy line). Also shown are two modelled profiles. The full line corresponds to a steady state at the present conditions. The dash-dotted line depicts the following scenario: Starting from a steady state with 10 degree K colder surface temperatures than at present, an increase of surface temperatures by 8^{0}K during 2000 years and a subsequent increase by 2^{0}K during 8000 years until present, is assumed. (The acutal warming following the ice age occured sooner and much more rapidly). The models reproduce the upper part of the measured temperature profile quite well. The minimum temperature calculated by the steady-state model (-22.9°C) is 0.8^{0}K colder than the measured minimum temperature; this is within the tolerances due to inaccurate model input. The minimum temperature in the time-dependent model, which corresponds to a rather extreme scenario, appears to be too cold. The depths of the calculated temperature minima are, however much larger than that of the measured profile. We attribute this difference to the 3-D ice deformation occurring in the convergent subsurface-channel and not accounted for by the models. The extra vertical strain which develops in the subsurface channel can be estimated from the difference in relative depth of the minima of modelled and measured temperature profiles. Based on this estimate we conclude that the temperate basal layer is some 30% thicker in the actual ice stream than shown by the steady state model.

References

Clarke, T. and Echelmeyer, K. (1989). [Abstract] High resolution seismic traverse across Jakobshavns Isbrae, Greenland. *EOS*, 70(43):1080–1080.

Echelmeyer, K., Clarke, T., and Harrison, W. (1991). Surficial glaciology of Jakobshavns Isbrae, West Greenland: Part I. Surface morphology. *Journal of Glaciology*, 37(127):368–382.

Echelmeyer, K. and Harrison, W. D. (1990). Jakobshavns Isbrae, West Greenland: Seasonal variations in velocity - or a lack thereof. *Journal of Glaciology*, 36(122):82–88.

Echelmeyer, K., Harrisson, W., Clarke, T., and Benson, C. (1992). Surficial glaciology of Jakobshavns Isbrae, West Greenland: Part II. Ablation, accumulation and temperature. *Journal of Glaciology*, 38(128):169–181.

Funk, M., Echelmeyer, K., and Iken, A. (submitted). Mechanisms of fast flow in Jakobshavns Isbrae, Greenland; Part II: Modeling of englacial temperatures and comparison with measured ones. *Submitted to Journal of Glaciology.*

Iken, A., Echelmeyer, K., and Harrison, W. (1988). A lightweight hot water drill for large depths: experiences with drilling on Jakobshavns Glacier, Greenland. In *Proc. International Symposium on Ice Core Drilling*, Grenoble, France. October 1988.

Iken, A., Echelmeyer, K., Harrison, W., and Funk, M. (1993). Mechanisms of fast flow in Jakobshavns Isbrae, Greenland, Part I: Measurements of temperature and water level in deep boreholes. *Journal of Glaciology.* In press.

Smith, G. D. and Morland, L. W. (1981). Viscous relations for the steady creep of polycristalline ice. *Cold Regions Science and Technology*, 5:141–150.

Estimation of thermal zones on the Greenland ice sheet

Hisashi Ozawa
Geographisches Institut, Eidgenössische Technische Hochschule
CH-8057 Zürich, Switzerland

Gorow Wakahama
Institute of Low Temperature Science, Hokkaido University
Sapporo 060, Japan

Near surface thermal condition of the Greenland ice sheet was examined using a quantitative method of zonation that was recently developed by the authors. A preliminary analysis suggests that *temperate infiltration zone*, where 10-m depth temperature is at the melting point, exists along south-eastern part of the ice sheet.

Method

Figure 1 shows glacier zones defined by temperature (temperate or cold) and structure (snow or ice) at the isothermal depth (10-m depth). We investigated heat conduction process, meltwater percolation process and formation process of superimposed ice within the near surface layers of glaciers, and revealed that each zone boundary can be given by the balance between three amounts of water (percolation water Q_p, internal accumulation Q_f, and surface balance b_s) as follows (Ozawa, 1991):

(1) temperate ablation zone: $Q_f \sim 0$
(2) cold ablation zone: $Q_f > 0$ and $b_s + Q_f < 0$
(3) superimposed ice zone: $Q_f > 0$ and $-Q_f < b_s < \alpha Q_f$
(4) temperate infiltration zone: $Q_f < Q_p$ and $b_s > \alpha Q_f$
(5) cold infiltration zone: $Q_f = Q_p > 0$ and $b_s > \alpha Q_p$
(6) dry snow zone: $Q_p \sim 0$

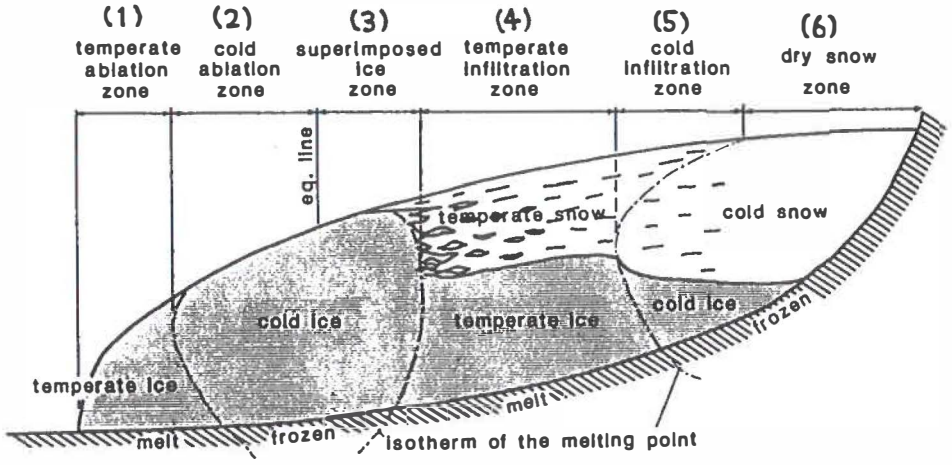

Fig.1. Six different thermal zones of an ideal glacier.

Here α is an index of ice formation ($\rho_s/(\rho_i-\rho_s)$) about 1 depending on snow density ρ_s. It is reasonably understood that the two cold ice zones (2 and 3) will disappear when winter is mild and $Q_f \sim 0$. This is the so-called *temperate type* glacier. In dry regions, such that annual precipitation ($P=Q_p+b_s$) is less than $(1+\alpha)Q_f$, the temperate infiltration zone (4) will disappear. This is the *cold type* (sub-polar) glacier. It should be noted that, in cold ($Q_f>0$) and humid ($P>(1+\alpha)Q_f$) climate regions, glacier should be an *inversion type* having the temperate infiltration zone and the cold ice zones. The cold ice zones will act as a 'dam' against the movement of the glacier.

Zonation of the Greenland ice sheet

Figure 2 shows zonal distribution on the ice sheet predicted by the above mentioned method. Percolation water (Q_p) is calculated by an empirical equation given by Reeh (1989). Surface balance (b_s) is $P-Q_p$; P is compiled by Ohmura and Reeh (1991). Internal accumulation (Q_f) is calculated by air temperature and precipitation during winter (Ozawa, 1991). The preliminary result suggests that the ice sheet mainly consists of cold zones (2, 3, 5 and 6). However, the temperate infiltration zone (4) is suggested to exist in high precipitation regions along the south-eastern margin of the ice sheet. Although few attention has been paid to this region, we think it is important for the ice sheet dynamics since several outlet glaciers flowing from this regions show surge-like behavior (Weidick, 1988).

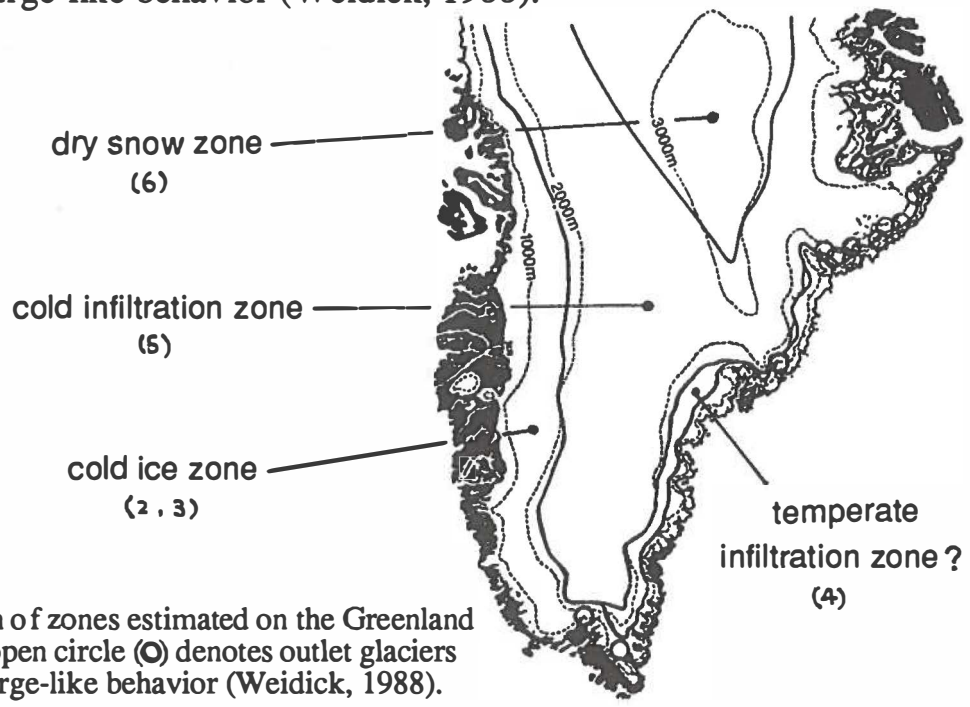

Fig.2. Dirstribution of zones estimated on the Greenland ice sheet. The open circle (O) denotes outlet glaciers showing surge-like behavior (Weidick, 1988).

[References]
Ohmura, A. & Reeh, N. *J. Glaciol.* 37 (125) 140-148 (1991)
Ozawa, H. Ph.D. thesis, Hokkaido Univ., Sapporo (1991)
Reeh, N. *Polarforschung* 59 (3) 113-128 (1989)
Weidick, A. *Rapp. Grønlands geol. Unders.* 140, 106-110 (1988)

ETH Greenland Ice Sheet Climate Programme: An Overview

Atsumu Ohmura
Geographisches Institut, ETH Zürich
Zürich, Switzerland

The objective of the present programme is to understand the relationship between the climate and the mass balance of the Greenland Ice Sheet under the present climate.

To achieve this objective, a programme was organized in the following four branches: 1) Investigation of the surface energy balance at the height of the climatic equilibrium line, including the studies of the structure of the atmospheric boundary layer which somehow keeps the supply of sensible heat from the atmosphere to the ice sheet surface much smaller than present-day theories imply; 2) Estimation of the large scale distributions of the important energy balance parameters, in particular, the surface albedo and the temperature, as well as the distribution of the melt-zone; 3) Investigation of the moisture source for the ice sheet; and 4) the Investigation on the relationship between the shift of the equilibrium line and the change in annual mass balance.

The micrometeorological experiments on the climatic equilibrium line were carried out at the ETH Camp (69°34'37"N, 49°16'09"W, 1155 m a.m.s.l.) during the 1990 and 1991 summer seasons for the period from the late dry snow to the entire melt season. The results of the energy balance for the surface and the interior of the snow cover will soon be published as a doctoral thesis of T. Konzelmann. One of the most important results in this branch of the programme is the discovery that the amount of sensible heat flux from the atmosphere to the surface is as envisaged indeed very small, despite large vertical temperature gradient. The existence of the zero wind-shear zone happens within the layer of the surface inversion, which makes the layer very stable. The layer is so stable that substantial part of the momentum exchange takes place in form of the internal wave rather than turbulence. The material for this conclusion came from the 30-m tower with the profile and the turbulence measurements and the radio-, rawinsonde observations.

At the moment the surface albedo and temperature are estimated for the cloud-free scenes with the NOAA data. The in situ measurements of the albedo and surface temperature at the ETH Camp are used to activate the algorithm. The differences in albedo and the surface temperature between the cloud-free and overcast sky conditions are also investigated both from the

observations and in theory. This information is necessary to estimate the climatic values only with the information from the cloud-free scenes. The results will become available in two years in a form of the doctoral thesis by M. Haefliger.

The moisture transport and the divergence over Greenland is studied by P. Calanca as the main part of his doctoral dissertation, by using the analyses made at the ECMWF, Reading. Presently it is confirmed that the agreement between the negative divergence and the total precipitation for Greenland at the monthly level is very good and the further analyses can be made for searching the moisture source.

The annual accumulation which M. Anklin determined at nine locations of the EGIG line (T5 to T43) gave the first possibility, when used together with the ten years long mass balance measurement for the lower areas by the GGU, to calculate the total mass balance of the sector of the ice sheet concerned. It is also possible to determeine the sensitivity of the mass balance against the shift of the equilibrium line. The results of the mass balance for the period 1982/83 to 1988/89 are presented in Table 1. The relationship between the mean specific mass balance and the ELA is given in Figure 1. The mass balance sensitivity of the west slope of the Greenland Ice Sheet revealed in the present analysis is 14 cm WE/100 m which is one of the least sensitive relations found so far. This result confirms that the variability of the accumulation, that is precipitation carries an importance for determining the mass balance of the ice sheet.

The observed elements during this expedition are presented in Figures 2 and 3.

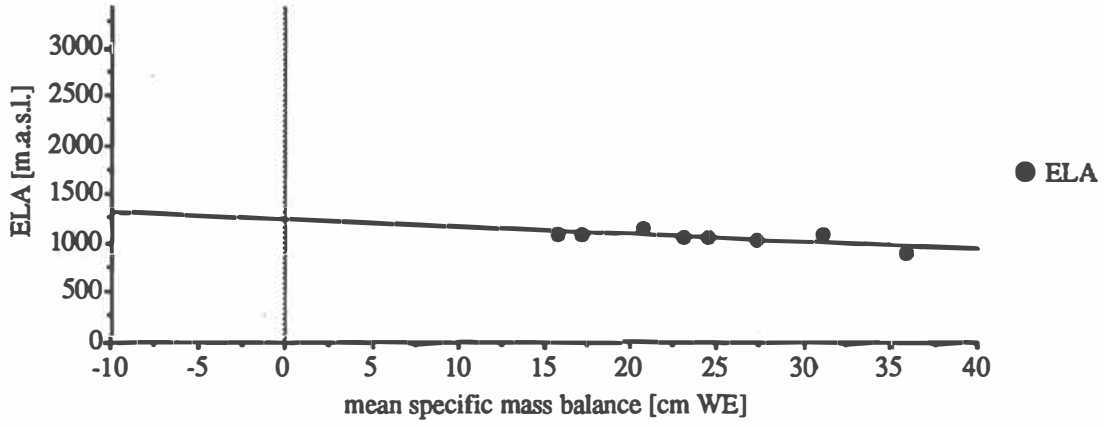

Fig. 1: Relationship between the annual mean specific mass balance and the equilibrium line altitude for the mid-west slope of the Greenland Ice Sheet

Mass Balance Observations along the EGIG Line, 1982-1989

Altitude range m.a.s.l.	Stake		82/83	83/84	84/85	85/86	86/87	87/88	88/89	Mean	Rel. Area in %
3000-3200	T43	3171	28.1	30.0	23.9	23.0	27.3	23.9	22.1	25.5	25.8
	T41	3149									
2800-3000	T31	2961	40.3	43.2	34.8	38.9	43.5	38.2	29.5	38.3	17.3
	T27	2867									
2600-2800	T21	2692	45.1	51.9	38.8	46.3	54.6	44.2	31.5	44.6	12.7
2400-2600	T17	2530	47.2	48.7	43.4	48.6	57.3	42.0	35.6	46.1	8.7
2200-2400	T13	2373	47.1	48.2	39.1	48.1	61.4	45.5	37.4	46.7	9.2
2000-2200	T9	2107	46.8	44.8	34.6	56.5	50.9	35.8	29.6	42.7	6.4
1800-2000	T5	1907	47.6	37.1	55.8	29.9	28.5	38.4	38.6	39.4	5.1
1600-1800											3.4
1400-1600											2.5
1200-1400											2.5
1000-1200	12	1070	(45)	(-5)	(-50)	-5.7	-81.4	-93.2	-72.9	-35.5	2.3
	11.5	1020									
800-1000	11	965	-15.6	(-64)	(-150)	-94.2	-176.6	-172.1	-124.8	-113.9	1.8
	10	890									
	9	850									
600-800	8	780	(-65)	(-123)	(-169)	-129.9	-216.5	(-211)	(-138)	-150.3	1.0
	8	720									
	7.5	720									
	7	615									
400-600	6	560	(-107)	(-234)	(-268)	-222.8	(-290)	-284.0	-207.1	-230.4	0.8
	5	415									
200-400	many		-247	-317	-343	-304	(-360)	-358	-280	-315.6	0.4
Mean specific mass balance			36.0	31.1	20.8	27.2	23.1	17.1	15.7	24.5	0.3 for h<200
ELA m.a.s.l.			925	1110	1150	1050	1090	1100	1100	1075	

Tab 1: Mass balance observations along the EGIG line, 1982-1989 (Source: H. Thomsen, personal communication. Anklin, M., 1991)

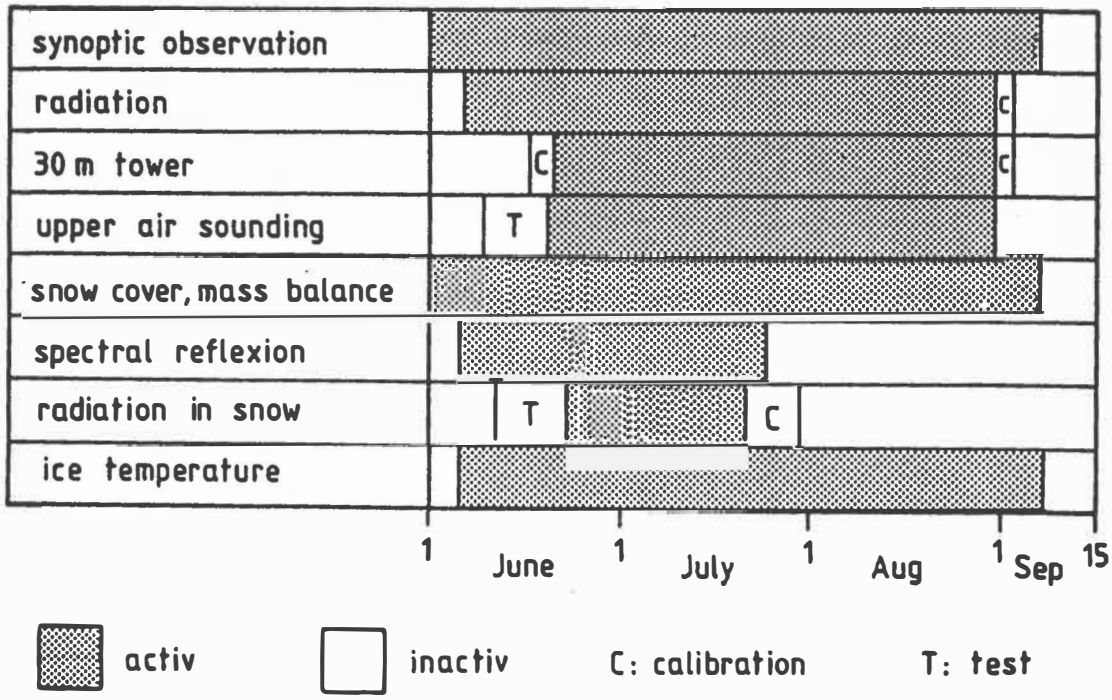

Fig. 2: Graphic timetable of the various measurements for 1990. Sonic measurements were performed at irregular intervals between July 4 and August 28.

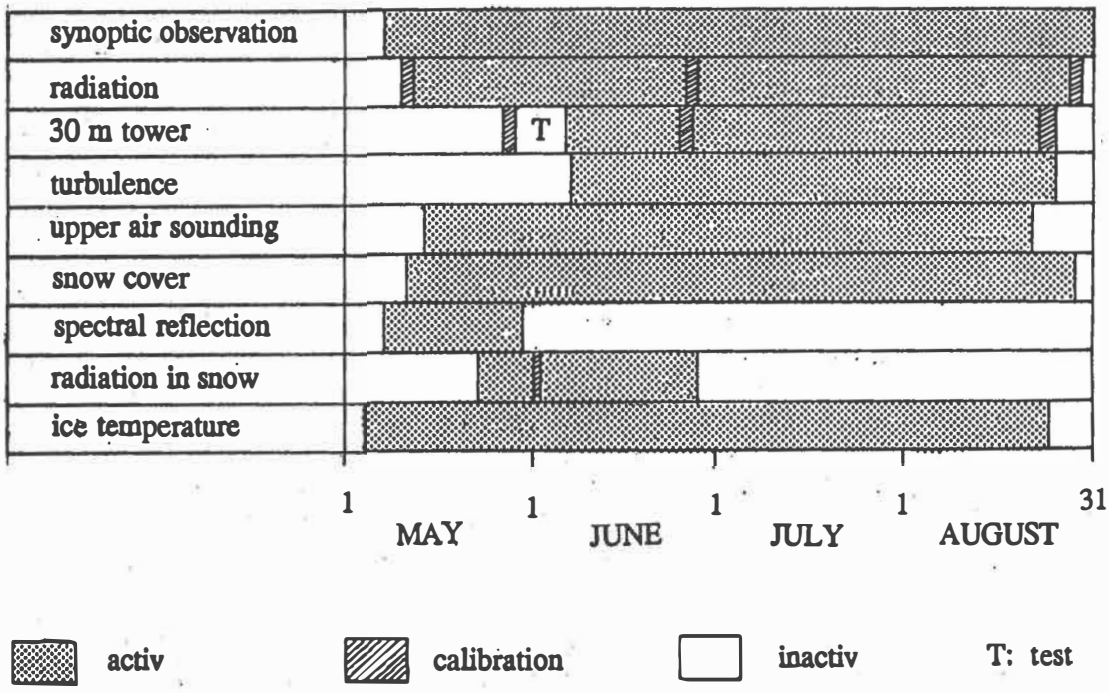

Fig. 3: Graphic timetable of the various measurements for 1991. Sonic measurements were performed at irregular intervals between June 7 and August 25.

Parameterization of short- and longwave incoming radiation for the Greenland Ice Sheet

Wouter Greuell, Roderik van de Wal en Richard Bintanja
Institute for Marine and Atmospheric Research, Utrecht University
Utrecht, The Netherlands

Thomas Konzelmann and Ayako Abe-Ouchi
Geographisches Institut, ETH
Zurich, Switzerland

Edwin Henneken
Faculty of Earth Sciences, Free University of Amsterdam
Amsterdam, The Netherlands

Parameterizations of short- and longwave incoming radiation are needed in numerical models of the surface energy balance for the Greenland Ice Sheet. These models are used for the calculation of ablation and the sensitivity of ablation to climatic change. They are generally forced by meteorological variables measured at simple climatological stations, for instance screen-level temperature (T_a), screen-level vapour pressure (e_a), 10 m-wind speed, cloud amount (n) and precipitation. The fluxes are then computed by means of parameterizations, containing the forcing variables, topographic variables (like elevation) and internally generated variables (like albedo) as independent variables.

Two parameterizations (daily mean values) for the incoming shortwave radiation are based on measurements from Ambach's experiments in Camp IV (1004 m) and Carrefour (1850 m), from the GIMEX expeditions (340 to 1520 m), from the ETH Camp (1155 m) and from Summit (3230 m). In the first parameterization only extinction by clouds is considered. Therefore, cloud amount and elevation are the only independent variables. In the second parameterization absorption and scattering due to air molecules, ozone and water vapour, and multiple scattering are computed explicitly. Hence, screen-level temperature, screen-level vapour pressure and albedo are also used as independent variables.

The uncertainty of calculations with these parameterizations is 3% for clear skies and 5-6% in the presence of clouds. Calculations with these parameterizations were compared to calculations with parameterizat-ions developed with data from the Alps. Differences appeared to be considerable.

The parameterizations for longwave incoming radiation are exclusively based on the measurements from the ETH Camp. These measurements were first compared to calculations made with LOWTRAN7, a numerical radiative band model using upper air soundings as input. Measurements and calculations appeared to be compatible, if the ranges of uncertainty are taken into account.

Two equations for longwave incoming radiation (L↓) were derived, one for instantaneous values and one for daily means. The latter reads:

$$L\downarrow = [\, 0.23 + 0.483\,(e_a/T_a)^{1/8}\,]\,\sigma\,T_a^4\,(\,1 + 0.300\,n^3\,)$$

The term between square brackets is termed the clear-sky emittance. Its form is a modified version of an expression introduced by Brutsaert. LOWTRAN7 calculations, using test profiles as input, indicated that this is the most appropriate form. The values of two of the constants are also based on these calculations. Thereafter, the value of the remaining constant (0.483) was determined from the data. The term ($1 + 0.300n^3$) describes the increase of the radiation due to clouds.

The residual standard deviation is approximately 8 % on average for all kinds of cloud conditions, but is only 3 % for clear skies. The expression was tested by means of Ambach's measurements. The average difference between these measurements and calculations with the present parameterizations is only +3 W/m^2.

The parameterizations presented in the paper are based on summer measurements in West Greenland only. The uncertainties in calculations with these expressions will increase when they are applied during other seasons and in other parts of the ice sheet. High-quality measurements in other parts of the ice sheet and other seasons could provide new data for confirmation or improvement of the proposed parameterizations.

Publications:

Konzelmann, T., R. S. W. van de Wal, W. Greuell, R. Bintanja, E. A. C. Henneken and A. Abe-Ouchi: Parameterization of short-and longwave radiation for the Greenland Ice Sheet. Submitted to Global and Planetary Change.

Greuell, W. and T. Konzelmann: Numerical modelling of the energy balance and the englacial temperature of the Greenland Ice Sheet. Calculations for the ETH-Camp location (West Greenland, 1155 m a.s.l.). Submitted to Global and Planetary Change.

Van de Wal, R. S. W.: An energy balance model for the Greenland Ice Sheet. Submitted to Global and Planetary Change.

Turbulence measurements in the stable atmospheric boundary layer at the ETH camp, Greenland ice sheet

(69°34'25,3"N, 49°18'44,1"W, 1155 m a.s.l)

Jann Forrer
Department of Geography, Swiss Federal Institute of Technology
CH-8057 Zürich, Switzerland

Three 3-D ultrasonic-anemometers operated from June 1991 to August 1991 during selected periods and at different heights. The sensors were mounted on the 30 m tower, usually at 2, 10 and 30 m. The uppermost level could be moved to other levels for experiments. The three components of the wind vector (u, v, w) and the sound velocity were recorded with a frequency of 21 s^{-1}. A total of 31 experiments covering 266 hours of measurements were performed.

The main objective of this study was the better understanding of the turbulent transport mechanism in a stably stratified atmospheric boundary layer (SBL) over the Greenland ice sheet. The SBL is a difficult subject, because it occurs in various manifestation, each dominated by different physical processes, for example topographical slope effects and internal gravity waves (Nieuwstadt, 1984). Therefore the investigation is limited to an intensive measuring period, which lasts from the 25.7.91 00.00 UTC to the 26.7.91 04.00 UTC. During this time two interesting runs (29, 31), where different processes occur, were sampled with the ultrasonic-anemometers. Additionally eight radiosondes were launched to observe the atmospheric profiles to higher altitudes.

Table 1: Some important parameters for runs 29 and 31: (Q: sensible heat flux; u*: friction velocity; L: Obukhov length; Rf: flux Richardson number; U: mean wind speed; z: height above ground; all values on 2 m, expect Rf on 30 m).

Run	Q (W/m2)	u* (m/s)	L (m)	Rf	U (m/s)	z/L
29	-70 (± 5)	0.45 (±0.04)	200 (±100)	0.09 (±0.01)	11 (±0.3)	0.013
31	-40 (±8)	0.27 (±0.04)	45 (± 10)	0.17 (±0.06)	6 (±0.4)	0.043

RUN 29

The sounding profiles show a katabatic wind regime during run 29 with a distinct maximum of wind speed at about 100-200 m above ground and a distinct inversion layer (Fig.1). The stability during this run was relatively low (low Rf in Table 1). The vertical profile of the momentum flux is more or less constant with height up to 30 m but the sensible heat flux shows a maximum at 10m.

RUN 31

An inversion layer with high Rf (Table 1), but no wind maximum was observed during this run (Fig.1). Wave like fluctuations appear in the time series of the three wind speed components and the temperature. A spectral analysis yields a fairly consistent period of 280 s. An estimate of the wavelength can be made by assuming that the wave drifts with the mean wind. The 280 s period then corresponds to a wavelength of about 2000 m. This peak appears at all heights in the spectrum for the u-component. For the vertical motion the peak disappears 2 m above ground (Fig.2). The vertical component of the wind vector seems to be influenced more strongly by the surface.

During this run the momentum flux and the sensible heat flux decrease with height. The momentum flux decrease more slowly than the sensible heat flux.

BOTH RUNS

In the turbulent part of the spectra the size of the eddies that contain the maximum of the energy were determined. The eddies in the more stable case (run 31) are smaller. Strong stability dampens vertical motions and therefore compresses the eddies.

The cospectra show a contribution of the wave to the vertical transport of momentum but no contribution to the turbulent transport of sensible heat. The phase angle gives the same information. Vertical motion (w) and temperature (T) are about 90 degrees out of phase. This is an indication for a gravity wave (Stull, 1988). For the u and w component of the wind vector the phase angle is significantly different from 90 degrees (Fig.3).

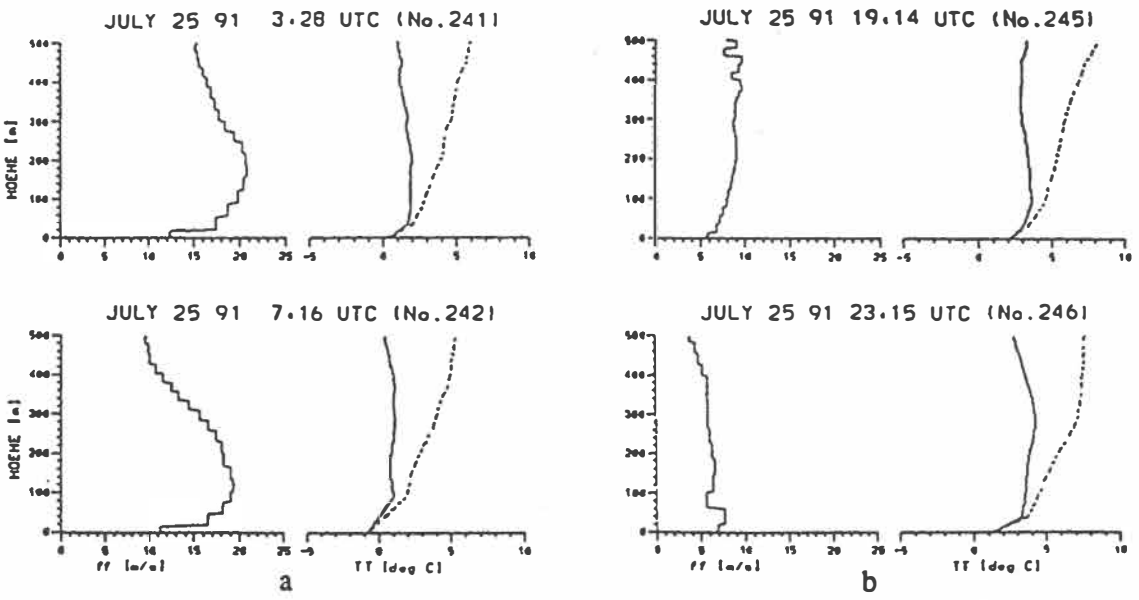

Fig 1: Two radiosonde profiles of wind speed, temperature and potential temperature (dashed line), during run 29 (a) and run 31 (b)

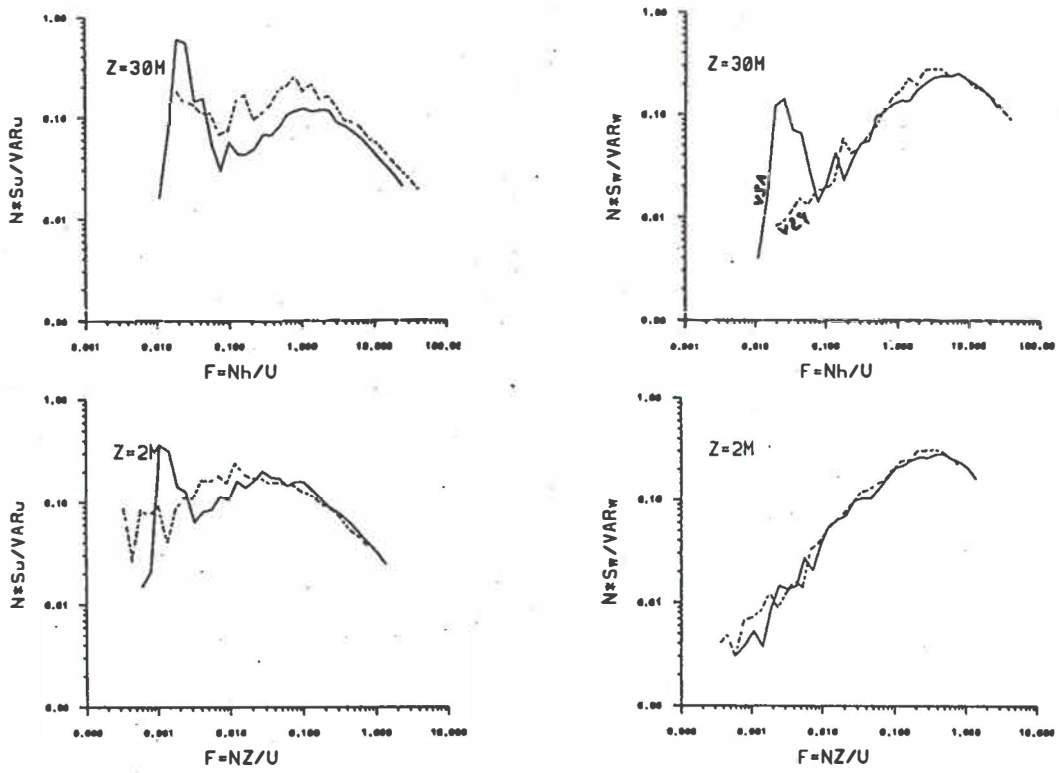

Fig.2: Spectra of the u- and w-component for run 29 (dashed line) and run 31 (solid line) on 2 and 30 m.

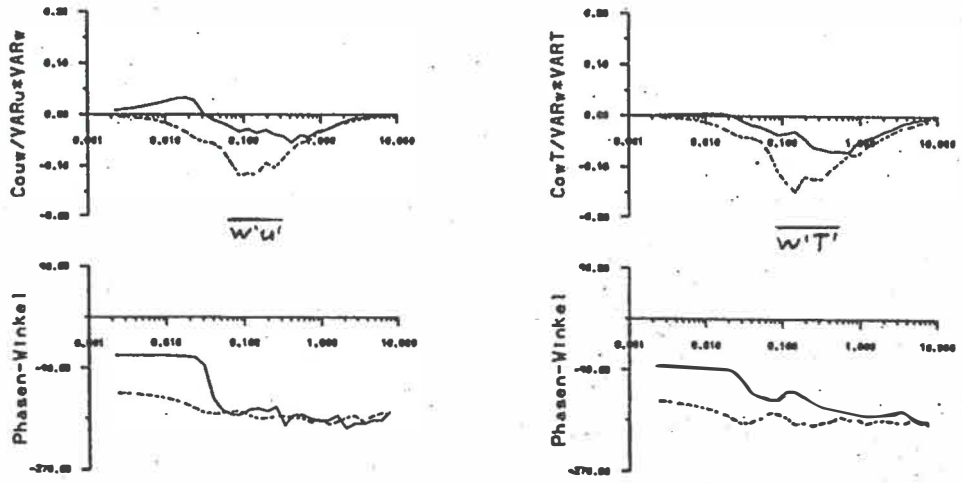

Fig.3: Cospectra and phase (on 30 m) for Reynolds stress and turbulent flux of sensible heat for run 29 (dashed line) and run 31 (solid line)

References

Nieuwstadt, F.T.M., 1984a: The turbulent structure of the stable nocturnal boundary layer. *J.Atmos.Sci.* , 2202-2216.

Stull, R.B., 1988: *An introduction to Boundary Layer Meteorology*, Kluwer Academic Publishers, Dordrecht, 666pp.

Energy Balance and Melt at the VU–GIMEX Camp

Edwin A.C. Henneken
Faculty of Earth Sciences, Department of Meteorology
Free University Amsterdam

We present the energy balance (and associated melt) for the period of July 2nd till July 25th 1991 at the site of the VU–GIMEX camp (67°02′ N, 49°17′ W, at an altitude of about 1500 meters a.s.l.). The energy balance, Q_t, is defined to be (see Henneken *et al.*, 1992),

$$Q_t \equiv R_n + H + LE + Q_b \tag{1}$$

and consists of the net radiation, R_n, the sensible heat flux, H, the latent heat flux, LE and the sub–surface heat loss, Q_b. We assume a positive energy balance, in which the fluxes contributing to melt are counted as positive, to be used fully for the process of melting. The amount of melt on a given day (in meters water equivalent), $\mathcal{W}$, then readily follows from the integration of the melting rate with respect to time over an entire day, i.e. equation (1) divided by the latent heat for melting, L_m, and the density of water, ρ_w. This amount of melt is approximated by

$$\mathcal{W} = 8.64 \cdot 10^4 \frac{Q_{av}}{\rho_w L_m} \tag{2}$$

where Q_{av} (unit W m^{-2}) denotes the energy balance, Q_t, averaged over the day, i.e. the amount of energy (per square meter) avaible for melt (per unit of time); a Q_{av} of 39 W m^{-2} results in a melt of 1 cm w.e.

The net radiation has been determined using a net radiometer, the turbulent fluxes were estimated with the help of a eddy correlation system and the sub–surface heat loss was established employing a number of thermistors.

The evolution of each energy balance component in the forementioned period has been depicted in figure 1; it also shows the energy balance, the sum of the components. From the energy balance, as defined by equation (1), and equation (2) we have estimated the amount of melt (in cm w.e.) for each day. The ablation, i.e. cumulative melt, which follows from this calculation is to be found in figure 2. This figure also lists the amount of ablation (in cm w.e.) as estimated from stake–observations; to be able to convert the amounts of melt (in cm) as determined by the stake–measurements we adopted a density

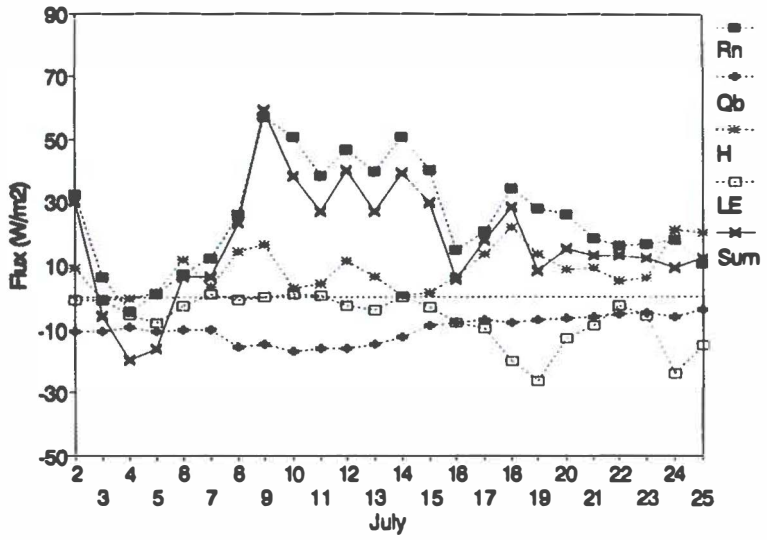

Figure 1. *The evolution of the energy balance and its constituting components in the period of July 2nd till July 25th at the VU-GIMEX camp.*

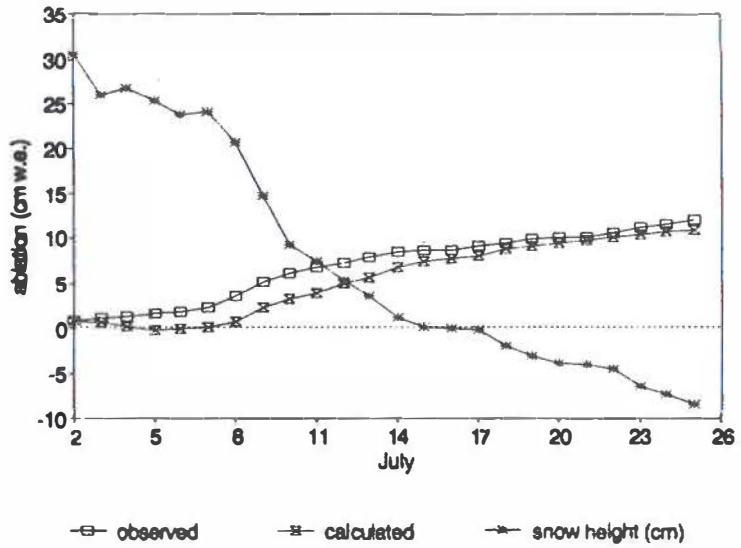

Figure 2. *Ablation measured at the VU-GIMEX camp as calculated using an energy balance and measured with the help of stake-measurements. Also the evolution of the snow height is shown.*

ρ_s (which is the effective density for the snow/ice volume at the position of the stake) which increases linearly in time. The interpretation of figure 2 is far from trivial; e.g. a change in snow height may well have originated from densification of the snow pack.

Figure 2 shows that the observational period can be divided into two periods: the first characterized by the presence of a snow cover, which has disappeared in the second period. The transition takes places at July 14^{th}. In this light it is observed that, on average, the second period is characterized by more evaporation. This means that in the second period less energy becomes available for melt. It is also observed that most of the time H and LE have opposite signs.

It follows from figure 1 that the net radiation, R_n, is indeed an important component, but quite often one or more of the remaining components have a non–negligible contribution.

References

Henneken, E.A.C., Bink, N.J., Vugts, H.F., Cannemeijer, F. and Meesters A.G.C.A. (1992). A Case Study of the Daily Energy Balance at the VU–GIMEX camp. Submitted to Global and Planetary Change.

Henneken, E.A.C. (1992). Boundary Layer Measurements over the Greenland Ice Sheet. Circumpolar Journal 3-4: 24–33.

Katabatic flow and surface energy balance near the boundary line between glacier and tundra during GIMEX-91

Peter G. Duynkerke and Michiel R. van den Broeke

Institute for Marine and Atmospheric Research Utrecht, The Netherlands

The Greenland Ice Margin EXperiment (GIMEX) was carried out in the Søndre Strømfjord area 67° N 50° W, in south-western Greenland during the summers of 1990 and 1991. A major goal was to study the relation between the meteorological conditions and the mass balance of the Greenland ice sheet. The unique set up during GIMEX was that masts were erected from a point 90 km up the ice cap, right through the melting zone, down to a point 5.8 km inside the tundra area. The x-axis is from west to east and the y-axis from south to north, the origin of the coordinate system being the base camp. The ice front is then at about x = 400 m. The locations of the different sites are indicated in Table 1.

site	x [km]	height [m]	|v|	T	RH
SS	-20	50	10	2	2
3	0	149			
base camp	0	149	4.9	2, 4.9	2, 4.9
4	2.6	341	0.5, 6	0.5, 6	0.5, 6
5	7.3	519	2, 6	2, 6	
6	38.8	1028	2, 6	2, 6	
9	90.	1519	4, 8	2, 8	2, 8

Table 1 The location of Søndre Strømfjord (SS) and the sites at which the masts were erected. The heights at the masts, used in this paper, at which the wind speed (|v|), temperature (T) and relative humidity (RH) are measured.

The set up provided us with the opportunity to study the energy balance along a transect perpendicular to the ice edge. The large difference in the radiation and the thermal characteristics of the ice sheet and the tundra has some important influences on the dynamics of the katabatic flow, especially during summer. In Figure 1 the x-component (u) of the wind is shown as a function of time at sites 4, 5, 6, base camp and 9. The wind speed far above the ice cap (site 6 and 9) shows little diurnal variation, the highest wind speeds being recorded during the night and early morning. As the air flows down the ice cap the wind speed increases slightly, probably due to the increase in the slope of the ice cap. During day-time there is a clear increase in the u-velocity, due to the enhanced pressure gradient as a result of the heating of the tundra. At site 4 retardation of the flow is observed during night-time due to the cooling of the boundary layer over the tundra. It is clear from the discussion above that the flow near the boundary line between tundra and ice cap is influenced by the difference in the energy balance of the tundra and the ice surface.

We have calculated the friction velocity (u_*), sensible heat flux (H) and latent heat flux (LE) using the profile method. This is applied at sites 4, 5, 6 and 9 using the wind speed,

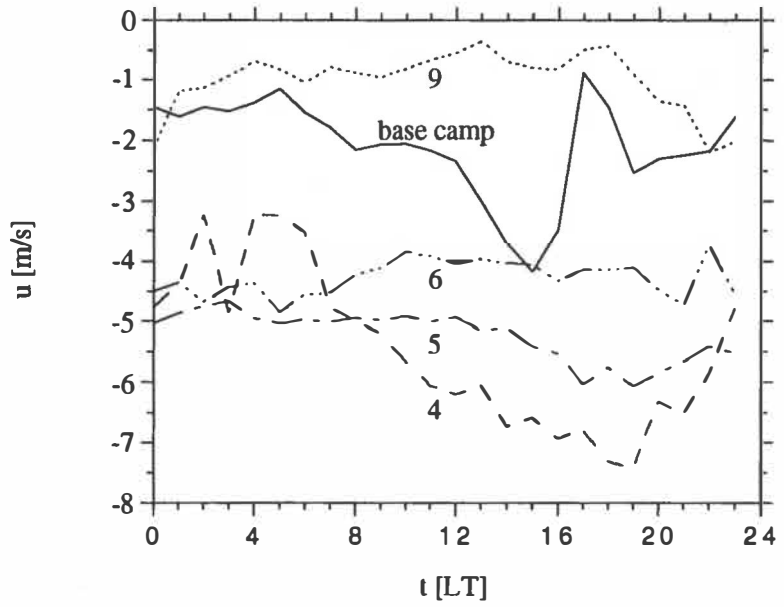

Figure 1 The component of the wind speed perpendicular to the ice edge at the various sites on 22 July 1991.

temperature and relative humidity measurements at the heights summarised in Table 1.The average fluxes over the entire period are given in Table 2. The net radiation at site 4 is 120 W/m^2, which means that about 20 % of the energy for melting is provided by the sensible heat flux. At site 9 all three terms, net radiation, sensible and latent heat flux, are important in the energy balance. The calculated sensible heat flux indicates that there is a transport of heat from the air in the katabatic layer towards the ice, whereas the calculated latent heat flux indicates that moisture is added to the katabatic layer as a result of evaporation. This is in agreement with the observed decrease in potential temperature and increase in specific humidity as the air flows down the ice cap.

site	u_* [m/s]	z_0 [cm]	H [W/m^2]	LE [W/m^2]	Q [W/m^2]
4	0.21	0.08	-34.1	11.0	120
5	0.26	0.4	-13.7		
6	0.45	4	-44.1		
9	0.30	0.8	-30.2	28.7	22.5

Table 2 The average friction velocity (u_*), sensible heat flux (H), latent heat flux (LE) and net radiation (Q) for the period of 10 June to 31 July at site 4, 10 June to 30 July at site 5, 10 June to 24 July at site 6, and for the period of 27 June to 28 July 1991 at site 9.

REFERENCES

Duynkerke, P.G. and M.R. van den Broeke, 1993. Surface energy balance and atmospheric boundary layer structure near the boundary line between glacier and tundra during GIMEX-91, submitted for publication to *Global and Planetary Change*.

Van den Broeke, M.R., P.G. Duynkerke and J. Oerlemans, 1993. The observed katabatic flow at the edge of the Greenland ice sheet during GIMEX-91,*Global and Planetary Change*.

SIMULATION OF THE KATABATIC WIND AND ITS INFLUENCE ON THE ENERGY BALANCE

Antoon Meesters, Institute of Earth Sciences, Free University, Amsterdam, Netherlands.

1) Introduction.

The katabatic wind plays an important role in the climate of the ice sheet of Greenland. This wind is almost permanently present. It is caused by the cooling of air by contact with the surface, and deflected by the Coriolis force. In the ablation zone at the margin of the ice sheet, the wind can be accelerated in consequence of the ice-tundra temperature difference at daytime.

The katabatic wind is one of the factors determining the ablation and mass balance of the ice sheet. It transports heat and hence determines the air temperatures. Further, the wind speed influences the exchange of heat between air and ice. At the other hand, the wind is itself driven by the temperature difference between air and ice, and also by horizontal temperature differences.

Because of this complicated interrelation, it is impossible to quantify the change of the sensible heat contribution to the ice energy balance in response to a change in the external conditions, unless a dynamic atmosphere model is used. Such a model should describe the energy fluxes at the surface, the resulting wind system, and the feed-back to the fluxes.

The present model has been set up specifically for this purpose. Its primary observational background is constituted by the data which have been gathered by the GIMEX expeditions in 1990 and 1991.

2) Set-up of the model.

A 2-dimensional atmospheric model has been set up for the western margin of the Greenland ice sheet. The model contains for each surface point a multilevel box for the ice and for the tundra, whereas a constant temperature is prescribed for the sea surface. The atmospheric part of the model has been set up along the usual lines for mesoscale models. Infrared radiation is calculated from temperature and moisture profiles. The influence of infrared radiation divergence on the air temperature profiles is also computed. The turbulent exchange is dependent on the Richardson number.

3) Model results.

Figures 1 and 2 show the wind and temperature at reference height, as calculated by a preliminary model version, for a certain day with clear sky (17 july 1991). The synoptic wind at the 500 hPa level is SE, so that the katabatic wind is stronger than usual. The diurnal variation of the wind field is small for this day. The spatial variation is large, which is a consequence of the strong heating above the tundra, among others.

Concerning the temperature field (figure 2), a strong daytime heating is seen above the higher parts of the ice cap (where the average temperature is lowest) and above the tundra. In the ablation zone, there is little diurnal variation since the surface is at the melting point most of the time.

Most results are in satisfactory agreement with GIMEX observations for this day, and with climatological data. The most notable exception is the exaggerated afternoon temperature above the tundra, which is probably caused by a wrong initialization of mid-tropospheric temperatures above the ice sheet. Indeed, model results are rather sensitive with respect to this initialization.

4) Consequences of the katabatic wind for the energy balance of the ice.

As seen in figure 2, the air in general becomes warmer as it flows down the ice sheet. This is due to compression. Hence, an air temperature can be maintained which is usually higher than the surface temperature, so that the sensible heat flux can be directed from the air into the ice during both "day" and "night". This, together with the relatively low net radiation for the ice sheet (mainly due to the high albedo) causes the sensible heat flux to be an important term in the energy budget of the ice. However, matters are complicated by the existence of a latent heat flux, which is comparable in magnitude with the sensible heat flux but which has the opposite direction (ice to air).

reference: Meesters, Henneken, Bink, Vugts, Cannemeijer (1993), Simulation of the atmospheric circulation near the Greenland ice sheet margin. Submitted to 'Global and Planetary Change'.

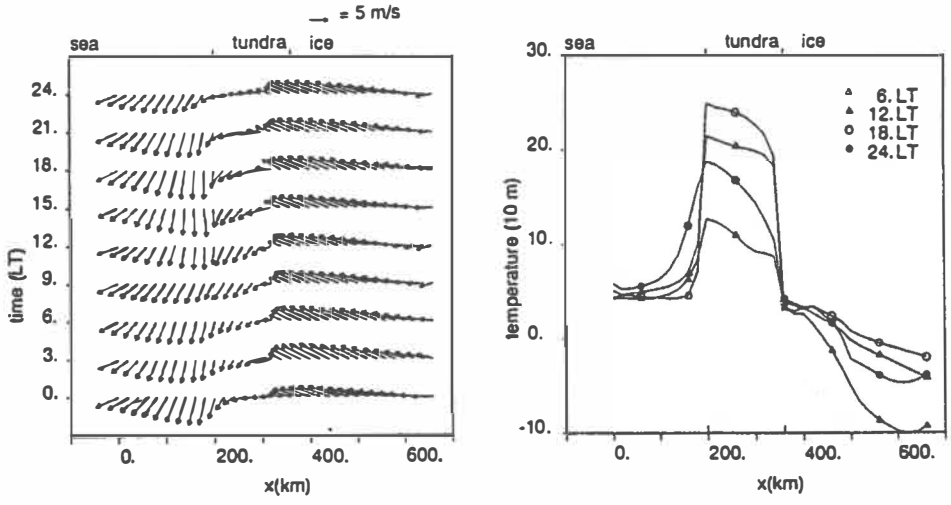

Is there a 13-hour inertial oscillation in the windfield on the Greenland Ice Sheet?

Hans F. Vugts
Institute of Earth Sciences
De Boelelaan 1085
1081 HV Amsterdam, The Netherlands

The dynamics of the atmosphere can be simply represented by equations of motion as:

$$\frac{du}{dt} = -\frac{1}{\rho}\frac{\partial p}{\partial x} + fv + F_x \qquad (1)$$

$$\frac{dv}{dt} = -\frac{1}{\rho}\frac{\partial p}{\partial y} - fu + F_y \qquad (2)$$

in which p is the pressure, ρ the density, F the friction force and f the Coriolis force while u and v are the velocity components in the x - and y direction. If there is no friction then for midlatitude synoptic scale situations the pressure gradient balances the Coriolis force, we find:

$$\frac{\partial p}{\partial x} = \rho f v \qquad (3)$$

$$\frac{\partial p}{\partial y} = -\rho f u \qquad (4)$$

If the pressure field is horizontally uniform so that the horizontal pressure gradients vanish, we will find a balance between the Coriolis force and the centrifugal force:

$$\frac{V^2}{R} - fV = 0 \qquad (5)$$

in which V is the horizontal windspeed and R the radius of curvature. This equation may be solved for $R = V/f$. Because there are no accelerations the speed must be constant and therefore the radius of curvature, R , must be constant, neglecting the latudinal dependence of f . The flow is circular and the period of this oscillation is $P = 2\pi R/V = \pi/\Omega \sin\varphi$. At midlatitudes the period will be about 15 or 16 hours and the period is often referred to as one-half pendulum day. These inertial oscillations are quite often found in the oceans (Tolmazin, 1985). Since this situation is actually caused by the inertia of the fluid, this type of motions is rarely found in the atmosphere, because the motions are damped by friction or because other forces are more important in controlling the evolution of the motion. In a boundary layer with strong friction the damping will be considerable, within a few hours the phenomena will be died out. Only a few observations are known from literature. This kind of oscillations were observed by Kraus *et al*, 1985, and by Kottmeijer, 1988, most

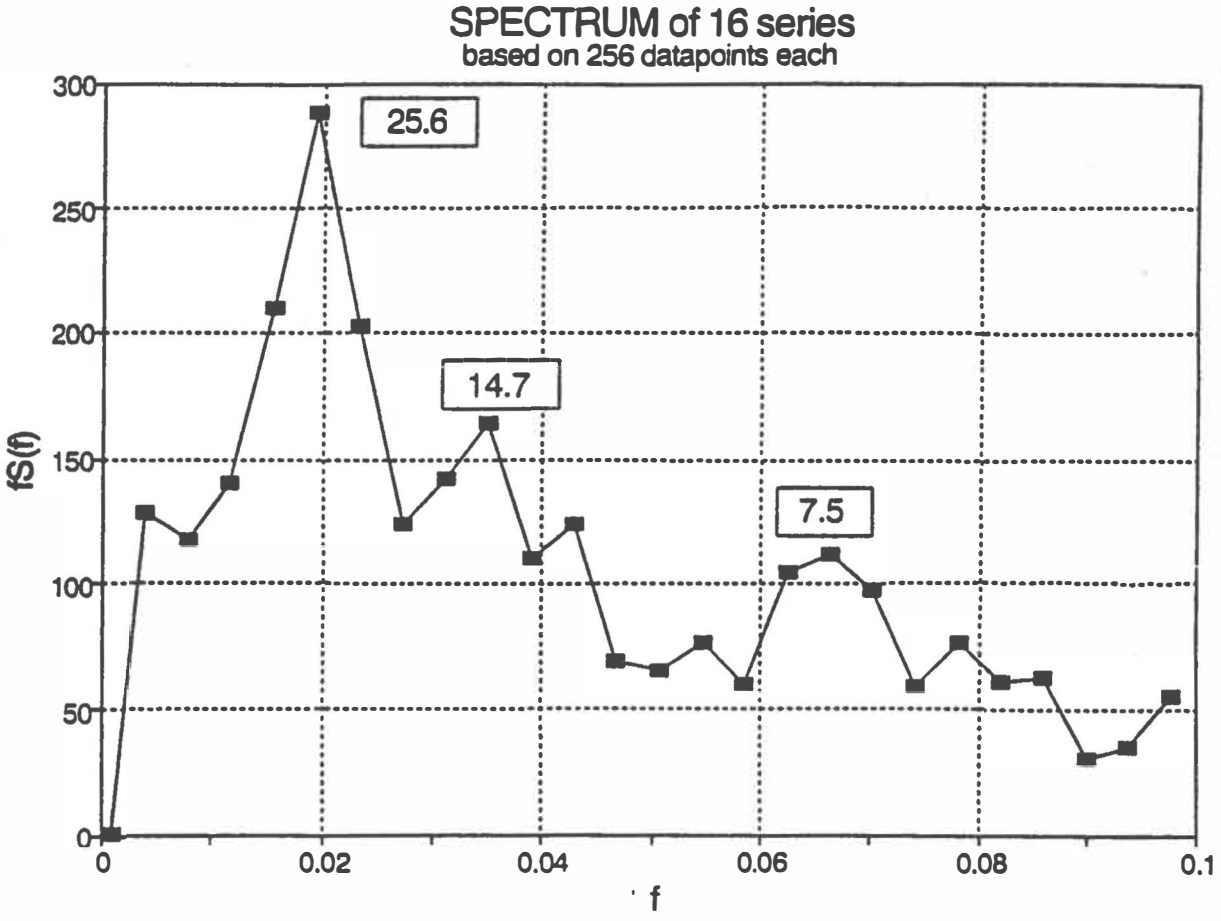

Figure 1. Spectrum of 16 series of 256 datapoints each. Data obtained from site 6, IMAU, 1990 and 1991 and site 9, VUA, 1991. Sampling interval is 30 minutes; periodicities are given in hours near the peaks.

of time during low level jet situations. As at midlatitudes nights last only 8 to 16 hours, the full cycle of the oscillation might not be realized before sunrise, when the nocturnal jet will be destroyed by mixing.
In modelling the dynamics of flows generated when stably stratified air overlies a sloping surface inertial oscillations appear which are considered as unrealistic (Egger and Schmid, 1988) and special arrangements are needed to save computertime in calculating a steady-state solution (King, 1989).
In the boundary layer at the VU-GIMEX site, Greenland, with weak friction, there might be a possibility to detect such inertial oscillations. Analysing windirection data were carried out for site 6 and 9 (Oerlemans and Vugts, 1992). Due to missing values 16 sets of 256 half hour winddirection averages could be obtained from site 6 in 1990 and 1991, and from site 9 in 1991. For these subsets only a few estimates had to be made to complete them. The total average result is given in figure 1.

References

Egger, J. and Schmid, S., 1988. Elimination of spurious inertial oscillations in boundary-layer models with time-dependent geostrophic winds. Bound. L. Met., **43**, 393-402

King, J.C., 1989. Low-level wind profiles at an Antartic coastal station. Ant. Sc., **1**, 169-178

Kottmeijer, Ch., 1988. Atmosphärische Strömungsvorgänge am Rande der Antarktis. Berichte des Instituts fur Meteorologie und Klimatologie der Universitat Hannover. Band 33

Kraus, H., Malcher, J. and Schaller, E., 1985. A nocturnal low level jet during PUKK. Bound. L. Met., **31**, 187-195

Oerlemans, J., and Vugts, H.F., 1992. A meteorological experiment in the melting zone of the Greenland Ice Sheet. Accepted in: Bull. Am. Met. Soc.

Tolmazin, D., 1985. Elements of dynamic oceanography. Allen & Unwin. London

MELTWATER REFREEZING IN THE LOWER ACCUMULATION AREA OF THE GREENLAND ICE SHEET

Roger J. Braithwaite
Geological Survey of Greenland, Copenhagen, Denmark

Climate warming will cause extra melting at the margin of the Greenland ice sheet, and an immediate rise in World sea level. In contrast, increased meltwater from the surface snow in the lower accumulation area of the ice sheet will initially refreeze within the near-surface firn layer and have no immediate effect on sea level. However, the refreezing will gradually reduce permeability of the firn and eventually create an impermeable surface so meltwater will then run off to the sea. Refreezing is therefore an important factor for Greenland's contribution to sea level rise but is still little understood.

Fieldwork was carried out by the Geological Survey of Greenland (GGU) in 1991 and 1992 to study relations between snow melting, refreezing and runoff, with the eventual goal of determining the effects of these on future sea level changes.

The lower accumulation area east of Ilulissat/Jakobshavn was chosen as the study area because GGU has worked in the nearby ablation area since 1982 and the nearby 'Swiss Camp' could be used for logistics and as a source of climate data. The work is a Danish contribution to a 10-nation study on causes and effects of sea level changes supported by the European Community through the European Programme on Climatology and Natural Hazards (EPOCH).
In the 1991 fieldwork the main approach was to study melting conditions in a profile from the ablation area to well within the lower accumulation area at 1620 m a.s.l. This involved mass balance measurements in spring (May) and at the end of summer (August) as well as placement of thermistor strings to measure temperatures to a depth of 10 metres. There is no clearly defined equilibrium 'line' but rather an equilibrium 'zone' which was around 1200 m a.s.l. in 1991. The runoff limit was around 1400 m a.s.l, agreeing with the lack of visible hydrological features on the snow surface

above this elevation. The depth of meltwater percolation was between 2 and 4 metres in the firn in the stretch 1440-1620 m a.s.l. which shows the area belongs to the wet snow zone. The 10-metre temperatures show a 'firn warming' in the same area of about 4.7 to 6.7 deg °C due to latent heat release by refreezing of meltwater.

As the 1991 field work strongly suggested that the firn-ice transition is a key process determining the extent and location of the refreezing zone, the 1992 work concentrated on studying density variations in the firn area. The main control on density in the near-surface firn layer (5-10 metres depth) is the formation of ice layers by meltwater refreezing. The mean density of near-surface firn decreases with elevation due to a decrease in melt rate with elevation. There is a surprising decrease in firn density at depths of more than about 4 metres below the 1991 summer surface which reflects lower melt rates and/or higher accumulation in the early 1980s and late 1970s when this firn was passing through the surface layer. The formation of such low density firn may have partially contributed to the 1978-85 thickening of the ice sheet observed by satellite radar altimetry.

Results from the field work have been used to validate a simple model relating the runoff limit to climate, and model experiments are now being made to study effects of climate change on the refreezing zone.

Acknowledgements. The work was supported by the European Programme of Climatology and Natural Hazards (EPOCH) through contract EPOC-CT90-0015 which is coordinated by Professor D. Smith (Coventry University, U.K.).

Published and in press

Braithwaite, R. J., N. Reeh & A. Weidick. 1992: Greenland glaciers and the 'greenhouse effect', status 1991. *Rapp. Grønlands geol. Unders.* 155, 9-13.

Braithwaite, R. J., W. T. Pfeffer, H. Blatter & N. F. Humphrey. 1992: Meltwater refreezing in the accumulation area of the Greenland ice sheet: Påkitsoq, summer 1991. *Rapp. Grønlands geol. Unders.* 155, 13-17.

Braithwaite, R. J. & M. Laternser. In press. Measurements of firn density in the lower accumulation area of the Greenland ice sheet: EPOCH 1992. *Rapp. Grønlands geol. Unders.*

Longwave Radiation Balance Derived from AVHRR for the Greenland Ice Sheet

Marcel Haefliger
Department of Geography, Swiss Federal Institute of Technology,
CH-8057 Zurich, Switzerland

Abstract

Correlations between surface temperature, water vapor amount in the atmosphere and incoming longwave radiation are examined, providing an incoming longwave radiation retrieval algorithm for the Greenland ice sheet. Out of surface temperature the outgoing longwave radiation can be calculated so that the longwave radiation balance is easily retrievable.

Ice Surface Temperature

A common approach for estimating surface temperatures is to relate satellite data to surface temperature observations with a regression model. A good overview of the theoretical algorithms for satellite derived surface temperatures is presented in Barton et al. (1989). Satellite thermal radiances are modeled with a radiative transfer model. The AVHRR channels 4 and 5 (10.5-11.5 μm, 11.5-12.5 μm) are used to retrieve ice surface temperatures. This method was applied for open ocean areas (McClain et al., 1985; Minnet, 1990) as well as for sea ice areas (Key and Haefliger, 1992). Temperature, pressure and humidity profiles, cloud observations and skin temperatures from the ETH camp were used in LOWTRAN7 (Kneizys et al., 1988). Through a statistical analysis of the daily clear sky profiles the coefficients for following equation were determined (see also Haefliger et al., in press):

$$T_{ice} = a + bT_4 + cT_5 + ((T_4 - T_5)\sec(\Theta)) \quad (1)$$

T_4 and T_5 are the satellite-measured brightness temperatures in Kelvin and Θ is the sensor scan angle (0° to 55°). The next table shows coefficients and root mean square error based on NOAA 11 AVHRR channels 4 and 5.

a	b	c	d	RMS
-4.257151	3.473293	-2.470502	-0.141503	0.320

Measured and calculated (AVHRR) ice surface temperature (IST) at the ETH Camp are shown in the following table. Due to the uncertainty of the exact location (registration error of 1/2 pixel for NOAA AVHRR) the mean temperature of 3 by 3 pixels are also calculated.

Date	Measured IST	Calculated IST		Delta IST
		1 pixel	Mean of 9 pixels	1 pix/9 pix
	(K)	(K)	(K)	(K)
6-21-90	271.0	271.4	271.6	+0.4/+0.6
6-23-90	271.3	271.2	271.0	-0.1/-0.3
6-24-90	271.5	271.4	271.1	-0.1/-0.4
6-27-90	271.3	271.3	270.8	0.0/-0.5
6-28-90	270.8	271.2	271.1	+0.4/+0.3
6-29-90	270.2	270.8	270.7	+0.6/+0.5
7-1-90	271.9	271.5	271.3	-0.4/-0.6
7-2-90	271.0	271.5	271.5	+0.5/+0.5

Longwave Incoming Radiation

Ice surface temperature and the brightness temperature of AVHRR channels 4 and 5 can be used to calculate the water vapor amount of the atmosphere:

$$WV = a + bT_{ice} + c(T_4 - T_5) \tag{2}$$

T_{ice} is the surface temperature in Kelvin and T_4 and T_5 are the satellite-measured brightness temperatures in Kelvin. Surface temperature and water vapor amount of the atmosphere are used to calculate the incoming longwave radiation $L^{\downarrow}$ as follows:

$$L^{\downarrow} = a + bT_{ice} + cWV \tag{3}$$

T_{ice} is the surface temperature in Kelvin and WV is the water vapor amount of the atmosphere in $kg\ m^{-2}$.

Out of equations 1, 2 and 3 follows:

$$L^{\downarrow} = a + bT_4 + cT_5 + (d\sec(\Theta) + 1)(T_4 - T_5) \tag{4}$$

T_4 and T_5 are the satellite-measured brightness temperatures in Kelvin and Θ is the sensor scan angle (0° to 55°). Coefficients and root mean square error based on NOAA 11 AVHRR channels 4 and 5 are following in the next table.

a	b	c	d	RMS
-749.330261	12.376310	-8.803085	-0.362533	8.10

Measured and calculated (AVHRR) incoming longwave radiation ($L^{\downarrow}$) at the ETH Camp.

Date	Measured $L^{\downarrow}$	Calculated $L^{\downarrow}$		Delta $L^{\downarrow}$
		1 pixel	Mean of 9 pixels	1 pix/9 pix
	(Wm^{-2})	(Wm^{-2})	(Wm^{-2})	(Wm^{-2})
6-21-90	231	235	235	+4/+4
6-23-90	236	234	233	-2/-3
6-24-90	239	235	233	-4/-6
6-27-90	231	234	232	+3/+1
6-28-90	231	234	233	+3/+2
6-29-90	221	232	232	+11/+11
7-1-90	243	235	234	-8/-9
7-2-90	232	235	235	+3/+3

Summary and Conclusion

The relationship between clear sky NOAA 11 thermal radiances and the measured surface temperature and incoming longwave radiation of the Greenland ice sheet is examined through forward calculations of radiative transfer equation using LOWTRAN7. Pressure, temperature and relative humidity profiles and cloud observation from the ETH camp are used. Using the split window channels 4 and 5 and scan angle, the RMS errors in the estimated IST and $L^{\downarrow}$ are 0.4 K and 9 Wm^{-2}, respectively.

Further studies are needed in order to know the accuracy of the method for the whole Greenland ice sheet.

References

Barton, I.J., A.M. Zavody, D.M. O'Brien, D.R. Cutten, R.W. Saunders and D.T. Llewellyn-Jones, 1989: Theoretical algorithms for satellite-derived sea surface temperatures, J. Geophys. Res., 94(D3), 3365-3375).

Haefliger, M., K. Steffen and C. Fowler, in press: AVHRR surface temperature and narrow-band albedo comparison with ground measurements for the Greenland ice sheet, Annals of Glaciology.

Key, J. and M. Haefliger, 1992: Arctic ice surface temperature retrieval from AVHRR thermal channels, J. Geophys. Res., 97(D5), 5885-5893.

Kneizys, F. X., E. P. Shettle, L. W. Abreu, J. H. Chetwynd, G. P. Anderson, W. O. Gallery, J. E. A. Selby and S. A. Clough, 1988: Users guide to LOWTRAN7, Rep. AFGL-TR-88-0177, 137 pp, Environmental Research Papers, No. 1010, Air Force Geophys. Lab., Bedford, Mass.

McClain, E.P., W.G. Pichel and C.C. Walton, 1985: Comparative performance of AVHRR-based multichannel sea surface temperatures, J. Geophys. Res., 90, 11587-11601.

Minnett, P.J., 1990: The regional optimazation of infrared measurements of sea surface temperature from space, J. Geophys. Res., 95(C8), 13497-13510.

On the dynamics of Storstrømmen, an outlet glacier from the North-East Greenland ice sheet

Niels Reeh, Danish Polar Center/The Geological Survey of Greenland, Øster Voldgade 10, DK-1350, Copenhagen K, Denmark

Carl Egede Bøggild, Hans Oerter, Alfred-Wegener-Institut für Polar- und Meeresforschung, D-2850, Bremerhaven, Germany

In the summers of 1989 and 1990 a glaciological field programme was carried out by the Alfred-Wegener-Institut on Storstrømmen (77° 20'N, 23°W), an outlet glacier from the North-east Greenland ice sheet (Reeh et al., 1989, 1990). As part of this programme, a glacier-dynamic study was performed comprising measurements of surface velocities, surface-elevation change and changes in ice-front position (Bøggild et al., submitted).

Surface velocities

Ice surface velocities were determined by different methods:

1. Repeated doppler satellite positioning of 8 poles in a 60 kilometre transect from the eastern margin of Storstrømmen in Germania Land to north of Ymer Nunatak, see map in Fig.1. Positions were determined in July-August 1989 and 1990.
2. Repeated GPS positioning (differential mode) of stakes located between 2.5 and 10 km from the ice margin. Observations were made in 1990, and again in 1992 during a short field trip to Storstrømmen. During this field trip, the poles in the transect established in 1989 were also positioned by differential GPS measurements.
3. In the region between 700 m and 1000 m elevation, several lakes forming lake ogives are found (Reeh et al., 1991). The ogives are formed annually (Echelmeyer et al. 1991), and velocities were obtained by measurements on aerial photographs taken in 1978.
4. Comparison of distinct surface features seen on aerial photographs taken in 1964 and 1978, respectively, allowed displacements and consequently velocities to be determined in the lower region of Storstrømmen (A Higgins, unpublished material).
5. Repeated positioning of poles by angle-distance measurements from stations on the ice-free land in 1989, 1990 and 1992 provided ice surface velocities near the ice margin in Germania land.

The observations show that a large central part of Storstrømmen between 120 km and 50 km from the front moves as a block with velocities between 250 and 300 m/yr. The increase of the velocity from very small values near the margins to the "block-flow" values in the central part of the glacier takes place through narrow

zones less than 1 kilometre wide. So far, velocities have not been measured closer to the front than 50 km. However, balance-velocity calculations indicate a velocity increase to about 800 m/year at the calving front.

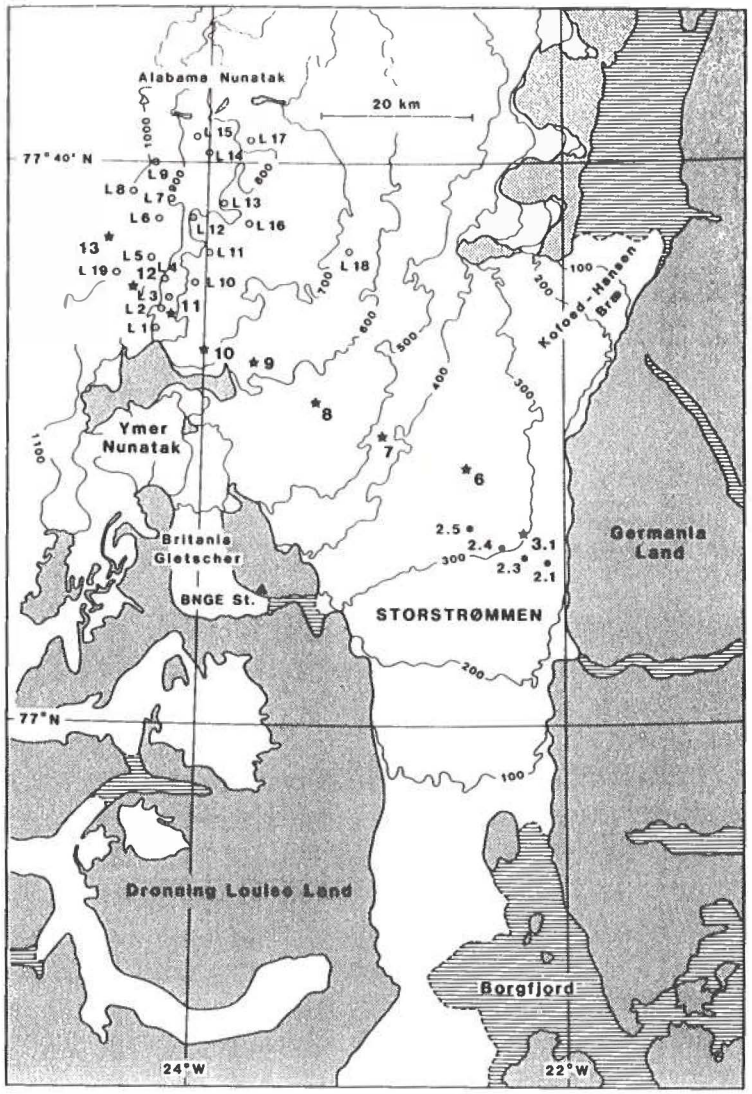

Figure 1. Map of Storstrømmen. Stars indicate points positioned by means of Doppler satellite receiver. Dots indicate points positioned by means of differential GPS observations. Points denoted by L are "lake ogive" velocity points.

Surface elevation change

Surface elevations of points determined by Doppler satellite and GPS observations in 1990 and 1992 have been compared to elevations at the same locations on maps compiled by the Geological Survey of Greenland (GGU, 1990,1992) based on aerial photographs taken in 1978. The Doppler and GPS elevations have been reduced by 40 m in order to convert elevations above the ellipsoide to elevations above sea

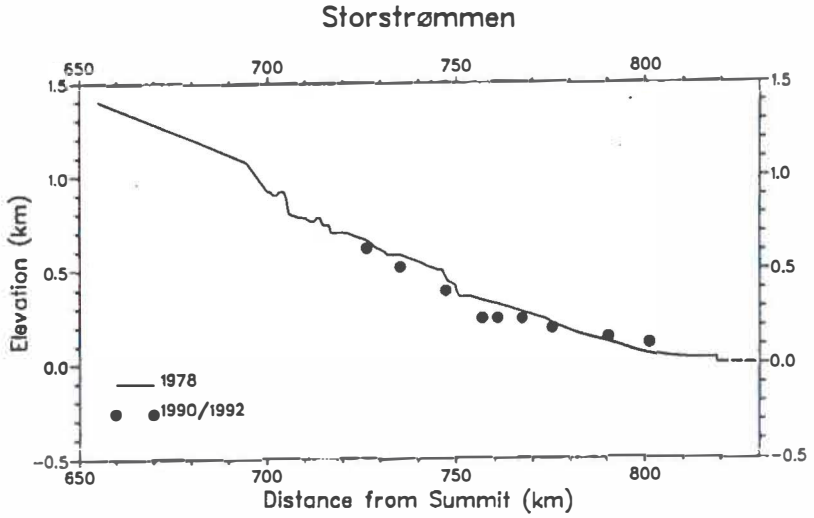

Figure 2. Surface elevation profile along centerline of Storstrømmen based on the 1978 aerial photography (line). Dots indicate surface elevations of points determined by Doppler satellite and GPS observations in 1990 and 1992.

surface. Figure 2 shows the surface elevation profile along the centerline of Storstrømmen based on the 1978 aerial photography (full line) and point surface elevations determined by Doppler and GPS observations (dotts). Generally, the Doppler and GPS points were not located on the center line. In Figure 2, the actual point locations have been shifted to centerline positions along elevation contour lines. This means that elevation changes are displayed correctly in the figure. As appears from the figure, the surface between kilometres 725 and 775 has gone down by up to 90 m during the period 1978-1990, and gone up by up to 60 m between kilometres 775 and 800 during the same period. Accurate Doppler and GPS measurements in 1989, 1990 and 1992 show that points at kilometres 755 and 760, which are the points that have been subject to the largest surface lowering between 1978 and 1989/90, have now started to move up, indicating glacier thickening in this area, whereas points farther up-glacier do not show a similar recent thickening. The positions of points down-glacier of kilometre 760 have only been determined once (i.e. in 1992), and consequenly, the present trend of the surface elevation change for these points is not known.

Frontal variations

The frontal part of Storstrømmen merges with L. Bistrup Bræ, an outlet glacier draining the Inlandice south of Dronning Louise land, to form a common calving front (Bredebræ) in Borgfjorden, see Figure 1. The eastern part of Storstrømmen terminates with a second calving front between Germania Land and a semi-nunatak. In the following this front is referred to as "Northern Front". Figure 3 shows front positions as recorded since 1912-13, when the first reliable observation was performed by Koch and Wegener (1930). Maps based on aerial photos taken

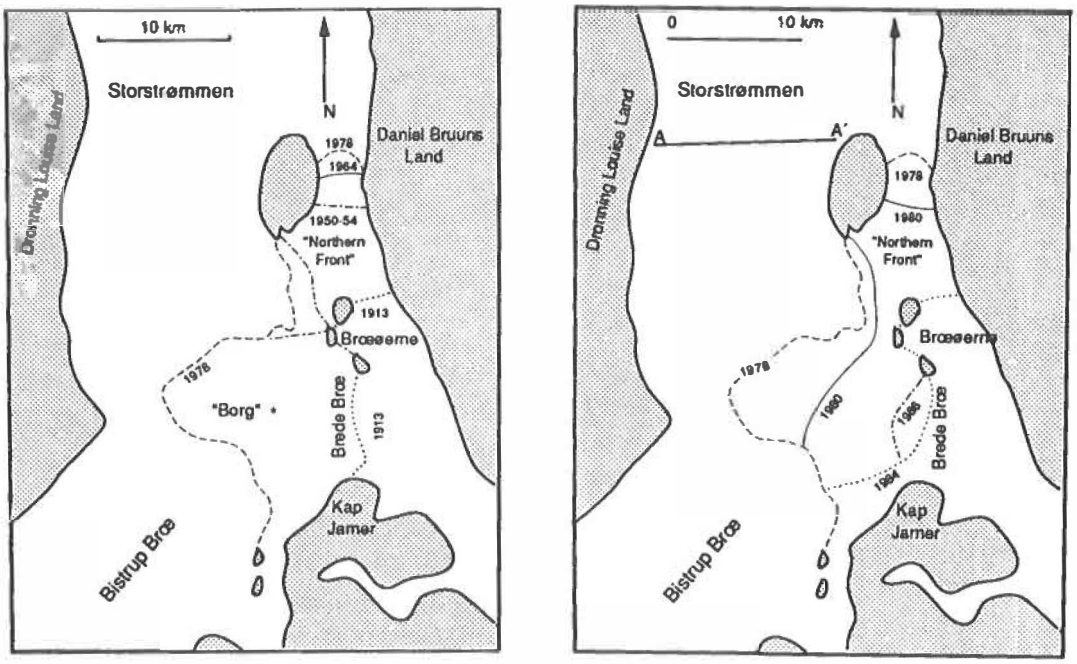

Figure 3. Frontal positions of Storstrømmen between 1912-13 and 1978 (left) and between 1978 and 1986 (right).

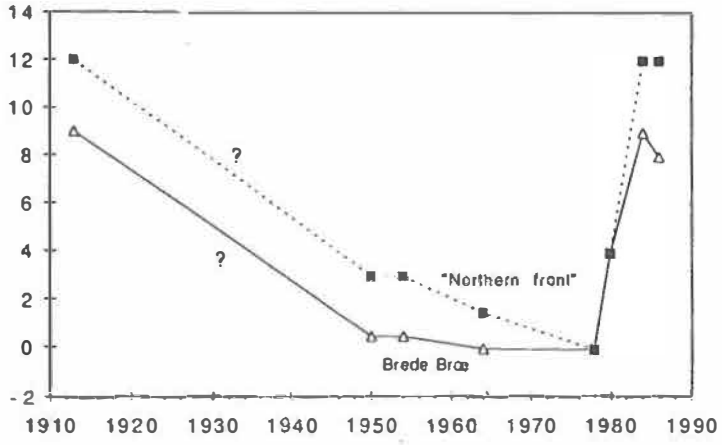

Figure 4. Frontal variations of Storstrømmen since 1912-13. The front position in 1978 is used as datum.

in 1950 by the British North Greenland Expedition (Hamilton, et al. 1956) show much retreated front positions as compared to 1912-13. Aerial photographs from 1954, 1964 and 1978 indicate either unchanged front position (Bredebræ) or further retreat (Northern Front) as compared to the 1950 positions. The maximum retreat (1978) amounts to 9 km and 12 km for Brede Bræ and "Northern Front", respectively, as compared to the 1912-13 front positions, see Figure 3a.

Between 1978 and 1980 major advances of about 5 km occurred along both Brede Bræ and "Northern Front" (Figure 3b). Between 1980 and 1984 further advances of about 8 km took place along both fronts, making the 1984 front positions almost identical to the 1912-13 positions. After 1984, the fronts have remained virtually stationary, although recently, frontal disintegration and retreat seem to have started. The frontal variations since 1978 have all been documented by means of LANDSAT satellite images. The observed frontal variations since 1912-13 are further illustrated in Figure 4.

Discussion

The observed pattern of surface elevation change (indicating glacier thinning in the upper reaches and glacier thickening near the front) in a period overlapping the period of the large, rapid front advance impels to describe the event as a surge or "surge-like" event. About 50 km^3 of ice was transferred from the upper to the lower reaches of Storstrømmen between 1978 and 1984, in which period velocities at the front must have reached at least 2 km/year. The frontal advance is unlikely to be a normal response to mass balance changes, since in that case glacier thickening should have taken place along the entire length of the glacier. Therefore, reduced basal friction and/or side drag must be the cause of the "surge". The "surge" hypothesis is further supported by the present frontal disintegration and retreat of Brede Bræ initiated in 1984, which indicates that the advanced front position is unstable. It is likely, that the glacier front will retreat back to the relatively stable position occupied at least during a 28 year period from 1950 to 1978. The observed present rise in surface elevation in the region previously subject to the greatest thinning accompanied by a present decreasing trend in ice flow velocity in the same region can also be taken as indication that this part of the glacier is now recovering from the surge. A planned continuation of the glaciological field programme in 1993 and 1994 will make possible to study the trends of surface elevation and velocity in two more years.

Acknowledgements

State Geodesist Frede Madsen, National Survey and Cadastre (formerly Geodetic Institute), Copenhagen, Denmark is thanked for lending us a JMR-1 Doppler satellite receiver in 1989 and 1990 and for spending time on instructing us in how to use the instrument. Likewise, Frede Madsen lent us two ASHTECH GPS receivers in 1990 which were operated in the field in co-laboration with I. Hauge Andersson, National Survey and Cadastre (now at the Danish Polar Center, Copenhagen, Denmark), who's help is also very much appreciated. State Geologist Niels Henriksen, The Geological Survey of Greenland, Copenhagen, Denmark and I. Hauge Andersson, Danish Polar Center are thanked for their exellent way of organizing logistics in 1989/1990 and 1992, respectively. The research was supported by the European Programme on Climatology and Natural Hazards under EC Contract EPOC CT90-0015, and by the Commission for Scientific Research in Greenland (Reg. nr. 28829).

References

Bøggild, C.E., N. Reeh and H. Oerter, submitted. Apparent large scale surge of Storstrømmen, an outlet glacier from the Northeast Greenland ice sheet. Submitted to Global and Planetary Change.

Echelmeyer, K., T. S. Clark and W. D. Harrison, 1991. Surficial glaciology of Jakobshavns Isbræ, West Greenland: Part I. Surface morphology. J. Glaciol., 37, 368-382.

GGU, 1990. Storstrømmen. Internal report, The Geological Survey of Greenland, Copenhagen Denmark. Topographic base map compiled by the Geological Survey of Greenland. Aerial photographs and ground points supplied by the National Survey and Cadastre, Denmark (A200/87).

GGU, 1992. Storstrømmen (front). Internal report, The Geological Survey of Greenland, Copenhagen Denmark. Topographic base map compiled by the Geological Survey of Greenland. Aerial photographs and ground points supplied by the National Survey and Cadastre, Denmark (A200/87).

Hamilton, R.A., et al., 1956. British North Greenland Expedition 1952-54: Scientific Results. Geographical Journal 122, 203-240.

Koch, I.P. and A. Wegener, 1930. Wissenschaftli che Ergebnisse der Dänischen Expedition nach Dronning Louise Land and quer über das Inlandeis von Nordgrönland 1912-13 unter Leitung ven Hauptmann I.P. Koch. Meddelelser om Grønland 75 (1), 676 p.

Reeh, N., H. Oerter and A. Letréguilly, 1989. Glaciological studies on the Inlandice margin 75° - 77.5°N. In: Express Report North-East Greenland 1989, The Geological Survey of Greenland, Øster Voldgade 10, 1350 København K, Danmark.

Reeh, N. and H. Oerter, 1990. Glaciological studies on the margin of Storstrømmen glacier, Germania Land, North-East Greenland. In: Express Report North-East Greenland 1990, The Geological Survey of Greenland, Øster Voldgade 10, 1350 København K, Danmark.

Reeh, N., H. Oerter and J. K. Neve, 1991. Supra-glacial lakes on Storstrømmen Glacier Northeast Greenland and their relation to ice dynamics. Abstract in: Programm, Deutsche Gesellschaft für Polarforschung, 16. Internationale Polartagung in Göttingen, 10-13 April 1991.

ABLATION RECONSTRUCTION AND MASS-BALANCE SENSITIVITY TO CLIMATE CHANGE - ASSESSED BY MODELLING ON STORSTRØMMEN, NORTH-EAST GREENLAND

Carl Egede Bøggild
Alfred Wegener Institut für Polar- und Meeresforschung, Bremerhaven, Germany

Niels Reeh
Danish Polar Center/ Geological Survey of Greenland, København, Denmark

Hans Oerter
Alfred Wegener Institut für Polar- und Meeresforschung, Bremerhaven, Germany

Overview:

A time series of ablation measurements has been performed along a transect of ablation stakes (A-A' in Fig.1) on Storstrømmen glacier during two seasons of glaciological fieldwork in 1989 and 1990. In 1992 this was followed up by a short visit. As part of the programme basic climate stations were operated during the field seasons. Ablation and temperature data has served as input for a degree-day model following the concept suggested by Reeh (1989), by which mass-balance has been determined in the lowest 1400 m of the glacier basin. From climatological data at the coastal station Danmarkshavn ablation and accumulation has been reconstructed on monthly basis back to 1949.

Initial results of the work showed that: **1**) the degree-day factor appears to be about 20% higher in North-East Greenland than the factor previously found in South-West Greenland (Braithwaite and Olesen, 1989), **2**) summer temperatures at the ice margin in the Dove bugt area are lower than temperatures on the outer coast. This is also in contrast to conditions in South-West Greenland, where an inland heating has been documented at many locations.

Mass-balance for the period 1949-1991:

The modelled cummulative mass-balance deviations for the period 1949-1991 is shown in Fig. 2. The mass-balance reconstruction shows some destinct features; (1) there is no significant trend in the mass-balance over the period studied, since the values of cummulated deviation in 1949 and 1991, respectively, are almost the same. 2) However, during this period two severe negative mass-balance events of approximately 4 years duration have occurred, i.e. from 1949 to 1953 and from 1965 to 1969, respectively. In these two periods, ablation rates have been determined to be consistantly higher and accumulation rates consistantly lower, respectively, than the averages for the whole period. After 1986,

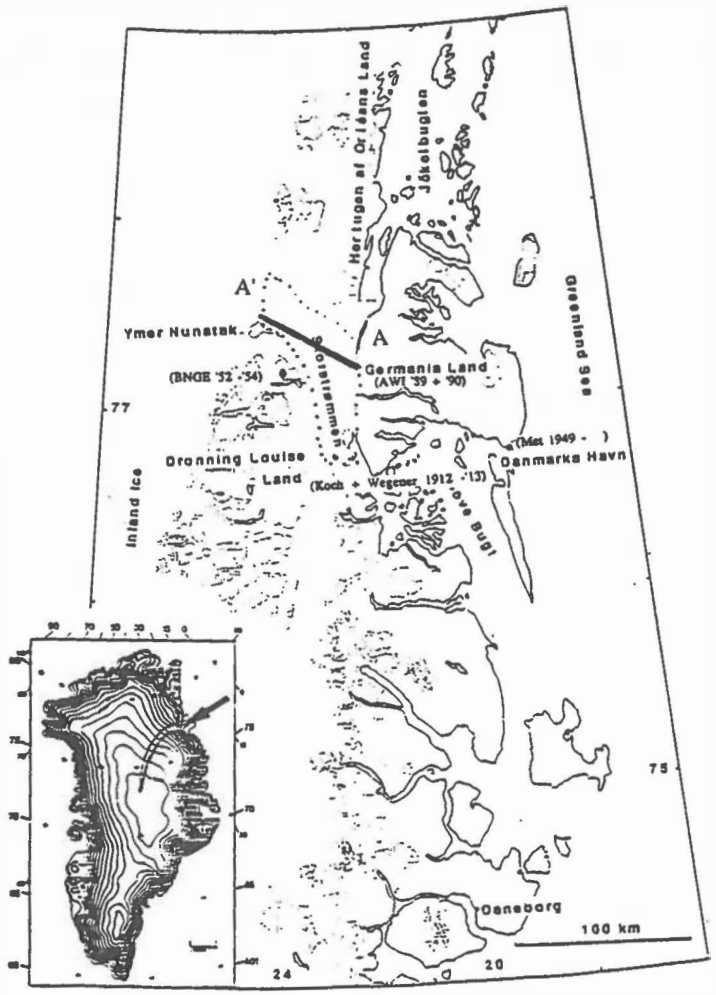

Fig.1. Location of Storstrømmen.

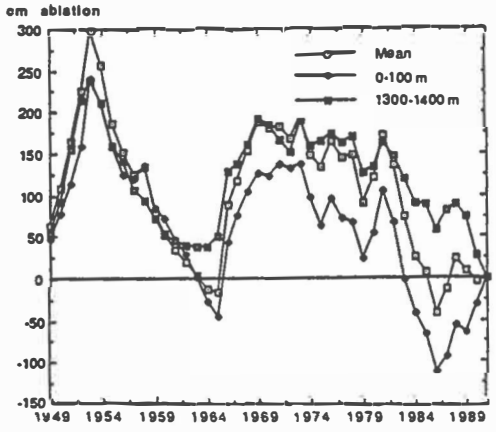

Fig.2. Cummulated ablation deviations with time. 0-100m and 1300-1400 m refer to the elevation band at sea-level and the top of the modelled elevation interval, respectively.

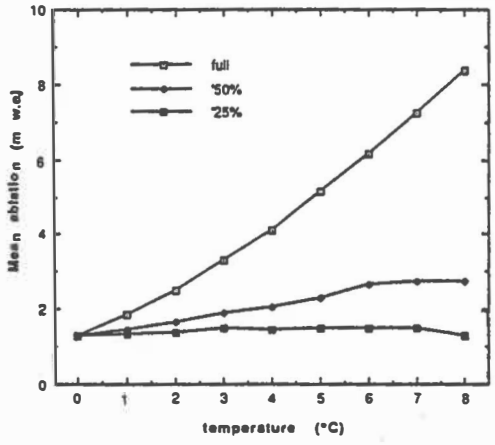

Fig.3. Mean ablation as a function of winter temperature. "Full" denotes equal Summer and Winter warming with a 5.3 $\%K^{-1}$ PTR. A $22\%K^{-1}$ PTR is used with the reduced Summer warmings (50% and 25% of the winter warming). For further explanation, see text.

both ablation and accumulation rates have increased. This has caused opposite trends in the uppermost and lowermost elevation bands (see Fig.2). In the lowest 100 m, net ablation has increased because there ice melting is the most important component for the mass-balance. In the 1300-1400 m interval the tendency is opposite due to the importance of snow accumulation. Theoretically, this difference should have led to a steepening of the glacier surface during the last 6 years.

Climate sensitivity:

Global Circulation Model (GCM) experiments with rising atmospheric CO_2 predicts the highest temperature rise to occur in Polar regions, increasing especially in the North-East Greenland area with 8-14 °K in the winter and by 2-4 °K in the summer (Mitchell et al., 1990 p 138-143).

During the last 30 years at Danmarkshavn the mean annual temperature has incerased by about 1.6 °K and the precipitation has increased by 80 mm. From change of temperature and precipitation, respectively, a local precipitation/temperature ratio PTR of 22 $\%K^{-1}$ has been derived, which is four times larger than the value of 5.3$\%K^{-1}$ derived from ice cores and used in other studies of sensitivity of the entire ice sheet to climate change (Huybrechts et al., 1991).

With a restricted summer heating of 25% of the winter heating and the local PTR ratio of 22% K^{-1}, the mean ablation at the ice sheet margin is essentially independent of a temperature change (Fig.3). This result is modified when considering the total drainage basin of Storstrømmen (which extends to Summit at 3229 m a a.s.l., see Fig.1). A temperature rise is likely to result in increased accumulation in the interior regions of the basin, and although both the temperature change and the PTR ratio are likely to decrease when going inland from the margin, a temperature increase could very well lead to an increased positive mass-balance for the total drainage basin of Storstrømmen. Since the Storstrømmen basin is a typical North-East Greenland drainage basin, it is temptating to extend this conclusion to the entire north-east sector of the Greenland ice sheet. Consequently, the greenhouse-warming induced sea-level rise from this part of the Greenland ice sheet is likely to be less than hitherto assumed. E.g. the scenario presented by Huybrechts et al. (1991) predicts a large increase of the mean ablation at the margin of Storstrømmen on the order of 1 m w.e. K^{-1}, from applying a full summer warming and a PTR of 5.3$\%K^{-1}$ (see also Fig.3). The present scenario of less summer heating than winter heating and a higher PTR, results in a very limited increase of the ablation.

ACKNOWLEDGEMENTS

The research was supported by the EC under Contract EPOC CT90-0015, and by the Commision for Scientific Research in Greenland (Reg. nr. 28829).

REFERENCES:

Braithwaite, R., Olesen, O.B., 1989 A. Calculation of glacier ablation from air temperature, west Greenland. In: J. Oerlemans (editor), Glacier Fluctuations and Climate Change, Kluwer, Doerdrecht: 219-233.

Bøggild, C.E., N. Reeh and H. Oerter, submitted. Apparent large scale surge of Storstrømmen, an outlet from the Northeast Greenland ice sheet. Submitted to Global and Planetary Change.

Bøggild, C.E., N. Reeh and H. Oerter, submitted. Modelling ablation and mass-balance sensitivity to climate change of Storstrømmen, North-East Greenland. Submitted to Global and Planetary Change.

Huybrechts, P., Letreguilly, A., Reeh, N., 1991. The Greenland ice sheet and greenhouse warming. Paleogeogr., Paleoclimatol., Paleoecol. (Global Planet. Change Sect.) 90: 385-394.

Mitchell, J.F.B., Manabe, S., Meleshko, V., Tokioka, T. 1990. Equilibrium Climate Change - and its Implications for the Future. In: Houghton, J.T., Jenkins, G.J., and Ephraums, J.E. (eds.), Climate Change, the IPCC Scientific Assessment, Cambridge University Press, pp. 131-172.

Reeh, N., 1989 (published 1991). Parameterization of melt rate and surface temperature on the Greenland ice sheet. Polarforsch. (59): 113-128.

$\delta^{18}O$ studies on the margin of Storstrømmen, North-East Greenland

Hans Oerter,
Alfred-Wegener-Institut für Polar- und Meeresforschung, Bremerhaven, Germany

Niels Reeh,
Danish Polar Center, Copenhagen, Denmark

Introduction

Polar ice sheets and ice caps are rich sources of information on climate and environmental changes during the last glacial cycle, and probably even further back in time, as demonstrated by the results of deep ice-core drillings. Due to ice flow the old ice found at depth in the central regions of the ice sheets can also be retrieved from the surface of the ice-sheet margins (Lorius & Merlivat, 1997; Reeh et al. 1987, 1991). Here the time sequence shows the oldest ice nearest to the ice edge. The detailed $\delta^{18}O$ profile obtained by analysis of surface ice samples from the ice margin at Paakitsoq, central West Greenland could be correlated over the last glacial cycle with $\delta^{18}O$ profiles obtained from deep ice cores (Reeh et al. 1991). This allowed an interpretation of the Paakitsoq record in terms of Emiliani isotopic stages (EIS) and a translation of the $\delta^{18}O$ record into a Greenland temperature record covering the past 150 000 years. Here, we report on two new detailed $\delta^{18}O$ records obtained by analysis of surface ice samples from the margin of Storstrøm-men, an outlet glacier from the North-East Greenland ice sheet (for a map see Fig. 1 of Reeh et al., this volume. The sampling location at the margin is marked by a star.).

Sampling

The records were sampled along two parallel lines about 500 m apart, and perpendicular to the ice margin. More than 2000 samples were collected along the first profile line (profile N) covering a 2.2 km section at a spacing of 1 m or less, starting at the ice margin. The first 100 m of this profile consisted of moraine covered ice (5-10 cm thick layer). Along the second profile line (profile NS), more than 1500 samples were collected over a 1500 m section. In this profile, the 1100 m nearest to the ice margin were sampled at a spacing of 1 m, whereas the sampling distance for the remaining 400 m was 2.5 m.

Dust bands on the surface

Looking at the glacier surface in the marginal area, especially by bird eyes view, one recognizes alternating dark and light coloured bands running parallel to the margin. The light appearing surface is generally coarser than the dark appearing ice. Moreover, chryoconite holes containing dark material (dirt particles and blue-green algea) are more abundant in the light bands than in the dark bands in which the dirt particles seem to be more uniformly distributed on the surface. The alternating bands, as mapped at the intersection with the N-profile line, are plotted together with the $\delta^{18}O$ record in Fig. 1. It appears that light and dark coloured ice is associated with relatively high and low $\delta^{18}O$ values, respectively. A similar correspondence between surface ice colour and $\delta^{18}O$ values was found on the ice margin at Paakitsoq in West Greenland.

Blue band ice

The profile N (Fig. 1) displays several single-point spikes, with $\delta^{18}O$ values generally up to 15 ‰ higher than those found in the adjacent ice. These spikes can all be referred to ice from blue bands which are of common ocurrence, running roughly parallel to the ice margin, often

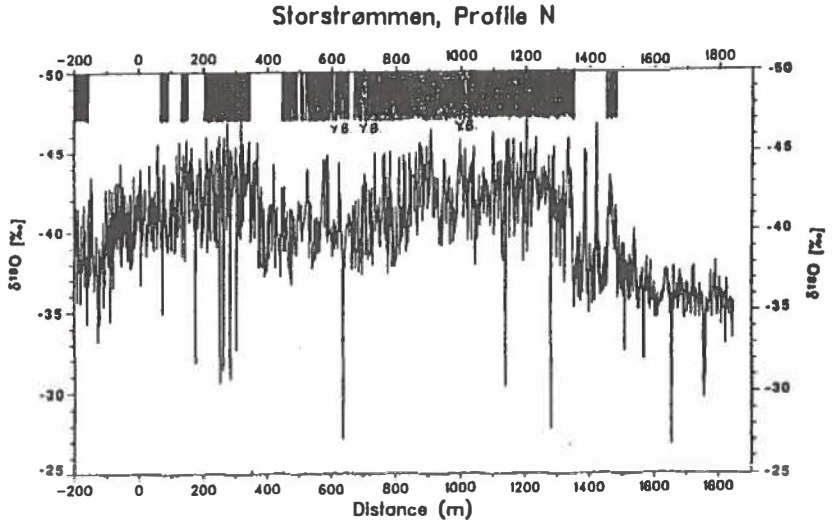

Figure 1: Ice margin Storstrømmen, North-East Greenland: $\delta^{18}O$ values along profile N (raw data). Distances are referred to stake NE0289, appr. 200 m inland from the very edge of Storstrømmen. The black colour on top marks dark and white appearing glacier surface. Y.B. = yellow bands.

continuous over several hundred metres. The explanation of the $\delta^{18}O$ anomaly of the blue bands is not yet known, but to judge from detailed sampling across the bands, they do not seem to break the continuity of the $\delta^{18}O$ record.

The points of intersection of the major blue bands with both profile lines could be determined. The correspondence between the profiles established in this way is illustrated in Fig. 2. From 100 m to 1300 m on the distance scale of the N-profile, the transformation is nearly linear. For distances larger than 1300 m, the blue-band correlation becomes ambigous, the bands split up, thus leaving two possibilities for interpretation. The one chosen, is shown on the graph by line segments.

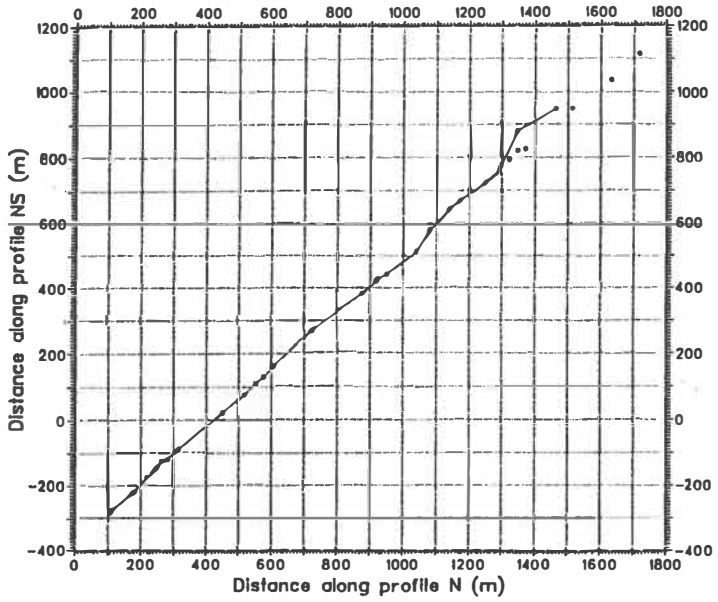

Figure 2: Correlation between intersection of blue bands with profile N and NS.

The $\delta^{18}O$ record of the profile N

The $\delta^{18}O$ record of the N-profile is shown in Fig. 1. The record shows large variations: a high frequency component with an amplitude on the order of 1.5 ‰ superimposed on variations with lower frequencies. In broad terms the low-frequency variations of the N-profile is characterized by relatively high $\delta^{18}O$ values (between -35 ‰ and -37 ‰) from 1550 m from the ice margin and inland. The marked $\delta^{18}O$ shift at 1475 m marks the Holocene-Pleistocene transition, and the "cold" $\delta^{18}O$ peak between 1440 m and 1475 m is interpreted as the Younger Dryas cold spell at the end of the last glaciation. For distances shorter than 1350 m the low frequency $\delta^{18}O$ record ranges between -38 ‰ and -45 ‰ except for the section between -100 m and -200 m, where the smoothed $\delta^{18}O$ record reaches values as high as -37 ‰. Tentatively, the $\delta^{18}O$ record from -100 m to 1475 m is interpreted as representing EIS stages 4, 3, and 2, whereas the section from -100 m to -200 m probably represents the end of EIS stage 5.

Comparison of the $\delta^{18}O$ records along profiles N and NS

The N- and NS-profiles are both shown in Fig. 3. The $\delta^{18}O$ spikes referred to blue band ice have been deleted from the N-profile; along the NS-profile these blue bands had not been sampled. The NS-profile is plotted on a distance scale obtained by transforming the actual scale by means of the correlation illustrated in Fig. 2. It appears that the two profiles matches well, e.g. 1) the marked drop in $\delta^{18}O$ at ca. 1350 m, 2) the pronounced isolated $\delta^{18}O$ peak at 950 m, 3) the relatively high mean $\delta^{18}O$ values in the interval from ca. 385 to 850 m. From about 1350 m inland of the margin the correlation between both profiles is less perfect. This point coincide with the point were the blue band correlation becomes ambigious, and it is close to the substantial shift of the $\delta^{18}O$ values which marks the transition from Holocene to Pleistocene. It is an open question whether one or both profiles were disturbed by folding, due to the large viscosity difference between ice deposited in the holocene and ice deposited in the late Wisconsian (Dahl-Jensen, 1985).

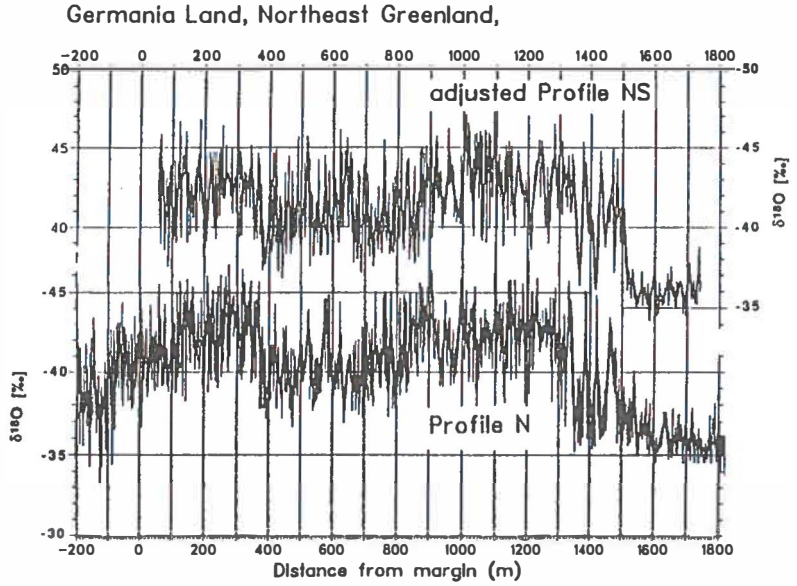

Figure 3: Comparison between profile N and profile NS. The distance scale of profile NS is adjusted according to Fig. 2.

Comparison of profile N with two Greenland ice cores

Finally, an attempt is made to correlate the N-profile with ice-core records from Renland and Camp Century (Johnsen & Dansgaard, 1992) (Fig. 4). A few ages are indicated, referring to the distance scale for Camp Century. The transition from Younger Dryas to Pre-boreal and the onset of the Bølling interstadials had been dated at 11 550 BP and 14 450 BP, respectively (Johnsen et al. 1992). The ages of 35 ka BP and 60 ka BP have been discussed by Beer et al (1988) for the Camp Century record and by Reeh et al. (1991) for the Paakitsoq profile. In a recent paper, Beer et al. (1992) accept the 35 ka ^{10}Be concentration to be present in the Camp Century record, but conclude that the second peak based on only one single high concentration value should not be considered without further confirmation. This comparison shows that profile N covers less than the past 100 000 years.

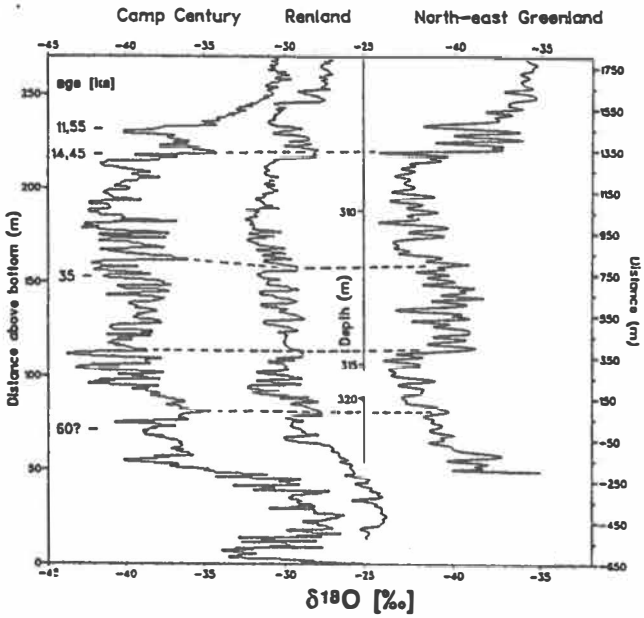

Figure 4: Comparison of profile N with two Greenland ice cores (Johnsen & Dansgaard, 1992). For the dating see text.

References

Beer, J., Siegenthaler, U., Bonani, G., Finkel, R.C., Oeschger, H., Suiter, M., and Woelfli, W., 1988: Information on past solar activity and geomagnetisme from ^{10}Be in Camp Century ice core. Nature **331**, 675-679.

Beer, J., Johnsen, S.J., Bonani, G., Finkel, R.C., Langway, C.C., Oeschger, H., Stauffer, B., Suiter, M., Woelfli, W., 1992: ^{10}Be peaks as time markers in polar ice cores. In: E. Bard & W.S. Broecker (eds.). The last deglaciation: Absolute and radiocarbon chronologies. NATO ASI Series **12**, Berlin, Heidelberg: Springer-Verlag, 141-153.

Dahl-Jensen, D., 1985: Determination of the flow properties at Dye 3, South Greenland, by bore-hole-tilting measurements and perturbation theory. J. Glaciology **31** (108), 92-98.

Johnsen, S.J. & Dansgaard, W., 1992: On flow model dating of stable isotope records from Greenland ice cores. In: E. Bard & W.S. Broecker (eds.). The last deglaciation: Absolute and radiocarbon chronologies. NATO ASI Series **12**, Berlin, Heidelberg: Springer-Verlag, 13-24

Johnsen, S.J., Clausen, H.B., Dansgaard, W., Fuhrer, K., Gundestrup, N., Hammer, C.U., Iversen, P., Jouzel, J., Stauffer, B., Steffensen, J.P., 1992: Irregular glacial interstadials recorded in a new Greenland ice core. Nature **359**, 311-313.

Lorius, C. & Merlivat, L., 1977: Distribution of mean surface stable isotope values in East Antarctica, observed changes with depth in the coastal area. IAHS Publ. **118**, 127-137.

Reeh, N., Thomson, H.H., Clausen, H.B., 1987: The Greenland ice-sheet margin - a mine of ice for palaeo-environmental studies. Palaeogeogr., Palaeoclimatol., Palaeoecol. **58**, 229-234.

Reeh, N., Oerter, H., Letréguilly, A., Miller, H., Hubberten., H.W., 1991: A new detailed ice-age record from the ice -sheet margin in central West Greenland. Palaeogeogr., Palaeoclimatol., Palaeoecol. (Global and Planetary Change Section) **90**, 373-383.

Height determinations along the EGIG line and in the GRIP area

Hinrich Kock
Institut für Vermessungskunde, Technische Universität Braunschweig

Introduction

During four expeditions between 1989 and 1992 a lot of height determinations were carried out along the EGIG profile and at Dome Grip. As height determinations are always relative measurements related to a pre defined zero level the type of height depends on the reference system and on the observation technique: optical levelling as well as trigonometric levelling results in geoidal height differences dependent on the chosen route; GPS observations provide heights above the reference ellipsoid with its certain datum shift valid for the observed network. Finally, gravity measurements lead to potential differences. They can be used to convert levelled height differences to orthometric height differences. Due to their little influence no orthometric corrections were computed for this presentation. That is why the results are of preliminary character.

Measurements

During the last four years the following height related measurements were performed:

- GPS observations along the NST profile between Dome GRIP and Crête, along the EGIG profile between T1 and Cecilia Nunatak. All GPS measurements were linked to two fiducial stations Jacobshavn and Constable Pynt.
- Trigonometric levelling beginning at Dome GRIP to Crête and further on to T1, and from Cecilia Nunatak to Crête. Between T1 and T53 (Jarl Joset) the leve ling line was located along the 1959 positions of the EGIG stakes. Four lines to each direction beginning at Dome Grip app. 10 km long to determine the highest point of the ice cap.
- Continuous gravity observations along the whole EGIG line, and between Crête and Dome Grip.

Height of Dome Summit

In order to confirm the 1989 declared Dome Summit as the highest point of the ice cap a trigonometric levelling was performed to all 4 directions beginning at Dome Summit. It turned out that there were nearly no undulations except of normal roughness of the snow surface in the vicinity of the borehole site. A map derived from these measurements shows the true summit nearly 3 km south-east of the drill site with a height difference of only 0.3 m. Due to buildings erected at Dome Summit a lot of snow has been deposited around the structures in the meantime. So we can assume the highest point of Greenland directly at Dome Summit. However, if this is the more important ice devide, too, will be answered after computing velocity vectors using the strain net around Dome Summit.

A special point of interest for all glaciological work is the height above sea level for a certain point. Up to now the only heights of Dome Summit available were those calculated from GPS observations with a more or less rough model of the geoidal undulation in that area, and those from airborne surveying using radar altimetry techniques. A combination of the height difference between Dome Grip and Crête measured in 1989 and the difference determined this season between Cecilia Nunatak and Crete lead to a height above sea level of 3229.6 m for the center point of the strain network around Dome Grip. This calculation assumes the height difference between Dome Grip and Crête beeing constant through the last 3 years. The height of Dome Summit fits very well the radar altimetry measurements carried out by Steven Hodge /1/ and presented on a GRIP preparation meeting in Copenhagen 1988. He determined the highest point of the ice cap as a little more than 3230 m.

The EGIG line

In order to convert a height derived from GPS observations to one above sea level (geoidal height) you need the separation value between ellipsoid and geoid: $N = h - H$ with h as ellipsoidal height and H as orthometric height. Comparing our GPS calculations with our trigonometric levelling all along the EGIG line will be a contribution to improve the geoid of Greenland. At the moment we cann't provide definite computations. We have calculated the line between Dome Grip and Crête with unfortunately insufficient results, probably because of geodetic datum problems.

Levelling group A of the EGIG expedition 1968 /4/ observed the part from A14 at the west coast north of Jacobshavn to T53 (Jarl Joset). They calculated a height of 2865.33 m for T53 (surface). The second levelling group B started at Cecilia Nunatak and went on to Jarl Joset. So the height of Cecilia Nunatak can be determined to 1623.36 m. This height was used for the 1992 levelling beginning at Cecilia Nunatak and proceeding to Crête. It is of preliminary character as no time reductions were computed for the eastern section.

Assuming that no significant height changes occured at Crête during the last 2 years the two parts of the levelling (1990 between Crête and T1, 1992 between Crête and Cecilia Nunatak) can be fit together. The result is a profile between T1 and Cecilia Nunatak as shown in the graph below.

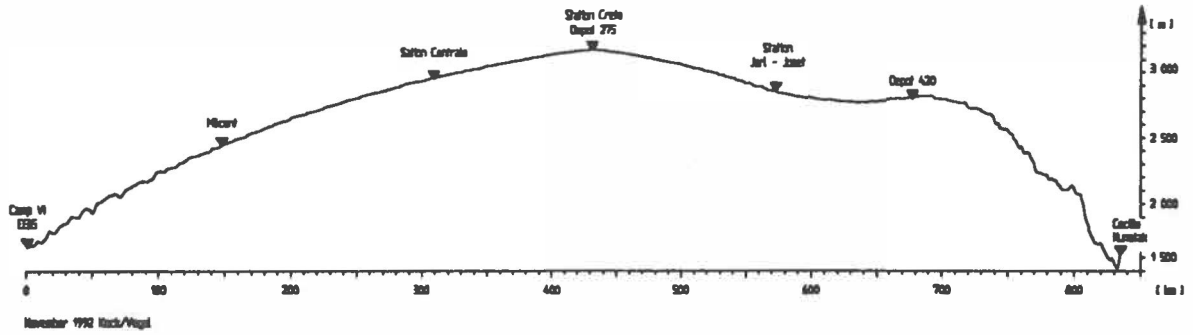

fig 1: cross-section of the ice cap

Comparing the 1959 profile /2/ with the new one it shows the same shape of the surface, i.e. all the waves especially in the western part are stable. As they don't move we can consider them as caused by the topography of the bedrock. The heights above sea level have decreased all along the line.

Seckel /5/ has compared the two levellings from 1959 and 1968, both of them beginning at A14 (westcoast) and reaching to T53 (Jarl Joset). West of T2 as well as east of T46 he found the surface decreasing. The center part was increasing 9 cm/a on the average. Comparing the 1992 observations with those from 1968 and 1959, respectively, lead to a decrease of the surface along the whole profile as shown in the following graph. The average values are -15 cm/a and -9 cm/a. Relative to the first time interval 1959 - 1968 the surface seems to flatten out and we can realize a shrinking of the ice cap. This result contradicts the radar altimeter measurements Zwally /6;7/ carried out. He claims a surface increase of up to 28 cm/a.

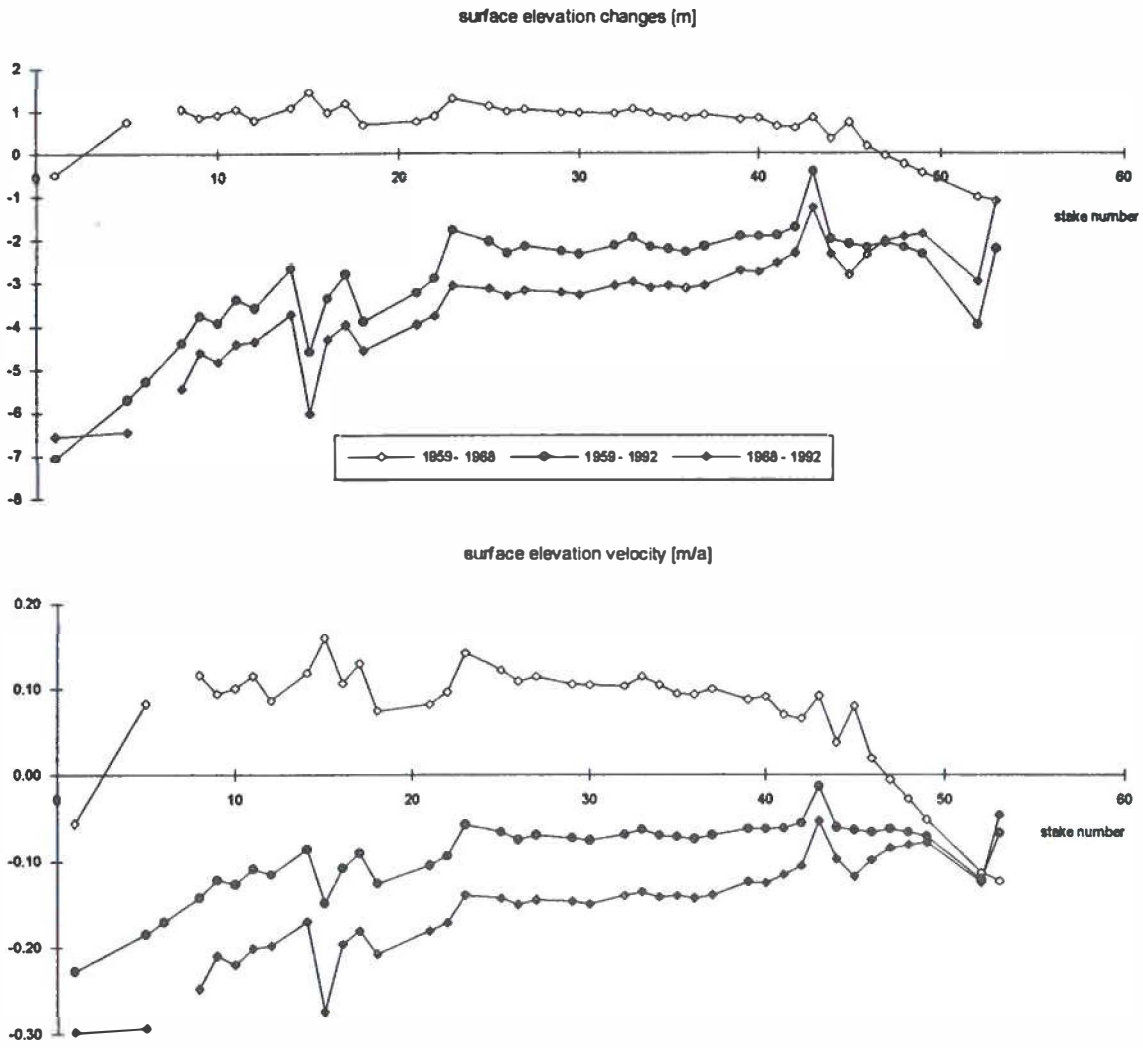

fig 2: surface elevation changes

References:

1. Hodge,S.: personal information
2. Mälzer,H.(1964): Das Nivellement über das Grönländische Inlandeis. Meddelelser om Grönland, Bd.173, Nr.7
3. Möller,D.: personal information
4. Seckel,H.(1977): Das geometrische Nivellement über das grönländische Inlandeis der Gruppe Nivellement A der Internationalen Glaziologischen Grönlandexpedition (EGIG) 1967-1968. Meddelelser om Grönland, Bd.187, Nr.3
5. Seckel,H.(1977): Höhenänderungen im Grönlandeis zwischen 1959 und 1968. Meddelelser om Grönland, Bd.187, Nr.4
6. Zwally, H. J.(1989): Growth of Greenland Ice Sheet: Measurement. Science, Vol. 246, pp. 1587-1589
7. Zwally, H. J.(1989): Growth of Greenland Ice Sheet: Interpretation. Science, Vol. 246, pp. 1589-1591

Strain Determination on the Greenland Ice Sheet

Ch. Homann, D. Möller
Institut für Vermessungskunde
Technische Universität Braunschweig

1. Introduction

From 1987 to 1992 several expeditions took place on the Greenland Ice Sheet. This project is financed by the "Bundesministerium für Forschung und Technologie". One goal of these expeditions is to determine the velocity of the ice movement along the EGIG-line and to calculate the strain rates on decided places.

This paper describes the deformation figures with their strain rates.

The condition for strain determination is the performance of geodetic measurements in two epochs.

There are two different methods of calculation to get information about the strain behaviour, out of which the field solution is the easier and faster one. On the other hand, it is possible to use different computer programs to get the same information, with the advantage of a higher precision and more detailed information compared with the field solutions. The "Institut für Vermessungskunde" provides such programs.

The geodetic measurements consist of angle, distance and azimuth observations. For the calculation of sets of coordinates it is necessary to have more measurements as needed to adjust the coordinates and, thus, increase the interior reliability.

With the help of the affine transformation it is possible to calculate both epochs. This special method has the advantage that not necessarily the same observations must be used in both epochs. Remeasurements are likely to be different from the first set of observations, if a point is missing in the second epoch. Perhaps, even if corresponding observations were carried out with different instruments, the two sets of observations can be compared.

After the affin transformation it is necessary to analyze the shifting of the points from the first to the second epoch. STRAINF is a special program for this step of the strain calculation.

2. Requirements for the deformation figure

The observations must be measured as exactly as needed. It depends on the time and the instruments available as well as on the time intervall between the two measurements.

The glaciological demand is three times the ice thickness as the distance from the center point to the exterior points of the deformation figure. This demand assures that the strain parameters are independent of local topographical influences. The time needed for the measurements shall be very short.

For all this demands, there are different possibilities for the shape of the deformation figures: The triangle, the quadrilateral or the pentagon. From the experience in Antarctica, the triangle is the best shape for this demand.

At special points along the EGIG-line the installed strain nets were designed as triangles. The observations were carried out from two central points . The exterior points of this triangle have a distance of 1600m to the center. These distances were measured with the KERN Mekometer 5000. This instrument can measure with an accuracy better than one millimetre. The angles were observed with a theodolite KERN DKM2AE and a tachymeter WILD TC 2000, which combines angle and distance measurements. For the orientation of the strain net, it is necessary to measure a sun azimuth with a theodolite or to measure an azimuth using the GYROSCOPE.

It is important to observe the exterior points a second time from the second central point. These measurements provide additional information and serve as a check for the observations.

After calculation and adjustment the paramters e1, e2 and t1 give us information about the strain behaviour at special parts of the ice sheet. Strain is the relative change between the points. Under the influence of strain a standard circle will get an elliptical form. The axes e1 and e2 of this ellipse inform about the extreme scale distortion. Table 1 and 2 show special strain figures in comparison. These results are preliminary. The second part of table 2 shows results from the EGIG-expeditions from 1959 to 1974. These values were calculated by Stober (1986).

Point	Date of measurement	Strain values t1	e1	e2
		[gon]	[10-5/a]	[10-5/a]
10010	1989 1990	125.1	+6.0	+2.2
10010	1989 1991	124.9	+5.0	+1.9
10011	1989 1991	113.0	+3.6	+2.0
10012	1989 1991	126.7	+4.9	+2.9
10013	1989 1991	164.9	+3.1	+1.6
10014	1989 1991	144.2	+5.6	+3.4

Tab. 1: Deformation figures at Summit

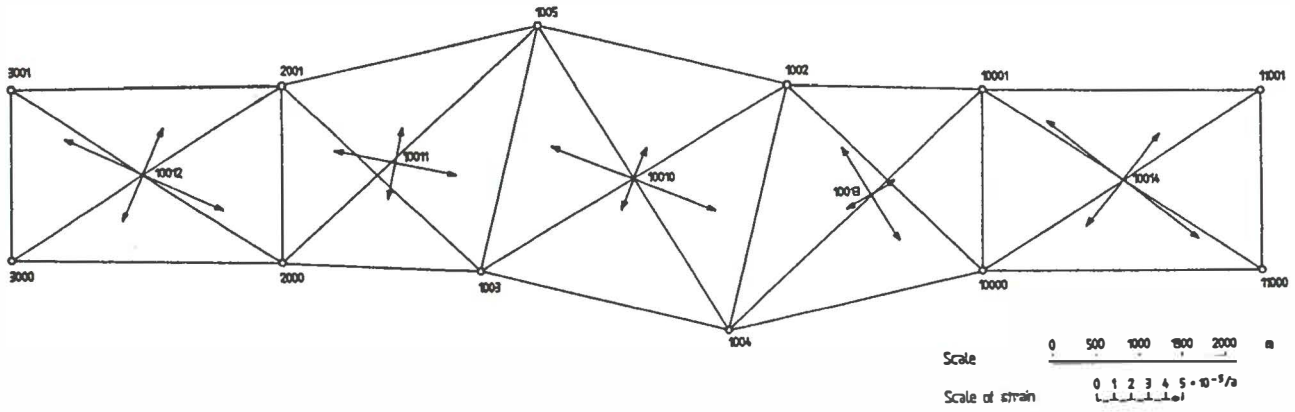

Point	Date of measurement	Strain values t1	e1	e2
		[gon]	[10-4/a]	[10-4/a]
T15	07.07.1990	90.9	+4.9	-1.9
	10.06.1991			
T31	24.06.1990	91.1	+2.2	-0.2
	20.06.1991			
T43	16.06.1989	83.2	+1.1	-0.1
	10.06.1990			
T15	1974-1968	E-W	+5.8	+1.7
	1968-1960		+4.0	-0.9
T31	1974-1968	E-W	+2.7	-0.5
	1968-1960		+2.1	-0.5
T43	1974-1968	80.2	+1.2	+0.1

Tab. 2: Deformation figures along the EGIG-line

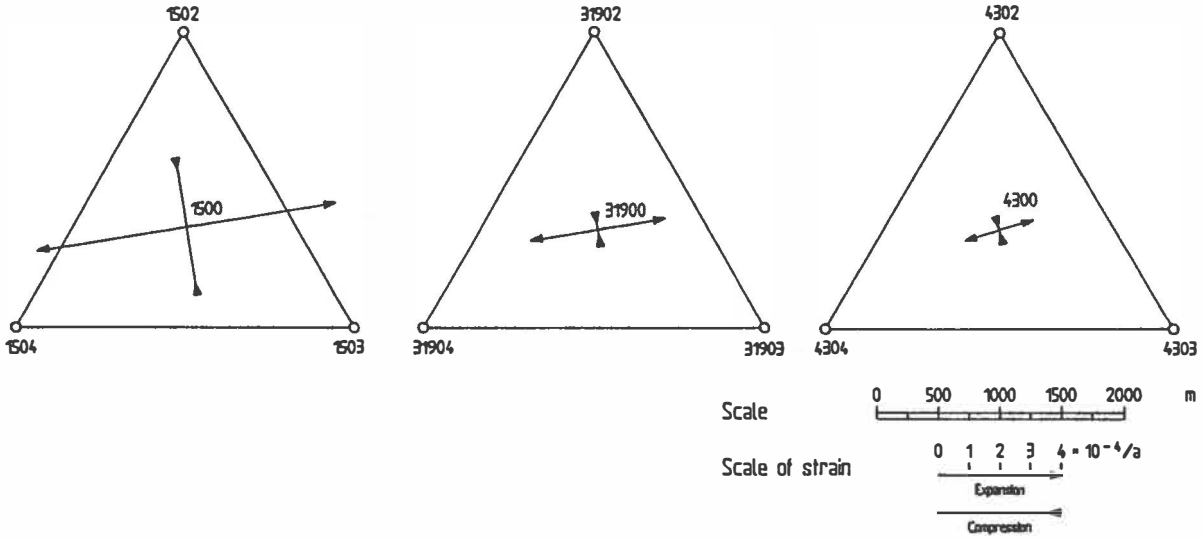

3. References

- Köhler, M.: Ein geodätischer Beitrag zur Erfassung und Darstellung des Verzerrungsverhaltens von Eisflächen unter der Anwendung der Kollokationsmethode. DGK, Reihe C, Heft 318, 1986

- Möller, D., Riedel, B., Ritter, B.: Strain and Velocity Determination on Ronne Ice Shelf, Seventh International Workshop of the Filchner-Ronne Ice Shelf Programme FRISP,61-68, 1992

- Stober, M.: Die Zwischenkampagne 1974, Beitrag aus: Die Deutschen Geodätischen Arbeiten im Rahmen der EGIG 1959-1974, DGK, Reihe B, Heft 281, 1986

- Timmen, L.: Untersuchungen zur Bestimmung des Verzerrungsverhaltens von Schelfeisoberflächen durch geodätische Beobachtungen. Diplomarbeit Hannover, Braunschweig 1988

Re-evaluation of the EGIG profile change

Atsumu Ohmura
Geographisches Institut, ETH Zürich
CH-8057 Zürich

The variation of the cross-section of the Greenland Ice Sheet along the EGIG line was evaluated by Seckel (1977a). One of the difficulties in the previous evaluation of the altitude change of the ice sheet is the error involved in repositioning the stakes surveyed in 1968 back to the locations of the 1959 traverse. Another approach to the problem of the height change is to use the characteristics of the Euler's substantial differential split into the local and into the advective derivatives. The major problem for the second approach was the uncertainty of the velocity field of the glacier surface. The reevaluation of the surface velocity by Heimes et al. (1986) made it possible to estimate the profile change based on the second method, and compare the results with the previous values calculated by Seckel (1977a).

Because the objective of the determination of the profile change is essentially the calculation of the local rate, the Euler's differential for the surface altitude H will be rearranged in the following manner:

$$\frac{\partial H}{\partial t} = \frac{DH}{Dt} - \underline{v}_H \bullet \underline{\nabla} H$$

where H is the altitude, $\underline{v}_H$ the surface velocity and t time. The substantial differentials for this calculation are due to Seckel (1977a), while the surface velocity values are owing to Heimes et al. (1986). By the error analysis it has become clear that the calculation needs extremely accurate surface topographical maps for computation of the surface gradient. Such topographical maps are available only in Seckel (1977b). For these sites the average surface gradients are calculated for the mid-points between 1959 and 1968 which are estimated from the velocity field. The result of the calculation is summarized in Table 1.

For the interior of the ice sheet where the advective term plays a lesser role, the present calculation shows similar results with those by Seckel (1977a). For the mid-range of the ice, however, the differences are significant, although the computation was not possible for the area lower than T4 (1850 m a.m.s.l.).

The dynamic response of the ice sheet due to the mass balance change will become measurable with more than a century time lag. This feature makes it possible to interprete the

height change over decades solely as a matter of the mass balance change. It is, therefore, urgently necessary to reconstruct the decadal mass balance history along the EGIG line at least after 1959.

References

Seckel, H., 1977a: Höhenänderungen im Grönländischen Inlandeis zwischen 1959 und 1968. Medd. Grønland, Bd. 187, Nr. 4.

Seckel, H., 1977b: Das geometrische Nivellement über das Grönländische Inlandeis der Gruppe Nivellement A der Internationalen Glaziologischen Grönland Expedition 1967-1968. Medd. Grønland, Bd. 187, Nr. 3.

Heimes, F.-J., W. Hofmann, A. Karsten, K. Nottarp und M. Stober, 1986: Die Deutschen geodätischen Arbeiten im Rahmen der EGIG 1959-1974, DGK, München.

Gross-balisen	Surface of snow, 1959 m a.m.s.l	Surface of snow, 1968 m a.m.s.l.	$\frac{DH}{Dt}$ m a^{-1}	u	v	$\frac{\partial H}{\partial x}$	$\frac{\partial H}{\partial y}$	$\underline{v}_H \bullet \nabla H$ m a^{-1}	$\frac{\partial H}{\partial t}$ m a^{-1} Ohmura	$\frac{\partial H}{\partial t}$ m a^{-1} Seckel
				m a^{-1}						
T4	1852.13	1846.98	-0.58	-90.0	-48.3	0.0060	0.0013	-0.61	0.03	0.04
T8	2064.03	2059.42	-0.51	-69.4	-41.7	0.0068	0.0042	-0.65	0.14	0.12
T11	2243.16	2239.62	-0.39	-56.4	-38.7	0.0085	0.0036	-0.62	0.23	0.12
T15	2451.42	2448.96	-0.27	-44.0	-18.7	0.0066	0.0048	-0.38	0.11	0.16
T20	2662.65	2662.32	-0.04	-32.3	-12.1	0.0033	0.0026	-0.14	0.10	0.07
T25	2823.44	2823.65	0.02	-22.5	-6.0	0.0040	0.0006	-0.09	0.12	0.12
T31	2963.68	2964.40	0.08	-14.7	-2.0	0.0025	-0.0007	-0.04	0.12	0.13
T35	3049.99	3050.59	0.07	-9.9	0.3	0.0027	0.0006	-0.03	0.09	0.09
T39	3119.88	3120.58	0.08	-5.9	1.8	0.0013	0.0003	-0.01	0.09	0.09
1	2	3	4	5	6	7	8	9	10	11

Source:

Col. 1-4 & 11: Seckel, H., 1977a: Höhenänderungen im Grönländischen Inlandeis zwischen 1959 und 1968. Medd. Grønland, Bd. 187, Nr. 4.

Col. 5 & 6: Heimes, F.-J., W. Hofmann, A. Karsten, K. Nottarp und M. Stober, 1986: Die Deutschen geodätischen Arbeiten im Rahmen der EGIG 1959-1974, DGK, München.

Col. 7 & 8: Seckel, H., 1977b: Das geometrische Nivellement über das Grönländische Inlandeis der Gruppe Nivellement A der Internationalen Glaziologischen Grönland Expedition 1967-1968. Medd. Grønland, Bd. 187, Nr. 3.

Table 1: The profile change of the EGIG line computed in this work and that after Seckel (1977a).

Accumulation during the last 2000 years along the EGIG line and to GRIP drill site derived from radio-echo soundings

Ludwig Hempel, Franz Thyssen, Monika Jonas
Institut für Geophysik, WWU Münster
Münster, FR Germany

During the Greenland expeditions in 1989 to 1992 extensive surface based radio echo soundings were carried out along the reconstructed EGIG line and to the ice core drill sites GRIP and GISP2. The main objectives were to obtain data from internal structures in the upper layers of the Greenland ice sheet and to get data from the bedrock topography on the same track. For the upper layers a 35 MHz high resolution single pulse radio echo sounder was developed and used. To calculate layer depths from the reflection times the velocity depth function of electromagnetic waves in ice was determined by Common Mid Point measurements. These were carried out at several points along the profil.

The reflections (Fig. 1) could be correlated with acid layers from volcanic eruptions in the GRIP ice core which were dated precisely (JOHNSEN et. al., 1992). As these reflections can be traced along the whole profile they give isochrones with high accuracy within the Greenland ice sheet.

Several of the stronger reflections which were picked from the records along the EGIG line and to GRIP drill site were correlated with volcanic eruptions, others had to be interpolated inbetween. From the reflection times mean annual layer thicknesses could be calculated by deviding the layer thicknesses by the corresponding time intervall. These annual thicknesses decrease with growing depth because of the strain effect. This time dependent strain effect was reversed by using the continuity equation for each layer. As a first approach a 2-dimensional model was used including the different development of the layers during the accumulation process. Surface velocity and strain rates were the values from the 1959/68 EGIG expeditions (HOFMANN, 1986). It was assumed that in the upper third of an ice sheet changes of strain rates and velocities with depth are negligible at least outside areas with rough bottom topography.

The strain corrected mean annual layer thicknesses lay within a deviation of ±8% in the eastern part of the EGIG line and to the drill site GRIP. They also fit close to the accumulation rates measured by Benson, GISP and GRIP (OHMURA and REEH, 1991) along the profil. In the western part of the EGIG line large variations in the surface strain rates and high velocities as well as vertical strain produced by bedrock topography cause bigger variations between thicknesses.

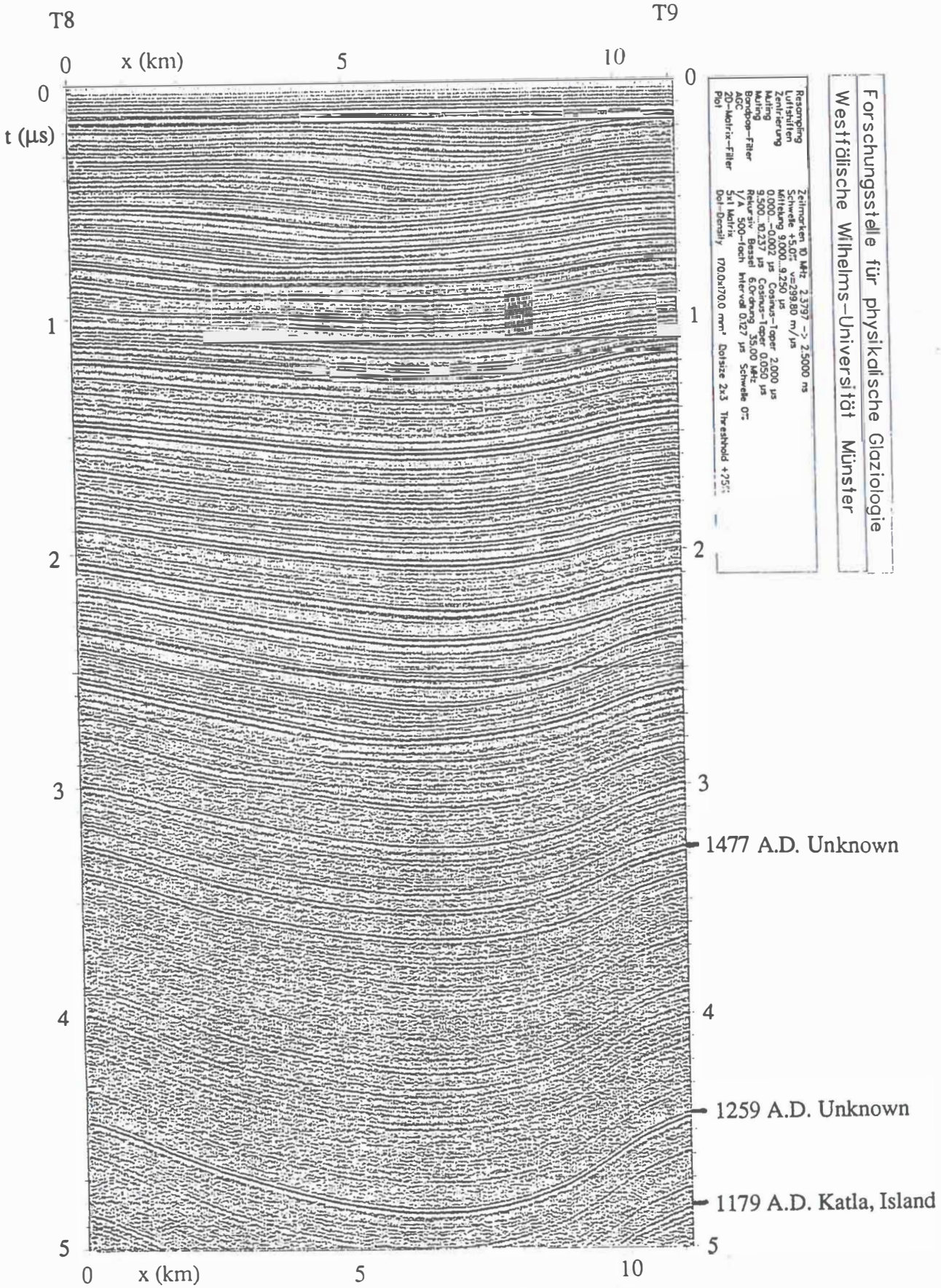

Fig. 1: A high resolution radio echo sounding between T8 and T9 on the EGIG profile.

The deviations are mainly due to incorrect correlation of layer depth with the interpolated ice core timescale for reflections that were not caused by directly datable volcanic eruptions because CMP measurements and start of recording could not be done precisely above the ice core drill hole. The main error sources are uncertainties in the velocity depth function of radio waves in ice which is app. 1% and errors that occurr while picking reflection phases from original data.

HOFMANN, W. 1986. Bewegung des Inlandeises im West-Ost-Profil von 1959 bis 1967. *Die deutschen geodätischen Arbeiten im Rahmen der internationalen glaziologischen Grönland-Expedition (EGIG) 1959-1974*. Deutsche Geodätische Kommission bei der Bayerischen Akademie der Wissenschaften, 43-61.

JOHNSEN, S. J., H. B. CLAUSEN, W. DANSGAARD, K. FUHRER, N. GUNDESTRUP, C. U. HAMMER, P. IVERSEN, J. JOUZEL, B. STAUFFER and J. P. STEFFENSEN. 1992. Irregular glacial interstadials recorded in a new Greenland ice core. *Nature*, **359**(6393), 311-313.

OHMURA, A. and N. REEH. 1991. New precipitation and accumulation maps for Greenland. *Journal of Glaciology*, **37**(125), 140-148.

Isotopic, Chemical and Glacio-Meteorological Studies along the EGIG Line

H. Fischer, K. Geis and D. Wagenbach
Institut für Umweltphysik, University of Heidelberg, Germany
M. Anklin and B. Stauffer
Physikalisches Institut, University of Bern, Switzerland
M. Laternser and W. Haeberli
VAW/ETH Zürich, Switzerland

1 Research activities

The annual snow accumulation and particulate matter input to Greenland firn and ice are of special interest to interpret the temporal alteration of atmospheric conditions and its natural and anthropogenic impurity load.

Evaluation of ice cores as an atmospheric data base with respect to this question however, requires detailed knowledge of meteorological, geographical and microphysical parameters governing the deposition processes.

For this purpose, the Institut für Umweltphysik, University of Heidelberg, in collaboration with TH Braunschweig, University of Bern and VAW/ETH-Zürich started field campaigns in 1990 and 1992. The developped sampling program was designed to attain following main objectives.

- to establish the present state distribution of the annual snow accumulation and firn temperatures along the EGIG line
- to investigate the chemical and isotopic change of Greenland snow properties related to various climatic and geographical situations

The program comprises the following sampling which was taken in two consecutive traverses along the EGIG line:

1990: Summit-Crête-T01

- snow pit and shallow (10m) firn core sampling at 10 sites
- in field determination of seasonal stratigraphy by means of H_2O_2-measurements, firn temperatures and snow density profiles. The H_2O_2-fluorescence method developped by A. Sigg at the University of Bern prooved to be a reliable tool for on site accumulation determination (Fig.1.1.).

1992: Summit-Crête-Caecilia Nunatak

- snow pit and shallow (10m) firn core sampling at 8 sites
- firn temperature profiles down to 15m and snow density measurements at 17 positions

Following these field measurements, various laboratory analyses are in progress at Heidelberg. These analyses concentrate on determination of:

1. stable isotopes of water (δO^{18}, δD, d) to delimit the climatic conditions with respect to precipitation formation and impurity input at the different drilling sites
2. major ions (NO_3, SO_4 as an prominent example for anthropogenic derived aerosol species, Cl as sea-salt indicator)
3. mineral dust components indicating crustally derived aerosol
4. Pb^{210} as an naturally produced radioisotope

2 Preliminary results

The advantage of a traverse coring program lies in the achieved temporal and spatial resolution for the subjects investigated. The accumulation rate, for example, reveals some interesting features (Fig.2.1)

- the annual accumulation in Fig.2.1. shows several predominant structures (ridges, valleys) along the spatial axis, prooving accumulation to be a large-scale phenomenon. Local disturbances only cause deviations from this overall behaviour.
- the change of accumulation rate along the temporal axis shows no significant trend. Also comparison with values of the mean accumulation rate found in the literature (e.g. Seckel, 1977) for previous time intervalls permits no unambigous answer.

The isotope measurements exhibit the empiric altitude and mass effects found in the literature (e.g. DAANSGARD, 1964 and 1973) and permit the determination of the annual mean air temperature. Additionally, the derived deuterium excess shows a small temperature gradient, reflecting kinetic effects during precipitation formation (JOUZEL AND MERLIVAT, 1984). The latter conclusion, however, needs further investigation and especially careful evaluation of the data set.

The measured 15m-firntemperatures show an altitude gradient of 1.2°C/100m (Fig.2.2). The rectangles named A and B in Fig.2.2 indicate points of approximately equal altitude but different latitude. The altitude corrected temperature/latitude gradient is approximately -0.48 °C/°lat for area B while points in area A are too scattered. Comparison with values for the firn temperatures given by DE QUERVAIN, 1969 for the time intervall between 1959 and 1964 indicates no significant change.

The chemical snow components investigated are also dependent on the geographical site of deposition. On the left of Fig.2.3. concentrations of various ions are plotted vs. distance from the coast. Cl as a sea-salt indicator shows the expected decrease of concentration with increasing distance from its source. NO_3 however seems to increase, SO_4 to remain approximately constant. On the right hand side concentrations of the same ions are plotted vs. the previous determined accumulation rates. Here NO_3 and SO_4 show an increase with decreasing accumulation, indicating this behaviour to be partially a dilution effect.

3 Summary

1. In situ H_2O_2 analysis of firn cores is a simple tool to clearly define seasonal snow stratigraphy.
2. Interannual variations of net snow accumulation appears to be a large scale phenomenon.
3. No systematic changes for the surface balance along the western EGIG line (T05-Crête) respectively the 15m-firntemperatures along the eastern EGIG line (Crête-Caecilia Nunatak) are observed over the last three decades.
4. δO^{18}, δD show an sytematic trend from T05 to Summit due to the according temperature change. Also the deuterium excess indicates such a behaviour.
5. Sea-salt aerosol decreases with distance from the coast.
6. Sulfate and nitrate concentrations slightly increase with distance from the coast probably due to lower snow accumulation.

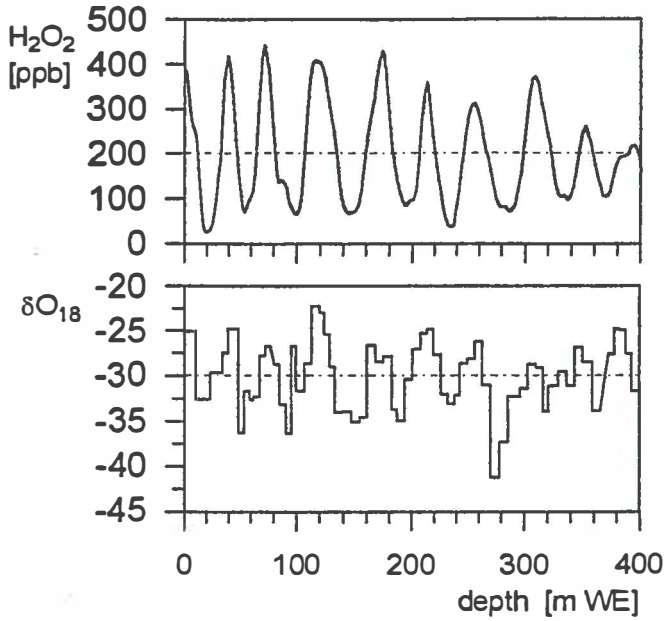

Fig.1.1 - Comparison of seasonal stratigraphy for drill site T21: At the top high resolution H_2O_2-measurement in the field, at the bottom coarse resolution of δO^{18} delimited by the H_2O_2 derived aliquotation.

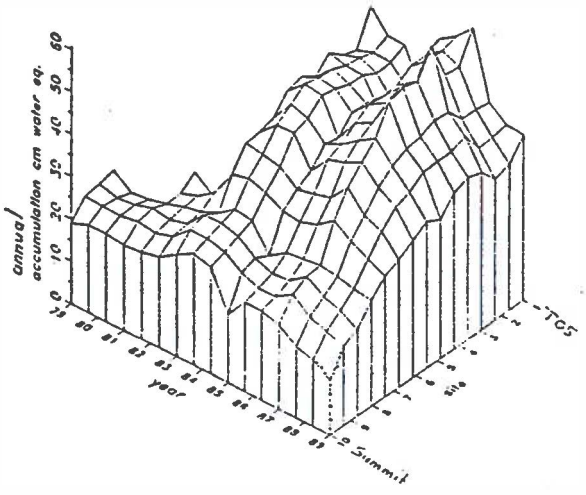

Fig.2.1 - Spatial and temporal distribution of the annual accumulation for the western EGIG line.

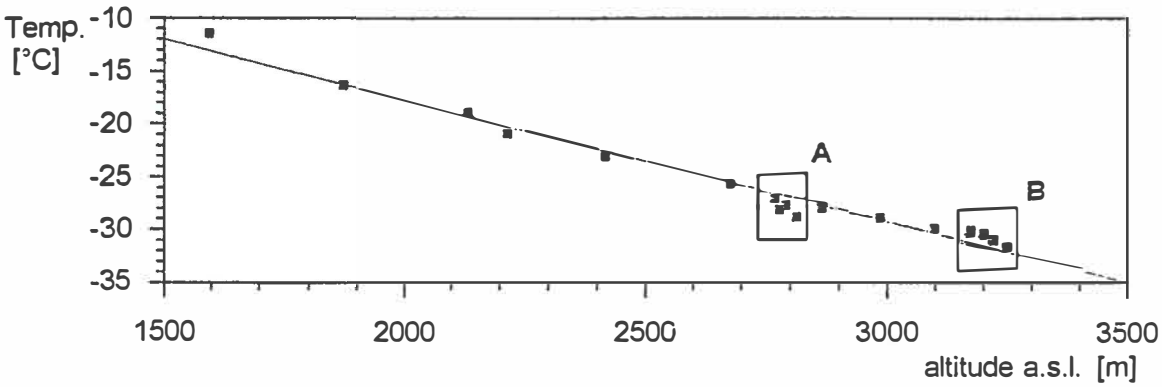

Fig.2.2 - 15m-firntemperatures of the drill sites along the eastern EGIG line related to their altitude a.s.l. . The rectangles A and B indicate consecutive points of approximately equal altitude but different latitude.

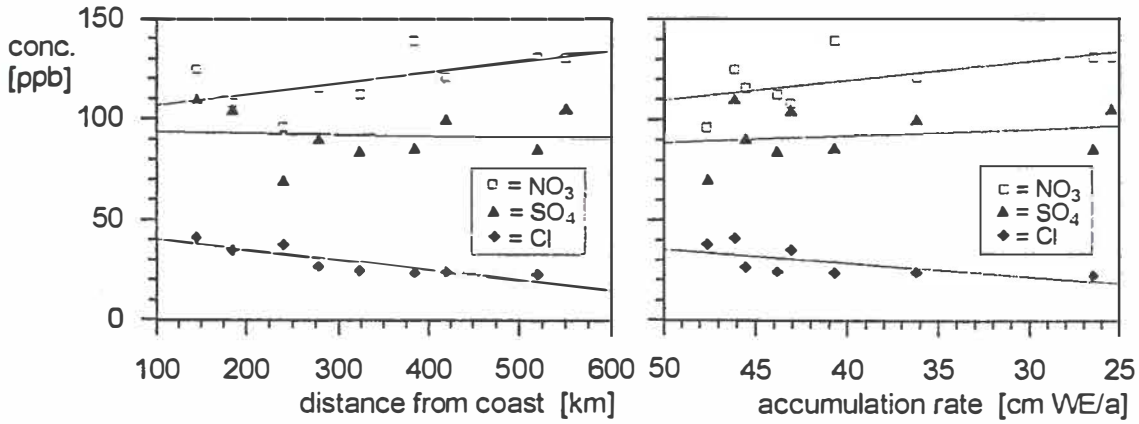

Fig.2.3 - Geographical variation along the western EGIG line for the mean concentrations of various ions compared to their accumulation rate dependence.

4 References

DAANSGARD, W., 1964, Stable isotopes in precipitation. *Tellus*, **16**,4.

DAANSGARD, W., JOHNSEN, S.J., CLAUSEN, H.B., GUNDESTRUP, N., 1973, Stable isotope glaciology. *Meddelser om Grønland*, **197**,2.

JOUZEL, J., MERLIVAT, L., 1984, Deuterium and oxygen in precipitation: Modelling of the isotopic effects during snow formation. *Journal of Geophysical Research*, **89**,D7.

DE QUERVAIN, M. ET AL., 1969, Schneekundliche Arbeiten der internationalen glaziologischen Grönlandexpedition (Nivologie). Expédition Glaciologique Internationale au Groenland (EGIG) 1957-60, Vol. 5, No. 1. *Meddelser om Grønland*, **177**,4.

SECKEL, H., 1977, Höhenänderungen im grönlandischen Inlandeis zwischen 1959 und 1968, extract from SECKEL, H., *Meddelser om Grønland*, **187**, Nr. 4.

Glaciation and Isostasy in the Søndre Strømfjord-Itivdleq system

Jaap J.M. van der Meer, Frank G.M. van Tatenhove
Fysisch Geografisch en Bodemkundig Laboratorium
University of Amsterdam, The Netherlands

Cees Laban, Erno Oele
Rijks Geologische Dienst, Marine Geology Division
Haarlem, The Netherlands

In the summer of 1992 the two institutions mentioned above joined forces in an effort to reconstruct in detail the Holocene glacial history of the Søndre Strømfjord. This combined effort was an extension of GIMEX, a major Dutch research project on the dynamics of the Greenland ice sheet (van der Meer, 1992; Oerlemans et al, 1992). The research theme of the physical geographers in GIMEX concerns the Holocene glacial history of the area between the airport Kangerlussuaq and the inland ice, more specifically the Russell and Leverett glaciers (van Tatenhove, 1992; van der Meer et al, 1992). Since fjords are important sediment traps an extension of the original research area towards the whole fjord was attempted together with the Marine Geology Division of the Rijks Geologische Dienst (Oele, 1992). It is to be expected that answers to questions arising from the on-land studies can be found in the sedimentary filling of the fjord or along the fjord. One of the questions that had come up over the last two years concerns the amount of isostasy near the head of the fjord. This has implications for the modelling of the dynamics of the ice sheet.

The airport Kangerdlugssuaq is situated on top of an extensive terrace at a level of about 40 m a.s.l. For this area an isostatic uplift of about 25 to 40 m is indicated by ten Brink (1975). In the adjoining figure the contour of a large former ice-dammed lake is indicated. This former lake is indicated on the basis of strandline terraces and deltas as mapped in the field. The total length of this former lake must have been in the order of 30 km. Given the position of this lake with regard to the general direction of Holocene ice retreat, one would expect the strandline terrace to show a distinct tilt caused by isostatic uplift. However, this is not the case; the terrace is traceable at the level of ca. 255 m a.s.l.
The findings of up to 40 m of isostatic uplift at the head of the fjord and no uplift less than 10 km to the N, are incompatible. One way to explain this difference is by assuming that the two areas have different uplift rates, e.g. because they are located on different tectonic blocks. Since there is no obvious sign for neotectonic activity along the major fault that runs from the head of the fjord to Russell glacier, this assumption can be discarded.

Another way out may be to look at the alleged isostatic uplift near the airport. For this it will be necessary to first describe the fjord system.

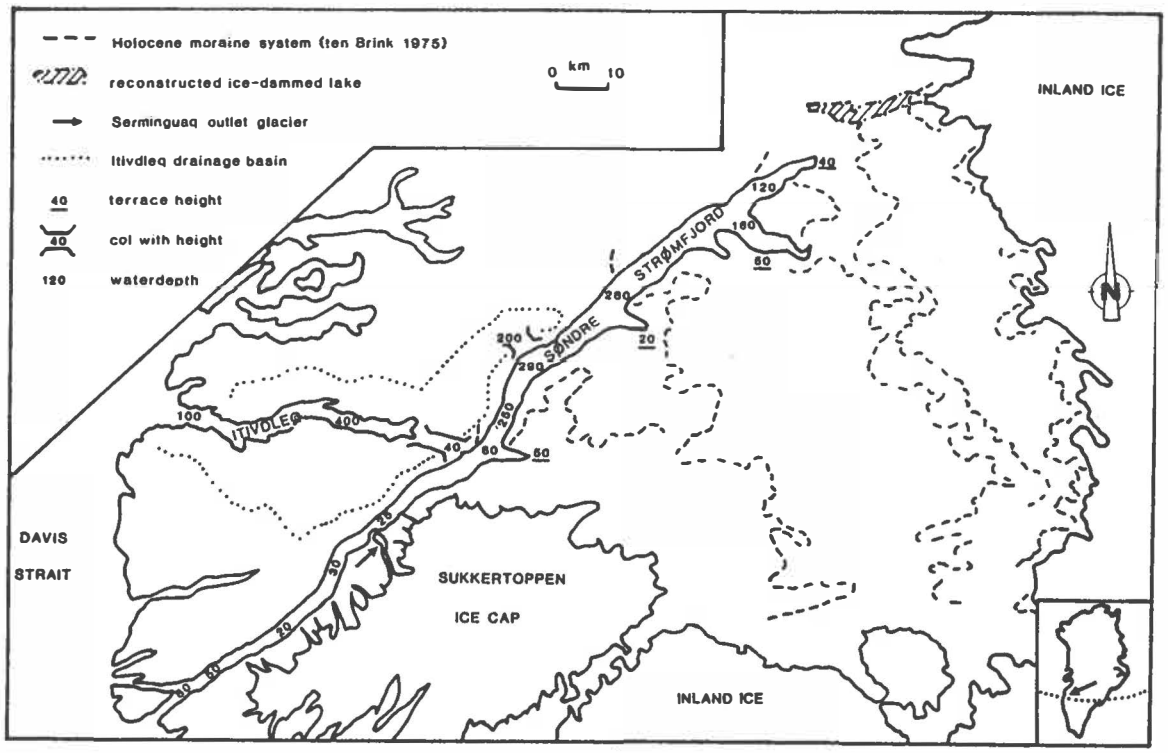

The adjoining figure indicates waterdepths (in round figures) for Søndre Strømfjord and Itivdleq. The latter fjord was included in the study because of air photo observations and relations suggested by Sugden (1972). These waterdepths clearly demonstrate that the main fjord can be divided in two sections of more or less equal length: an inner basin (290 m deep) and an outer sill (< 20 m deep, except for the channel). In this respect the depth of Itivdleq, approaching 500 m, is astonishing, because it drains a fairly small basin. Input from outside this drainage basin is only possible through two cols, one in the north at an elevation over 200 m, the other, a direct extension of the fjord, at 40 m a.s.l. Input through the northern col is only possible when the inland ice occupies the westernmost Holocene moraine system indicated in the map. Given the small drainage basin the infilling of more than 50 m (compared to several hundred metres in Søndre Strømfjord) in the deeper part of the fjord is most likely related to such an event.
Along the southeastern side of Søndre Strømfjord terraces can be found at the heads of all entrants. The lowermost terraces (except in one entrant, Angujârtorfik) are all located between 40 and 50 m (Sugden, 1972), coinciding in altitude with the terraces at the airport and the lowermost col to Itivdleq. If it is possible to find a common ground for these coinciding altitudes, this might explain the isostatic 'problem' at the head of Søndre Strømfjord.

The common ground may be the behaviour of Sukkertoppen, an independent ice cap, located near the coast at an altitude of more than 1500 m. Because of this it behaves independent from the inland ice sheet. The NW side of Sukkertoppen has several outlet glaciers, the largest of which is Serminguaq. The latter actually penetrates the fjord, with the (presumably) Little Ice Age moraines occupying its shallow part. An extension of this outlet glacier, caused by the independent behaviour of Sukkertoppen, could easily block

the fjord. A similar situation exists on the SE side of Sukkertoppen.
Blocking of the fjord would result in a rise of waterlevel until the level of the lowermost col to Itivdleq is reached. At that stage drainage will be resume, resulting in sediment-free water entering Itivdleq. In the mean time terraces will form at all major inputs into the ponded fjord.
Is there any evidence for such a blocking event ? Because of the very high tidal currents in the outer part of Søndre Strømfjord (up to 7 knots) there is hardly any sediment to be found there. Scree development on the steep rockfaces opposite Serminguaq hide any trace that might be left of the glacier reaching that shore. At this moment direct evidence of such an event is lacking. Indirect evidence can be found in the erosional channels that were observed in the sediment accumulation in Itivdleq; presumably these were cut by the sediment-free water entering the fjord. Further tests will concentrate on the sedimentary infilling of the westernmost part of the deep basin in Søndre Strømfjord. Likewise the evidence for the marine nature of terraces along the fjord as well as the dating of the incorporated shells will be studied.

References

Brink, N.W. ten, 1975 Holocene history of the Greenland ice sheet based on radiocarbon-dated moraines in West Greenland. Grønlands geol. Unders. Bull.113.

Meer, J.J.M. van der (ed) Greenland Ice Margin EXperiment 1991. Circumpolar Journal 6, 1-51.

Meer, J.J.M. van der, F.G.M. van Tatenhove, H. Jiskoot, J.Schoorl & E. Oosterbaan, 1992 Smeltende ijskappen, hogere dijken. Geografie 1, 40-43.

Oele, E. 1992 Cruise Report GIMEX-MAR '92. Marine Geology Division, Rijks Geologi sche Dienst Haarlem.

Oerlemans H., H. Vugts & J.J.M. van der Meer, 1991 Ice sheets and sealevel, the project behind GIMEX '91. Circumpolar Journal 6, 3-14.

Sugden, D. 1972 Deglaciation and isostasy in the Sukkertoppen ice cap area, West Greenland. Arc. & Alp. Res. 4, 97-117.

Tatenhove, F.G.M. van, 1991 A geomorphological branch on the GIMEX tree. Circumpolar Journal 6, 34-41.

Relations between ice margin and proglacial thermal regime near the Leverett Glacier as revealed from geoelectrical soundings

Frank G.M. van Tatenhove
Fysisch Geografisch en Bodemkundig Laboratorium
University of Amsterdam, The Netherlands

Within the context of the GIMEX project glacial geological research is carried out to constrain ice sheet models (van der Meer, 1991; Oerlemans et al, 1991; van Tatenhove, 1991). This abstract concentrates on the relations between the thermal regime of the glacier and its proglacial thermal regime as revealed from geoelectrical soundings and presents a preliminary analysis.

The 1992 geophysical sounding program: results, interpretation and problems

In the summer of 1992 geophysical soundings were carried out near the Leverett glacier (figure 1). The first area is between the present ice margin and a large morainic complex. The second area is between the morainic complex and the terrace area. The two sites reflect a different glacial history. SL6 has been covered by the Leverett glacier after the advance following the Holocene climatic optimum (hypsithermal). This advance ended probably around 700 yr BP. SL2 has been in the periglacial zone after deglaciation 4000-4500 yr BP. 11 geoelectrical profiles were measured, 4 Wenner arrays and 7 Schlumberger arrays. The location of the profiles is given in figure 1. Resistivity was recorded with an ABEM Terrameter SAS 300. To compare the geophysical properties of the two areas several profiles could not be used because the spread length was too short or the prerequisite of horizontal layering is not forefilled. Based on the location of the profiles, the depth penetration and the estimated influence of subsurface valley geometry, it seems to be reasonable to compare SL2 and SL6. SL2 is in the center of the inactive, unvegetated sandur plain in front of the morainic complex. SL6 is on the active sandur plain in front of the present ice margin. RESIST (Vander Velpen, 1988) is used for the interpretation of the curves. Because SL2 is the best possible profile regarding spread length and position within the valley, the resistivity values obtained with this profile were used to calculate the theoretical curves (i.e. to tune the depth-values) for the other profiles. This is especially necessary when the angle of the climbing part of the fieldcurve is approximately 45°. As different multi-layer models may give the same sounding graph, the most probable and simple model has been selected according to the results of terrain observations. Therefore all curves have been interpreted using a 3 or 4 layered model. An extensive discussion on the interpretation of the curves will be presented in a separate paper.
All curves have a similar lay-out: one or two surface layers followed by a layer with high resistivity (the 'high resistivity layer', HRL from now on). When the spread is long enough, this layer is followed by layer with a resistivity of a magnitude less than the HRL. SL2 revealed a value of 300 kΩm for the HRL and a value of 20 kΩm for the underlying layer.

The HRL is interpreted as frozen gravel/till/bedrock. Values of frozen debris of 10-900

kΩm are reported by King et al (1987). The layer underneath the frozen gravel/till/bedrock can be interpreted as frozen/unfrozen bedrock or unfrozen gravel/till. From this interpretation the uncertainty arises about the interpretation of the boundary between the HRL and the final layer. Does the change in resistivity reflect groundthermal conditions (permafrost or no permafrost, regardingless the material) or is it the boundary sediment (frozen) to bedrock (frozen or unfrozen)? The results of SL3 (close to a bedrock cliff) are in favor for the sediment - bedrock hypothesis. The resistivity of bedrock strongly depends on temperature according to Hoekstra & McNeill (1973) and King et al (1987). But the resistivity of frozen bedrock (10-20 kΩm for biotite granite at -2°C, compared to 4 kΩm unfrozen (Hoekstra & McNeill, 1973); 45 kΩm against 4.5 kΩm for unfrozen bedrock, King et al, 1987) is still an order of magnitude less than the resistivity of the HRL. With the available data it is difficult to evaluate the character of the boundary HRL and final layer. The HRL definitely indicates frozen material. Using the thickness of the HRL a minimum value for the permafrost thickness is obtained. It is not possible to determine the thermal conditions of the underlying bedrock i.e. no firm conclusions are possible about the permafrost thickness. Nevertheless near SL2 the minimum permafrost thickness is 130-150 m and near SL6 the minimum permafrost thickness is 50-100 m.

Conclusions

- If the permafrost thickness of 130-150 m at SL2 is in equilibrium with present climatological conditions, this could indicate a mean annual surface temperature (MAST) of -2/-2.5 °C (assuming a geothermal heat flux of 41 mW/m^2 and a thermal conductivity of 2.6 $Wm^{-1}K^{-1}$). According to local climatological data and reported relations between Mean Annual Air Temperature and MAST such an estimate is well possible.
- Based on the geoelectrical data and an analysis of the possible subsurface bedrock geometry the Leverett glacier advanced after the hypsithermal on a bed of sediment (probably frozen) and is still based on a sediment-bed (see also van Tatenhove et al , 1992).
- Using a simple analytical solution of the heat conduction equation (Gold & Lachenbruch, 1973; Lachenbruch et al, 1982) some implications of the existence of at least 50-100 m frozen material near the present margin at a site which has been subglacial in the period 700 - 100 yr BP could be:
  1. cold-based conditions of the Leverett glacier (basal temperature -0.5°C) during the advance to the morainic complex line followed by periglacial conditions with a MAST of -1 to -2.5°C during 100 or 700 years or 2. cold-based conditions of the Leverett glacier (basal temperature -1°C) during the advance to the morainic complex line followed by a warming of 0.5 °C in the last 100 yr or 3. temperate conditions during the advance (say in the period 1200 - 700 yr BP) followed by periglacial conditions after 700 - 100 yr BP with a MAST of -2°C to -3.5°C.
- Unfortunately, it is not possible to deduct the ice marginal thermal regime during glacier fluctuations from the measured geophysical properties, because no firm conclusions are possible about the permafrost thickness. A more detailed analysis is possible if groundtemperature data are available to a depth of ± 150 m. The use of geothermal models is useful to estimate possible scenarios. The study of the sediment-morphological properties of the morainic complex will also give information on the conditions at the former ice margin.

References

Gold, L.W., Lachenbruch, A.H., (1973): Thermal conditions in permafrost. A review of North American Literature. 2nd International Conference on Permafrost, 3-23.

Hoekstra, P and McNeill, D., (1973): Electromagnetic probing of permafrost. 2nd International Conference on Permafrost, 517-526.

King, L., Fisch, W., Haeberli, W., Waechter, H.P., (1987): Comparison of resistivity and radio-echo soundings on rockglacier permafrost. Z. f. Gletsch. und Glazialg., Bd.23, 77-97.

Lachenbruch, A.H., Sass, J.H., Marshall, B.V., Moses, T.H.Jr., (1982): Permafrost, heat flow and the geothermal regime at Prudhoe Bay, Alaska. J. of Geophysical Research 87, 9301-9316.

Meer, J.J.M. van der (ed), (1991): Greenland Ice Margin EXperiment. Circumpolar Journal 6, 1-51.

Oerlemans H., Vugts, H. & Meer, J.J.M. van der, (1992): Ice sheets and sealevel, the project behind GIMEX '91. Circumpolar Journal 6, 3-14.

Tatenhove, F.G.M. van, (1992): A geomorphological branch on the GIMEX tree. Circumpolar Journal 6, 34-41.

Tatenhove, F.G.M. van et al, (1992): Field Report of the Greenland Ice Margin Experiment (GIMEX) 1992. Unpublished report Fysisch Geografisch en Bodemkundig Laboratorium, UvA, 17 pp.

Ten Brink, N.W., (1975): Holocene history of the Greenland ice sheet based on radiocarbon-dated moraines in West Greenland. Medd. om Grønland, Bd. 201, Nr. 4, 44 pp.

Vander Velpen, B.P.A., (1988): RESIST's Users Guide. I.T.C. Delft, The Netherlands, 41 pp.

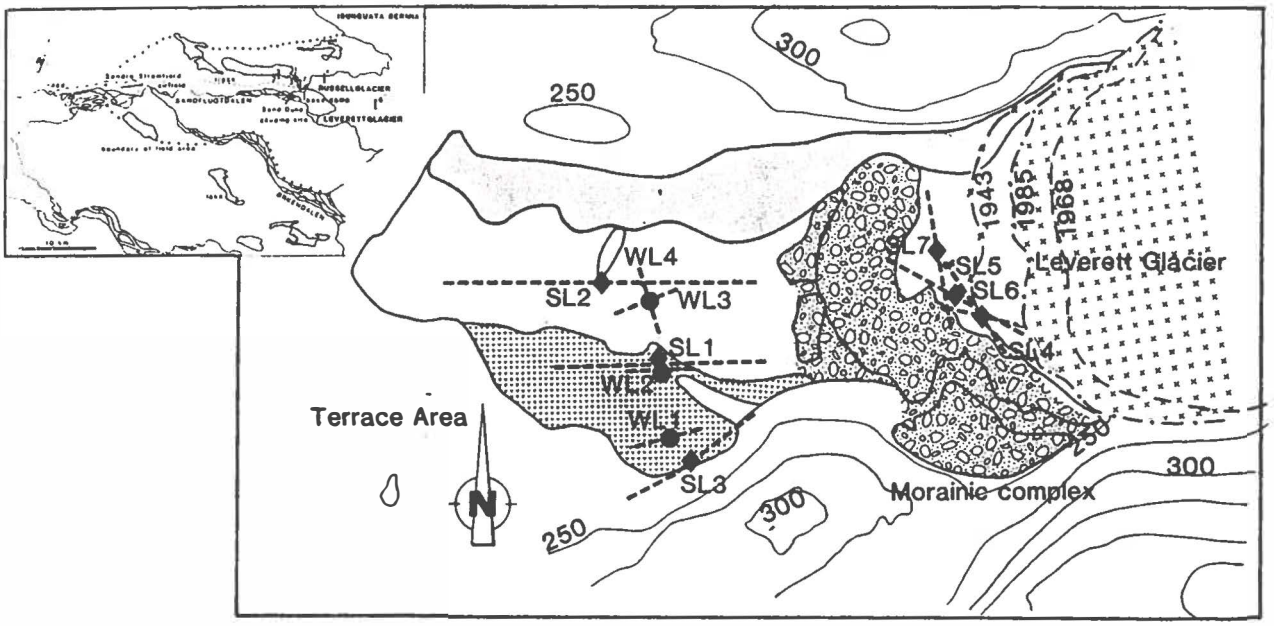

Figure 1: *Location of the geoelectrical soundings. SL* = Schlumberger array, WL* = Wenner array. 1943 - 1968 - 1985, position of ice margin at indicated year. Small dots = present active channel, vv = vegetated sandur.*

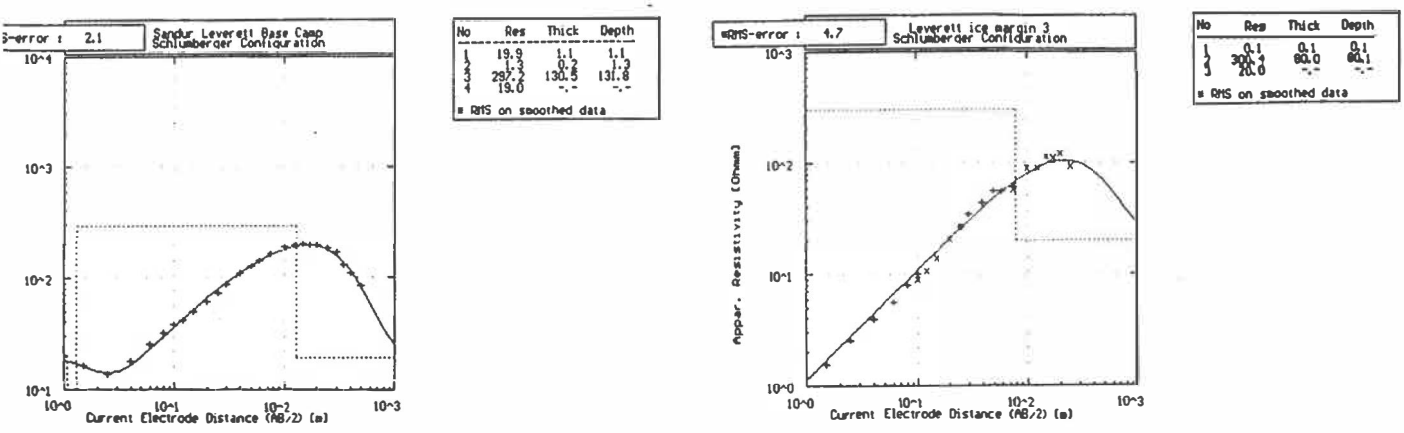

SL2 SL6

Figure 2: *Soundings SL2 & SL6. Note: apparent resistivity in kΩm.*

Controls on the varying morphological and sedimentological characteristics of outwash systems near Kangerlussuaq (Søndre Strømfjord), West Greenland

Andrew J. Russell
School of Geography, Kingston University, Penrhyn Road, Kingston Upon Thames, Surrey, KT1 2EE., U.K.

The morphology and sedimentology of four proglacial outwash streams near Kangerlussuaq (Søndre Strømfjord) was examined in order to characterise the role of variations in meltwater flow regime along an ice sheet margin.

Rivers examined emanate from the Øekendalen, Leverett, Russell, and Isunguata outlet glaciers. The Russell outwash plain were examined during the 1986, 1987 and 1988 meltseasons with further meteorological and hydrological studies undertaken during the 1990 and 1991 GIMEX expeditions. Preliminary studies were made of the proximal of the Ørkendalen river and the lower Leverett outwash plain (see location map).

Meltwater catchment areas are known to vary considerably between these rivers with base flow discharges increasing in the following order: Russell (80 m^3s^{-1}) (Russell, 1989, 1990; v.d.Wal & Russell, Submitted), Leverett (C. 200 m^3s^{-1}), Ørkendalen (10^2-10^3 m^3 s^{-1}), and Isortoq (10^2-10^3 m^3s^{-1}). Both Russell and Isortoq rivers include occasional jökulhlaup contribution providing additional discharges of at least 10^3 m^3s^{-1}. The Ørkendalen and Leverett rivers receive occasional discharges from the drainage of large supraglacial lakes augmenting flows by 25-30% for periods of 3-4 weeks (Russell, In Press).

The orientation and location of two subglacial outlets in relation to the ice and sandur margins determine proximal channel pattern of the Ørkendalen river system. The proximal sandur surface resembles a coalescent fan system characterised by cobble-sized sediment and high downstream gradients. Sedimentary evidence suggests that substantial deposition has taken place on top of river icings during winter or spring. The Leverett river displays less diurnal discharge variation than the nearby outlet from the Russell Glacier. The sedimentology of the Leverett outwash plain appears dominated by ablation controlled discharge events. One major subglacial outlet and several smaller marginal meltwater streams from the proglacial Isortoq river. High relief amplitude, sand bars and terrace fragments c. 5 m above observed river levels suggest large meltwater discharge variations. High relief amplitude bar and bedforms in the Russell river reflect high energy deposition during periodic jökulhlaups of 25 times greater discharge than normal flows (Russell, 1990).

Varying channel characteristics exhibited by each river reflect different controls on meltwater and sediment supply. The Ørkendalen and Isortoq rivers have a greater range of flow magnitudes than the Leverett probably due to meltwater input from large ice-dammed lake. Sediment supply variations, however, provide the main difference between the sand-dominated Isortoq and the other three coarser-grained rivers. In contrast the Leverett system having fewer ice-dammed lakes less discharge variation. The Russell river system, however, being very "flashy" almost perfectly preserves high magnitude flood deposits. Occasional meltwater contribution from the upper-middle ablation zone of the ice sheet by supraglacial lake drainage appears to have adding effect on river channel morphology and sedimentology other than by adding to base flows or perhaps depositing sediment on top of river ice in the winter months.

Proposed research

1. Detailed study of sedimentary characteristics within Ørkendalen, and Leverett rivers combined with river gauging programme.

2. Investigation of the role of supraglacial storage-release events for river flow regime.

3. Palaeohydrological reconstruction of flows within main outwash systems near Søndre Strømfjord.

References

Maizels, J.K. and A.J. Russell,´ 1992: Quaternary perspectives on jökulhlaup prediction. In QRA published book on *Application of Quaternary Research* Quaternary Proceedings, No.2, 30p.

Russell, A.J., 1989: A comparsion of two recent jökulhlaups from an ice-dammed lake, Søndre Strømfjord West Greenland. *J.Glaciology* **35**(120), 157-162.

Russell, A.J. and C. de Jong, 1989: Lake drainage mechanisms for the ice-dammed Oberer Russellsee, Søndre Strømfjord, West Greenland, *Zeitschrift für Gletscherkunde und Glazialgeologiie,* **24** (2), 143-147.

Russell, A.J., J.F. Aitken, and C. de Jong, 1990: Observations on the drainage of an ice-dammed lake in West Greenland. *J.Glaciology,* **36** (122), 72-74.

Russell, A.J., 1990: The geomorphological and sedimentological effects of jökulhlaups. *PhD thesis,* University of Aberdeen, 135pp.

Russell, A.J., 1990: Correspondence: Extraordinary meltwater run-off near Søndre Strømfjord, West Greenland. *J.Glaciology,* **36**(124), 353.

Russell, A.J., In Press: Correspondence: Supraglacial lake drainage near Søndre Strømfjord, West Greenland. *J.Glaciology.*

van de Wal, R.S. and A.J. Russell, Submitted: Energy balance and melt-water runoff modelling studies near Søndre Strømfjord, West Greenland, *Global and Planetary Science.*

AKULIARUSERSUP
Isortoq
Isungua ta sermia
AVGAT
Kûgssûp-glangua
Uiariaq
Qardligssuit
Qardligssuit tasiat
Sanguiarduk
SUNGUA
Manitsoq
Langsø erne
Aujuitsup tasia
Sáningássoq
RUSSELL
LEIGETT
Sandflugtdalen
Akuliarusiap Ssuk
Kegle
LUFTHAVN Flyveplads
JØRNITSUT
Rinssdal
Ørkendalen
Ravneklippen
Qaersorssuaq
Store Saltø
Brayasø
Taserssuatsiaq
Taserssuatsiaup kingingaera
Nunaqarfia
Taserssuatsiaup qalia
Nagtnán
ANGMA
Perserajut
13
67

ISSN 0903-7322